UNIVERSITY OF CALIFORNIA,
IRVINE

ESSAYS ON ASSET PRICING AND CRYPTOCURRENCY

DISSERTATION

submitted in partial satisfaction of the requirements
for the degree of

DOCTOR OF PHILOSOPHY

in Economics

by

Joy Diana Xiuyao Yang

Dissertation Committee:
Professor Gary Richardson, Chair
Associate Professor Ivan Jeliazkov
Professor Matthew Harding

2022

DEDICATION

To both my fathers who art in Heaven, for their unconditional and eternal love.

TABLE OF CONTENTS

LIST OF FIGURES

LIST OF TABLES

ACKNOWLEDGMENTS

I have been fortunate to find an intellectual home for the past five years in the Department of Economics at the University of California, Irvine, where I have the opportunity to work with superb researchers. I am grateful to many teachers, supervisors, and mentors who have enriched my life and thinking; who encouraged and supported me during the writing of this dissertation and my Ph.D. journey.

First and foremost, I am very indebted and thankful to my advisor Dr. Gary Richardson, who has provided me with outstanding guidance, mentoring, caring, and encouragement during the last five years of graduate study in Irvine. I have been so fortunate to have an advisor like him. I am profoundly grateful for the opportunity to learn so much from him, the help and inspiration he provided.

I thank Dr. Ivan Jeliazkov for the great inspiration, encouragement, and knowledge I received from him. His enthusiasm, teachings, caring, and generosity were influential to me and molded my framing of econometric analysis, Bayesian perspective, and teaching style. I value his confidence in my work and sincerely appreciate his guidance and wisdom.

I also thank Dr. Matthew Harding, who taught me Big Data and Machine Learning. I have been fortunate to work with him in the Deep Lab, and I appreciate the knowledge and wisdom I have received and benefited from him. I also deeply appreciate his generosity, encouraging words about the manuscript and the vital feedback and guidance he provided.

I would like to thank Dr. Guillaume Rocheteau for the rich feedback, fruitful discussions, and guidance in my research and writing. I thank Dr. Eric Swanson, Dr. Choi Michael, and Dr. Bill Branch for their guidance and advice. Working with them challenges my intellect and thinking in the best possible way.

I extend special thanks to the people who influenced me early in my study and career, Dr. Maxim Ivanov, Dr. Jeffrey Racine, Dr. Cathy Zhang, Dr. Amy Peng, and Dr. Haomiao Yu, for encouraging me to pursue my dream and becoming a professor.

I thank the friendship, love, support, and wisdom from Sara Kamali, Lan Wei, Frank Kuo, Dillon Flannery, Jaclyn Rosenquist, Kelsey Grey, Francisco Klapp, and Lucie Lebeau during my Ph.D. graduate student life. Their generous support and encouragement make me feel that I am not alone on this journey.

Finally, I would like to express special gratitude to my family - my mum Zhen, brother Qing and sister Susan Han, who have always been there supporting me and providing unconditional love. Without them, this dissertation would not have happened.

VITA

Joy Diana Xiuyao Yang

EDUCATION

Doctor of Philosophy in Economics **2022**
University of California, Irvine *Irvine, California*

Master of Arts in International Economics and Finance **2006**
Ryerson University *Toronto, Ontario, Canada*

Master of Science in Economics and Finance **2004**
Univeristy of York *York, Yorkshire, UK*

Bachelor of Arts in Finance **2002**
Shandong Univesity *Jinan, Shandong, China*

ABSTRACT OF THE DISSERTATION

ESSAYS ON ASSET PRICING AND CRYPTOCURRENCY

By

Joy Diana Xiuyao Yang

Doctor of Philosophy in Economics

University of California, Irvine, 2022

Professor Gary Richardson, Chair

This dissertation is composed of a theoretical chapter and an empirical chapter on asset pricing and cryptocurrency asset pricing.

The first chapter is a theoretical study and is motivated by the recent multiplication of privately produced cryptocurrencies and the questions raised about the dynamics of their prices. Through a New Monetary approach, I investigate a prominent question, which is, "What causes enormous price volatility in cryptocurrency?" Specifically, I study this question using a random matching search model and relax the assumption of rational expectation by introducing an adaptive learning algorithm. My model builds on Choi and Rocheteau (2021), who study the price dynamics of monies that are privately-produced through time-consuming mining technologies under rational expectation. They extended the Lagos-Wright model by adding a time-consuming mining technology and an occupation choice, to show that there exists a unique equilibrium where a positive money value reaches to steady state. Although their model has desirable results, the extreme price volatility in empirical data can not be explained in their rational expectation version of the model. I use bounded rational expectation to explore monetary theory price dynamics. my paper contributes to this under-explored study using an adaptive learning approach. The primary contribution of this study is that I use a constant-learning-gain to demonstrate how the learning gain affects monetary

equilibria, their dynamics and their stabilities. The main results are that with a relative high learning gain in the adaptive learning algorithm, a period of doubling bifurcation can occur, which can lead to chaos or explosive paths. These endogenous dynamic results shed some light on the intensity of cryptocurrency's price volatility. In addition, when buyers have higher bargain power, the price of cryptocurrency converges to a positive value. Ceteris paribus, however, when producers have higher bargain power, the price converges to zero equilibrium. The feedback effect, which plays a significant role in cryptocurrency's price volatility, provides the intuition behind this model.

The second chapter examines the cross-sector comovements that occurred in the U.S. stock market during the COVID-19 pandemic. This study constructs a dynamic factor model to illuminate the sources and implications of these comovements. Estimation of the model using a Markov Chain Monte Carlo method reveals that the latent sentiment is the driving force behind financial market behaviors. In addition, the latent factor had a weak daily oscillation pattern with a -0.09 autoregressive coefficient in an AR(1) process. This pattern explains the stock market's extreme comovements and high volatility. Moreover, this study estimates the impact of the monetary policy interest rate on each stock market sector. The results indicate that when the Fed Effective Funds Rate was reduced by one percentage point, utilities and non-durable goods stock returns substantially jumped by 11.35% and 7.328%, respectively. In addition, this study explores the impact of news shocks, including monetary policy news, fiscal stimulus news, and unemployment news, on cross-sector equity returns. For any given sector, the conventional and unconventional monetary policy news shocked the sector in opposite directions. Of the positive monetary news shocks, the strongest shocks were from the interest rate policy surprises, while unconventional monetary policy news had a more sluggish impact on stock returns. Conversely, fiscal stimulus news had the most substantial positive impact and triggered all sectors to rebound from the bear market at the end of March 2020. Furthermore, by applying Natural Language Processing (NLP) sentiment analysis, this study sheds light on the positive correlation between comovements and news

sentiment. Using the Wall Street Journal headlines as proxies of the market sentiment, the study finds a positive correlation, 0.31, at the 95% statistically significant level, between the comovements and market news sentiment. Finally, in estimating the associations between the cross-sector asset returns and the government's social distancing policy, this study finds that the stay-at-home orders and restrictions on transit have positive associations with asset returns. Conversely, increases in retail and recreation activities have negative associations with asset returns in general. Owing to the government's policies and restrictions enacted to protect public health by slowing the spread of COVID-19, some economic activities have been curtailed in the short term. However, in the long term, these government restrictions help the public's welfare and the economy. Future studies to explore the different impacts between government restrictions and voluntary social distancing could provide fruitful results.

Chapter 1

Adaptive Learning and Cryptocurrency's Price Volatility

This paper studies a question in monetary theory: Why is cryptocurrency extremely volatile? To investigate this question, I use a New Monetary model with an adaptive learning assumption. Specifically, using the baseline framework of Choi and Rocheteau (2021), this paper relaxes their perfect foresight assumption by replacing it with an adaptive learning assumption. I find that, under the adaptive learning assumption, the stability of steady state can be altered. With a high learning gain parameter in the adaptive learning algorithm, a period of doubling bifurcation can occur, which in turn can lead to chaotic regimes or explosive paths. These price dynamics from the model help explain the phenomena of the extreme price volatility in cryptocurrency.

Keywords: Cryptocurrency, Money Search, Expectations, Adaptive Learning, E-Stability

1.1 Introduction

The first cryptocurrency, Bitcoin, was introduced in 2009 and it took about ten years for it to go from an abstract idea to a multibillion-dollar market. Bitcoin started in early 2017 at \$998 [1] and reached \$19,783.06 [2] by December 17, 2017. Meanwhile, the total cryptocurrency market experienced phenomenal growth, rocking from \$18 billion to \$813 billion within 12 months. After this unprecedented boom in the cryptocurrency market, the capitalization collapsed 80% from its peak value back in January 2018, making the 2018 cryptocurrency crash worse than the Dot-com bubble crash. The market's boom and bust cycle and intense price volatility have sparked attention in both investment and academic fields. The market offers no consensus about its value. In academic areas, a growing body of literature has emerged studying this intrinsically worthless fiat money, and presenting with some heated debates.[3] However, few scholars have studied its extreme price volatility, leaving both the value of cryptocurrency and its high price volatility puzzles. The goal of my paper is to shed some light on these puzzles.

Through a New Monetary approach, I investigate a prominent question, which is, "What causes enormous price volatility in cryptocurrency?" Specifically, I study this question using a random matching search model and relax the assumption of rational expectation by introducing an adaptive learning algorithm. Most research papers in the New Monetary search field depend on rational expectation assumption; this assumption is standard and requires agents to have full knowledge of the equilibrium distribution of all economic variables, have complete information about other agents' preference and beliefs, and have unlimited computational power. Market clearing conditions are also assumed in rational expectation.

[1] In this paper, all monetary references are represented in the US dollar.

[2] Data from https://www.coindesk.com/sell-news-bitcoin-price-tests-20k-ahead-cmes-futures-launch

[3] A few Nobel laureates and famous economists are pessimistic about Bitcoin. For example, professor Joseph Stiglitz has described Bitcoin as "a bubble and should be outlawed." Professor Paul Krugman commented on Bitcoin as a bubble wrapped in techno-mysticism inside a cocoon of libertarian ideology.

Although rational expectation assumption can provide some robust results, it seems it is unrealistic and strong.

My paper builds on Choi and Rocheteau (2021) who study the price dynamics of monies that are privately-produced through time-consuming mining technologies under rational expectation. They extended the Lagos-Wright model by adding a time-consuming mining technology and an occupation choice, to show that there exists a unique equilibrium where a positive money value reaches to steady state. Although their model has desirable results, the extreme price volatility in empirical data can not be explained in their rational expectation version of the model. I use bounded rational expectation to explore monetary theory price dynamics. To the best my knowledge, few studies investigate cryptocurrency volatility based on agents' beliefs using the monetary search model, and my paper contributes to this under-explored study using an adaptive learning approach.

1.1.1 Empirical Motivation

From the empirical data, there exists substantial evidence to support that high price volatility is a salient characteristic of cryptocurrency. For example, Bitcoin's 60-day price historical volatility (See Figure (1.1)). The average one-year volatility of cryptocurrency is approximately six times that of gold and about 20 times that of the FOREX USD/EUR. Nobel Laureate Richard Thaler (2018) emphasizes, " The extremely high volatility in Bitcoin's price is due to irrationality." [4]In monetary theoretic studies, whether to assume rational expectation depends on the research question. A rational expectation version of the monetary model is unable to explain such price volatility; therefore, to reveal the cause of price

[4]Richard Thaler (2018) discusses the irrationality in the Bitcoin market that has led to the bubble, demonstrating the irrationality with the example of firms by adding the word " blockchain" to their names had largely increases their stock prices.

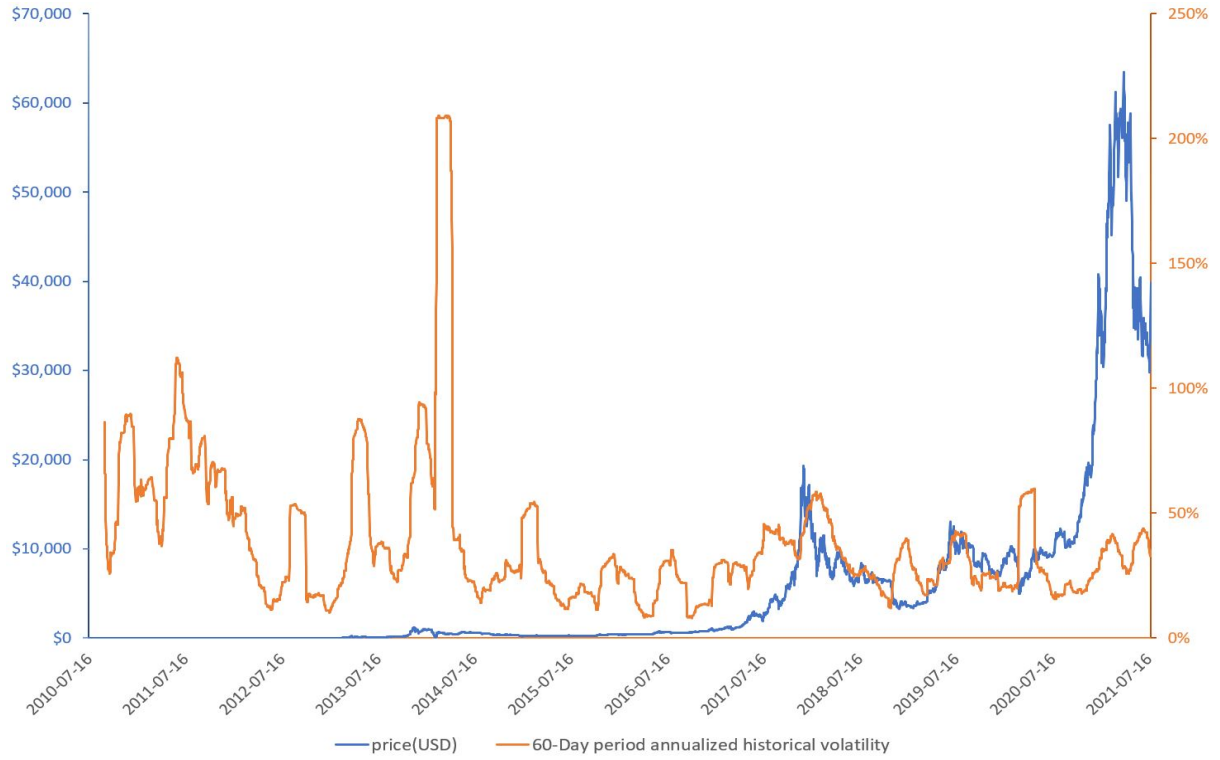

Figure 1.1: Daily Bitcoin Price and Historical Volatility (July 2010 - July 2021)

volatility in cryptocurrency, an alternative expectation assumption is imperative.

I analyze the monetary equilibrium in two settings. In the first setting, I adopt the standard framework from the monetary search literature of Lagos and Wright (2005) as the benchmark approach, in which results multiple equilibria: non-monetary and monetary equilibrium. I use discrete time instead of continuous time in my model. The only money in the economy is cryptocurrency, perfectly divisible, and it plays the role of facilitating trade. On the money supply side, I assume an exogenous supply path and based on the presumed mining technology[5], the numbers of miners required can be determined exogenously. On the money demand side, buyers and sellers have heterogeneous preferences and specialization in pro-

[5]For example, in Bitcoin mining, the block time (the time to mine a block to solve a Proof of Work puzzle) is relatively consistent at about 10 minutes, while in Ethereum with the Proof of Stake (PoS) algorithm, the block time is between 10 and 19 seconds.

duction, which creates a need for money. Buyers and sellers are randomly matched in the model, and the terms of trades are determined by Kalai bargaining. The conditions for the steady state equilibrium in perfect foresight are derived in the benchmark approach.

In the second setting of my paper, I extend the basic framework to bounded rational expectation instead of rational expectation. The expectation formation is influenced by the adaptive learning literature (e.g., Marcet and Sargent (1989); Evans and Honkapohja (2001). In the literature, agents are assumed to maximize their utility, and according to the cognitive consistent principle, agents follow an adaptive learning rule in which they make forecasts, at any given time, in the same way as econometricians do, formulating rules based on the available data and revising forecast over time as new data becomes available. Specifically, there are two main choices for the gain sequence in adaptive learning algorithms: (i) Decreasing-learning-gain algorithm, such as $g_t = \frac{1}{t}$, which is in line with standard recursive least squares algorithms, and (ii) Constant-learning-gain algorithm with $g_t = g$, where $g \in (0, 1)$. The key difference between the two cases is that for the constant-learning-gain algorithm, it is possible to have endogenous fluctuations, as the economy occasionally escapes from the basin of attraction of one steady state to the basin of attraction of another steady state (Evans and Honkapohja (2001)). Furthermore, a point emphasized in Hansen and Sargent (1990) and Sargent (1999) that it is possible in the constant-learning gain case, adaptive learning does not converge to the forecast rule and they can give rise to additional "persistent learning dynamics" not found in an REE. In my model, I use the constant-learning-gain algorithm, where the stability of the steady states is determined by the eigenvalues of the Jacobian matrix refers to Hommes (2013), convergences, chaos or bifurcations can occur.

The novelty of this paper is that I use a simple adaptive learning algorithm to shed light on the intense price volatility in cryptocurrency. The study of adaptive learning provides

a check on the robustness of the equilibrium. In a nutshell, the learning gain in adaptive learning plays a key role in this model, and the stability of price equilibrium can be altered with different learning gains. Adaptive learning offers a way of selecting among multiple equilibria, which can be a puzzle for many rational expectations models. My results show that with a relatively high learning gain in the adaptive learning algorithm, a period doubling bifurcation can occur, which can lead to a chaotic regime or to an explosive path. These dynamics from the model help to explain the phenomena of extreme price volatility in cryptocurrency. My work contributes to the literature on the price volatility of cryptocurrency.

1.1.2 Related Literature

The benchmark model builds on the monetary search-theoretic model of Lagos and Wright (2005), who built a tractable framework to analyze how frictions can impact the role of money as a medium of exchange. They showed that in bilateral trades, buyers and sellers with rational expectation negotiate via Nash bargaining. The Friedman Rule is still optimal, but it does not achieve the first best unless the buyer's bargain power is one. There are two steady states, a monetary and non-monetary steady state. A continuum of perfect foresight path converges from non-monetary steady state to the monetary steady state. I follow the framework of Choi and Rocheteau (2021), who extended the Lagos-Wright model by adding an occupation choice and a time-consuming mining technology. They used continuous time setting, which allows the model to eliminate some chaotic dynamics. They also showed that under perfect foresight, there exists a unique equilibrium where a positive money value reaches to steady state; and on the dynamics equilibrium path, prices can inflate and burst gradually overtime.

The literature on the existence of cycles and non-linear dynamics in monetary models is also well-known, such as Lagos and Wright (2005) and Rocheteau and Wright (2013). Nosal and Rocheteau (2011) have shown periodic cycles or chaos can be generated in a non-linear model. Gu et al. (2013) have shown non-linear perfect foresight dynamics in a model with endogenous debt limits. In essence, the perfect foresight model require a non-monotonic price equation to generate equilibrium dynamics in price.

Expectation plays the essential role for equilibrium stability. The tenuousness of monetary equilibria, originally studied by Wallace (1980), shows that in general, there exists a non-monetary equilibrium where fiat money values zero and a positive monetary equilibrium. Monetary equilibrium can always break down due to self-fulfilling beliefs. There are researchers focus on bounded rational and learning in macroeconomic models. The study of learning includes Bray and Savin (1986), Woodford (1990), Evans and Honkapohja (1999), and Hommes (2013). The adaptive learning rule is in the spirit of Marcet and Sargent (1989) and Evans and Honkapohja (2001), where agents behave like econometricians forming their forecast based on available data and revising their forecast to account for recent data. Under adaptive learning, Branch and McGough (2016) demonstrated that with the endogenous distribution of heterogeneous expectations, the stability can break down; as a result, complex dynamics can be created. There exists extensive literature that incorporates adaptive learning in an OLG model, such as Lucas (1986), Woodford (1990), and Evans and Honkapohja (2001). There are several similarities between the OLG and the monetary search models, however, the environments are different: agents in the monetary search model live forever and match randomly and bargain on trade. Therefore, the market structures are different. Rocheteau and Wright (2005) illustrated that variety of pricing mechanisms have different equilibria and monetary policy effects.

There is a growing literature on cryptocurrency and blockchains. Chiu and Koeppl (2019) used a search model to study the optimal design of a cryptocurrency protocol. Garratt and Wallace (2018) studied in an OLG setting, the competition and indeterminacy of exchange rates between cryptocurrencies and central bank currencies. In a model of an infinite horizon, Schilling and Uhlig (2019) discussed equilibrium where agents hold the cryptocurrency for appreciation purpose but not for payments. Pagnotta and Buraschi (2018) used a strategic oligopolistic game to model how miners incorporate the probability of earning mining rewards to their investment. Biais et al. (2019) formally analyzed the proof-of-work protocol as a dynamic coordination game for miners and showed the existence conditions required for an equilibrium path. Glaser et al. (2014) discussed how media coverage and sentiment impact Bitcoin's price volatility.

1.2 Economic Environment

This model builds on Lagos and Wright (2005). Time is discrete, extends forever and is indexed by $t \in N$. Each period is divided into two sub-stages, a decentralized market (DM) stage followed by a centralized market (CM) stage, in which different economic activities take place. There is a continuum of infinitely lived identical agents. There are two categories of goods: DM goods and CM goods. Agents can not consume their own produced DM good, but are able to produce a variety of DM goods that other agents can consume, which creates a need for trade. Money is perfectly divisible and storable, and the price of fiat money (in terms of the numeraire) is ϕ. Agents discount between the second stage CM and the following day DM at the rate of $r = \frac{1}{\beta} - 1$, where $\beta \in (0, 1)$.

There is a unit measure of agents in the model and each agent is a potential buyer with

the assumption that he can not consume his own goods in the DM and his initial money holding is $a_0 > 0$. At time t, there is a pool of m_t measure of miners who work on solving the Proof-of-Work (PoW) blockchain and the rest $1 - m_t$ measure of agents who work on producing goods. In addition, m_t is assumed as an exogenous variable, and an agent can be either a miner or a producer, but not both. In the DM, the random bilateral meetings and matching take place. The matching technology in the DM is described as follows. Let $\alpha(\cdot)$ be the matching function. As in the standard condition, $\alpha' > 0$, $\alpha'' \leq 0$. Let τ denote the market tightness, seller per buyer, thus $\tau = 1 - m_t$. The single coincidence that one agent likes the other's production DM goods is given by σ. As a result, the probability of matching a seller for each buyer is $\alpha(\tau)\sigma$, and for each seller, the probability of matching a buyer is $[\alpha(\tau)/\tau]\sigma$. Agents are anonymous and can not commit, as a result, no credit is available in this economy. The model also assumes no double-coincidence-of-wants matches, and all goods are non-storable and can not be transferred to later. To overcome all these frictions and to facilitate the trades, the miners create a medium of exchange called cryptocurrency.

Cryptocurrency is the only money in this model and is mined in the DM. Let $\tilde{a}_t$ be the supply of cryptocurrency at any time t and $\bar{A}$ be the total cap of money supply. Let $\tilde{d}_t$ denote the amount of new mined cryptocurrency during each period t and therefore $\tilde{d}_t = \tilde{a}_{t+1} - \tilde{a}_t$. Money supply is assumed to follow an exogenous path and the growth of production is designed to gradually decrease. For example, the total limit of Bitcoin is 21 million, the time to solve a proof-of-work (PoW) and validate one block is approximately 10 minutes and the reward per block is gradually reduced [6] [7]. One of the properties in cryptocurrency is that

[6]The number of Bitcoins rewarded per block is created to be reduced every four years, starting from 50 coins per block, halved to 25 coins, and currently miners have been receiving 12.5 Bitcoins for each block successfully processed.

[7]In another example, the block reward on Ethereum blockchain also has a decreasing algorithm. Initially, the block reward was 5 ETH per block in 2016 and was reduced to 3 ETH, then to 2 ETH after the Constantinople hard fork in 2019. This reduction from 3 ETH to 2 ETH is a -33% adjustment, hence also called "Thirdening".

successful miners receive the network's native tokens [8]. Incentives are paid to the first solver of the puzzle, either a single miner or a pool of miners, for which each miner receives a fraction of the total reward. Let $\frac{\tilde{d}_t}{m_t} = \Lambda$ be the average number of tokens rewarded to each miner, and for simplicity, Λ is assumed as constant.

The Centralized Market (CM) is a Walrasian market, in which all agents can produce or consume general goods. Buyers and sellers can re-balance their asset portfolios. The linearity of the utility and cost functions ensures that agents have the same money holdings at the end of the CM eliminating wealth effects.

An agent's preference is given by,

$$\mathcal{U}(\mathrm{x}, \mathrm{y}, \mathrm{X}, \mathrm{h}) = \mathrm{u}(\mathrm{x}) - \mathrm{c}(\mathrm{y}) + \mathrm{U}(\mathrm{X}) - \mathrm{h} \tag{1.1}$$

where x is the specialized consumption goods, y is the production goods in the DM, X and h are consumption and production labor of the general goods in the CM.[9] In general, x and y both depend on the money holdings of buyers and sellers. Later, I will use the numeraire good q to represent these DM goods. Let $u(\cdot)$ and $U(\cdot)$ be the utility functions in the DM and CM, respectively, and assume $u(0) = c(0) = 0$, $u' > 0$,$c' > 0$, $u'(0) = +\infty$, $u'' < 0$, $c'' \geq 0$, and $U' = 1$. There exists a $\bar{q}$, such that $u(\bar{q}) = \bar{q}$ and $\bar{q} < +\infty$.

The timing of this model is as follows (also see Figure (1.2)). Before the beginning of the first sub-period DM opens, based on the available information $\{\phi_i\}_{i=0}^{t-1}$, agents form their pre-determined expectations, (rational expectation in the benchmark model and adaptive

[8]There are different types of incentives in crypto blockchain mining: the native tokens, transaction fees, different form of tokens, privilege, and so forth.

[9]Refer to Lagos and Wright (2005), who comment on this: "although separability is not critical and is made merely to ease the presentation."

learning expectation in section 4). In the DM, agents are matched with the match function τ and the single coincidence σ, then Kalai bargaining follows. Trade price is based on the expected value of money ϕ_t^e formed at the beginning of this period and trades take place at the end of the DM. Agents then enter into the second sub-period CM observing the realized value ϕ_t. Based on the formed expectation ϕ_{t+1}^e at the beginning of this period, agents need to re-balance their money holdings by trading the general goods in the CM. Between closing the CM and the next day opening the DM, agents need to update their forecasts for ϕ_{t+1}^e and ϕ_{t+2}^e as the price ϕ_t is revealed in the CM. Note that, agents only update their forecast once at the end of each CM. Timing is an important assumption in the learning literature and change of the timing assumptions, such as price revelation and forecast updating, can cause variations of results.

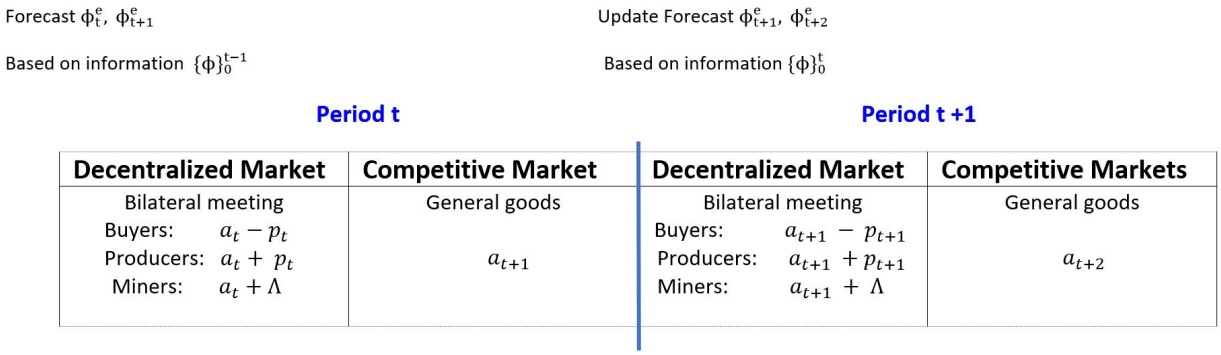

Figure 1.2: DM-CM

1.3 Equilibrium

1.3.1 Centralized market (CM) Bellman Equation

Agents enter the second sub-stage CM with a_t unit of money with price ϕ_t. A buyer from the first sub-stage DM would use labor to produce CM goods to increase his asset holdings, and

a producer or miner would purchase CM goods to reduce his asset holdings. By assuming that both the production cost and the utility function of CM goods are linear, the wealth effect is eliminated, and all agents readjust their asset holdings to leave CM stage with the same units of money, a_{t+1}.

Let $W_t(a_t, \phi_t)$ denote the value function for an agent, who holds $a_t \in \mathbb{R}_+$ unit of money at the beginning of the CM in the period time t.

$$W_t(a_t, \phi_t) = \max_{X_t, h_t, a_{t+1}} \{U(X_t) - h_t + \beta V^e_{t+1}(a_{t+1}, \phi_{t+1})\} \tag{1.2}$$

$$\text{s.t. } a_t\phi_t + h_t = a_{t+1}\phi_t + X_t \tag{1.3}$$

where ϕ_t is the value of cryptocurrency, $a_t\phi_t$ represents the real balance, and V^e_{t+1} is the expected value of DM for the period t+1.

1.3.2 Decentralized market (DM) Bellman Equations

The producer's DM value function,

$$\begin{aligned} V^p_t(a_t, \phi_t) = \alpha(\tau)\sigma\Big\{u[q(a_t, \phi_t)] + W^e_t[a_t - p(a_t, \phi_t)]\Big\} \\ + \frac{\alpha(\tau)}{\tau}\sigma\Big\{ - c[q(\tilde{a_t}, \phi_t)] + W^e_t[a_t + p(\tilde{a_t}, \phi_t)]\Big\} + \Big[1 - \alpha(\tau)\sigma - \frac{\alpha(\tau)}{\tau}\sigma\Big]W^e_t(a_t, \phi_t) \end{aligned} \tag{1.4}$$

Note, $\tilde{a_t}$ appears in the second term, which represents the number of tokens held by other agents, who can buy goods from the producer. The reason why it is $\tilde{a_t}$, but is not a is due

to there being no credit in this economy, therefore, the trade payment is essentially limited by the buyer's assets, not the seller's. I use $\tilde{a_t}$ to represent that it is the other agents' assets, which are not controlled by the producer.

The value function for a producer in the DM has three components. The first term on the right hand-side represents that anyone who holds asset a can potentially be a buyer as long as he does not run into a miner. Therefore, the probability of being a buyer is $\alpha(\tau)\sigma$. The terms of the trade (q, p) means that a buyer pays p unit of money for q units of DM goods. The second term is that a producer with a probability of $\frac{\alpha(\tau)}{\tau}\sigma$ to meet a buyer chooses to produce goods, costing $c(q)$ but earning p. The last term means that an agent chooses to be a producer, however, he does not meet a trading partner so trades do not occur; consequently, he ends up with the same asset a with which he entered the DM..

The miner's DM value function,

$$V_t^m(a_t, \phi_t) = \alpha(\tau)\sigma\Bigg\{u[q(a_t, \phi_t)] + W_t^e\Big([a_t - p(a_t, \phi_t) + \Lambda], \phi_t\Big)\Bigg\} + [1 - \alpha(\tau)\sigma]\Bigg[W_t^e\Big((a_t + \Lambda), \phi_t\Big)\Bigg] \tag{1.5}$$

where Λ is the average number of new coins rewarded to each miner.

The value function equation (1.5) for a miner in the DM can be broken down into two components: matched with a trade partner, thus trade; and not matched with any trade partner. The first term on the right-hand-side represents that a miner, holding asset a, is matched with a trade partner; consequently, he becomes a buyer while at the same time he engages in the mining activity. Therefore, with a probability $\alpha(\tau)\sigma$, he can trade with the term (q, p), spending p units of money, consuming goods, enjoying the utility of $u(q)$. He also knows

that success in mining is not guaranteed, but on average each miner is expected to get Λ units of new coins. The second term simply means when a miner is not matched with a trade partner, he engages in mining only and acquires the reward of Λ without consuming any goods in the DM.

Using the linearity of $W(\cdot)$, simplify function (1.4) and (1.5),

$$V_t^p(a_t,\phi_t) = \alpha(\tau)\sigma\Big\{u[q(a_t,\phi_t)] - p(a_t,\phi_t)\phi_t\Big\} + \sigma\frac{\alpha(\tau)}{\tau}\Big\{-c[q(\tilde{a_t},\phi_t)] + p(\tilde{a_t},\phi_t)\phi_t\Big\} + a_t\phi_t \tag{1.6}$$

$$V_t^m(a_t,\phi_t) = \alpha(\tau)\sigma\Big\{u[q(a_t,\phi_t)] - p(a_t,\phi_t)\phi_t\Big\} + \phi_t\Lambda + a_t\phi_t \tag{1.7}$$

Therefore, at the beginning of the CM the agent's maximum problem is,

$$W_t(a_t,\phi_t) = \max_{X_t,h_t,a_{t+1}}\{U(X_t) - h_t + \beta V_{t+1}^e(a_{t+1},\phi_{t+1})\} \tag{1.8}$$

$$\text{s.t.} \quad a_t\phi_t + h_t = a_{t+1}\phi_t + X_t \tag{1.9}$$

$$V_{t+1}^e(a_{t+1},\phi_{t+1}) = p_{t+1}^m V_{t+1}^m(a_{t+1},\phi_{t+1}^e) + (1-p_{t+1}^m)V_{t+1}^p(a_{t+1},\phi_{t+1}^e) \tag{1.10}$$

where p_{t+1}^m is the probability of an agent to be a miner at time $t+1$. Note, since the total population is a unit, m_t is exogenous and agents have the information of the m_t path, $p_{t+1}^m = m_{t+1}$. [10]

Agents' maximum problem for either miners or producers is the same, and it is simplified as

[10] I want to emphasize the fact that even if the probabilities are unknown, a_{t+1} does not depend on the probabilities. See Appendix A

below. (Details are illustrated in Appendix A.)

$$\max_{a_{t+1}} \left\{ -(\frac{\phi_t}{\beta\phi^e_{t+1}} - 1)\ a_{t+1}\phi^e_{t+1} \ + \ \alpha(\tau)\sigma\{u[q(a_{t+1})] - p(a_{t+1})\phi^e_{t+1}\} \right\} \tag{1.11}$$

It is obvious that from (1.11) the choice of the next period asset holdings a_{t+1} is independent of the current assets a_t. If $V^e_{t+1}(a_{t+1})$ is strictly concave, there is a unique solution to maximize the current value of $W_t(a_t, \phi_t)$. Therefore, in equilibrium when forward-looking agents make decisions for tomorrow, regardless of their occupations and the current asset holdings, miners and producers choose to hold the same assets a_{t+1} at the end of CM.

1.3.3 Kalai Bargaining

The terms of the bilateral trade, quantity, and payment (q, p) in the DM are determined according to the Kalai (1977) proportional bargaining rule. Buyers' and sellers' bargain power is assumed as θ and $1-\theta$, respectively, where $\theta \in [0, 1)$.[11]

The buyer's problem is,

$$\max_{q\geq 0, p\leq a} \quad \left\{ u(q) + W^e_t[a-p] - W^e_t(a) \right\} \quad \text{s.t.} \quad (1-\theta)\left[u(q) - p\phi^e_t \right] = \theta\left[-c(q) + p\phi^e_t \right] \tag{1.12}$$

From (1.12), Kalai proportional bargaining rule specifies a constant fraction of the total social surplus split between buyers and sellers based on their bargain power. During the bargaining process, both sides have common knowledge and same expectation of ϕ^e_t.

[11] Kalai Bargaining has several desired features that can not be achieved in Nash Bargaining, as discussed in Aruoba et al. (2007). I do not assume take-it-or-leave-it offer from buyers, because sellers would have no incentive to produce, there will be no trade at all, and all agents choose to mine.

As a result, output of the production q solves the buyers' problem,

$$q \in \arg\max \theta\Big\{u(q) - c(q)\Big\} \quad \text{s.t.} \quad p\phi_t^e \equiv (1-\theta)u(q) + \theta c(q) \leq a\phi_t^e \tag{1.13}$$

The bargain simply says, when $a \geq p*$, in an abundance liquidity economy, q^* is simply the first best solution to $p^*\phi_t^e = (1-\theta)u(q^*) + \theta c(q^*)$, and agents will bring the right amount of a to purchase the first best q^*. In a scarce economy, $a < p(q^*)$, buyers will spend all of their assets that they bring into the DM, therefore, q is the solution to $a\phi_t^e = (1-\theta)u(q) + \theta c(q)$. Consequently,

$$p \ = \min\Big\{\frac{(1-\theta)u(q^*) + \theta c(q^*)}{\phi_t^e}, a\Big\} \tag{1.14}$$

Similarly, the sellers' problem is as follows,

$$q \in \arg\max(1-\theta)\Big\{u(q) - c(q)\Big\} \quad \text{s.t.} \quad p\phi_t^e \equiv (1-\theta)u(q) + \theta c(q) \leq a\phi_t^e \tag{1.15}$$

1.3.4 Mining - Money Supply

The growth of money supply in the economy is exogenous,

$$\tilde{a}_{t+1} - \tilde{a}_t = \lambda(\bar{A} - \tilde{a}_t) \tag{1.16}$$

Where $\tilde{a}_{t+1} - \tilde{a}_t$ represents the number of new cryptocurrency that is minted during the period of t. On the right side of the equation (1.16), $\bar{A}$ is the total limited supply, and the amount of cryptocurrency left to mine is $(\bar{A} - \tilde{a}_t)$ at any given time t accordingly. The

parameter λ can be understood as a parsimonious representation of mining speed. Thus, the dynamics of the money supply path is exogenous with a decreasing growth rate. This decreasing-rate algorithm is chosen because it keeps the inflation rate low while also mimicking Bitcoin and gold growth.

In addition, as explained in the environment, the mining technology can be assumed as,

$$m_t\Lambda = \tilde{a}_{t+1} - \tilde{a}_t \tag{1.17}$$

where Λ is the average reward for each miner and is assumed as constant.

This equation implies that at any given time the total reward to miners, $m_t\Lambda$, equates the total of new minted coins. For example, one property of Bitcoin is that the network's native token is rewarded either to the first miner who discovers the solution or to a pool of miners, in which each miner receives a fraction of the total reward. On average, $\frac{\tilde{a}_{t+1}-\tilde{a}_t}{m_t} = \Lambda$ units of incentives are rewarded to each miner for investing his time and equipment.

Now, combining (1.16) and (1.17), the supply of money follows the rule below,

$$m_t\Lambda = \lambda(\bar{A} - \tilde{a}_t) \tag{1.18}$$

1.3.5 Equilibrium Definition

Definition 1 *Given the initial money a_0 and the expectation $\phi^e_{t=1}$, an equilibrium is a list of measure of miners $\{m_t\}^{\infty}_{t=0}$, money demand $\{a_t\}^{\infty}_{t=1}$, money supply $\{\tilde{a}_t\}^{\infty}_{t=0}$, money values$\{\phi_t\}^{\infty}_{t=0}$ and money value expectations$\{\phi^e_{t+1}\}^{\infty}_{t=1}$ and terms of trade $\{q_t, p_t\}^{\infty}_{t=0}$, such that,*

1. $\{q_t, p_t\}_{t=0}^{\infty}$, *solves the bargaining problem (1.13)(1.15).*

2. *Given* a_0, $\{m_t\}_{t=0}^{\infty}$, $\{\tilde{a}_t\}_{t=0}^{\infty}$ *and* $\{a_t\}_{t=1}^{\infty}$ *solve the money growth equation* (1.18).

3. *Given* a_0 and $\phi_{t=1}^e$, $\{\phi_t\}_{t=0}^{\infty}$ and $\{\phi_{t+1}^e\}_{t=1}^{\infty}$ *solve the first difference equation (1.22)* .

4. *Market clearing,* $a_t = \tilde{a}_t$.

Taking the F.O.C of (1.11) with respect to a_{t+1}, and recall that the matching function is $\alpha(\tau)$, the solution to the buyer's problem is,

$$-\{\frac{\phi_t}{\beta\phi_{t+1}^e}-1\}\phi_{t+1}^e+\alpha(1-m_{t+1})\sigma\theta\Big[u'(q_{t+1}(a_{t+1},\phi_{t+1}^e))-c'(q_{t+1}(a_{t+1},\phi_{t+1}^e))\Big]\frac{\partial q_{t+1}(a_{t+1},\phi_{t+1}^e)}{\partial a_{t+1}}=0 \tag{1.19}$$

then, from (1.13), the marginal benefit of holding one extra unit of numeraire asset gives,

$$\frac{\partial q(a,\phi)}{\partial a}=\frac{\phi}{(1-\theta)u'(q)+\theta c'(q)} \tag{1.20}$$

thus, divided by ϕ_{t+1}^e on both sides (1.19) becomes,

$$\phi_t=\beta\phi_{t+1}^e\left\{1+\ \alpha(1-m_{t+1})\sigma\theta\frac{u'(q_{t+1}(a_{t+1},\phi_{t+1}^e))-c'(q_{t+1}(a_{t+1},\phi_{t+1}^e))}{(1-\theta)u'(q_{t+1}(a_{t+1},\phi_{t+1}^e))+\theta c'(q_{t+1}(a_{t+1},\phi_{t+1}^e))}\right\} \tag{1.21}$$

In equilibrium, market is clear $a_t = \tilde{a}_t$ and money supply is exogenous and given, therefore (1.21) can also be rewritten as follows,

$$\phi_t=\beta\phi_{t+1}^e\left\{1+\ \alpha(1-m_{t+1})\sigma\theta\frac{u'(q_{t+1}(\tilde{a}_{t+1},\phi_{t+1}^e))-c'(q_{t+1}(\tilde{a}_{t+1},\phi_{t+1}^e))}{(1-\theta)u'(q_{t+1}(\tilde{a}_{t+1},\phi_{t+1}^e))+\theta c'(\tilde{a}_{t+1},q_{t+1}(\phi_{t+1}^e))}\right\} \tag{1.22}$$

$$\equiv F(\tilde{a}_{t+1},\phi_{t+1}^e) \tag{1.23}$$

The price of money today equals the discounted expected price of money tomorrow plus a liquidity premium. The liquidity premium is as following,

$$\beta\phi^e_{t+1}\alpha(1-m_{t+1})\sigma\theta\frac{u'(q_{t+1}(a_{t+1},\phi^e_{t+1}))-c'(q_{t+1}(a_{t+1},\phi^e_{t+1}))}{(1-\theta)u'(q_{t+1})+\theta c'(q_{t+1})}\geq 0 \tag{1.24}$$

which is the expected benefit of bringing one extra unit of numeraire asset into DM.

Now, let us look at the aggregate level on the demand side. Let $A^d(\phi_t)$ be the aggregate money demand for the whole population. There are two cases, and they can be expressed as follows,

$$A^d(\phi^e_{t+1}) = \Big[\frac{(1-\theta)u(q^*)+\theta c(q^*)}{\phi^e_{t+1}}, \bar{A}\Big] \qquad if \quad \phi_t = \beta\phi^e_{t+1} \tag{1.25}$$

$$= \{a_{t+1}\} \text{ where } a_{t+1} \text{ solves (1.22)} \qquad if \quad \phi_t > \beta\phi^e_{t+1} \tag{1.26}$$

If buyers expect that money is too costly to hold, they will bring just enough money to spend in the CM. As a result, $p_{t+1} = a_{t+1}$. If buyers expect that money is cost-less to hold, $\frac{\phi_t}{\phi^e_{t+1}} = \beta$, buyers will bring enough money in order to purchase q^* units of goods in the CM and maximize the match surplus, thus any amount of $a_{t+1}\phi_{t+1} \geq (1-\theta)u(q^*)+\theta c(q^*)$ is a solution to the demand side. In this paper, I focus on the price paths for the case of $\frac{\phi_t}{\phi^e_{t+1}} > \beta$, so that I can use F.O.C to determine the money demand. While the closed form solution does not exist in general, simulation can be used to solve money demand function.

Here I do not impose an initial condition ϕ_0, because the dynamics of equation (1.21) are forward looking, and the price of the money is not determined by the past; instead, it entirely depends on the future. In other words, ϕ_0 is an endogenous variable. I will discuss the expectation in the next section.

1.3.5.1 Perfect Foresight Equilibria

If agents hold perfect foresight beliefs, $\phi_{t+1} = \phi^e_{t+1}$ (rational expectations), a non-explosive equilibrium is a sequence $\{\phi_t\}$ that satisfies the equilibrium condition, $\phi_t \equiv F(\phi^e_{t+1})$, where $F(\cdot)$ is a non-linear function, whose shape depends on the specific property of utility, cost function and the value of the parameters. Thus, equilibria can take different forms, such as steady states, cycle or sunspot which depends on the initial conditions, the specific shape of $F(\cdot)$ and beliefs.

In a rational expectation steady state, money demand and supply are constant over time, $a = \tilde{a}$; there is no mining, $m = 0$; and $\phi_t = \phi^e_{t+1} = \phi^{ss}$. There are two types of steady state equilibrium: autarky equilibrium, where money has no value, $\phi^{ss} = 0$, and a positive value monetary steady state equilibrium with $\phi^{ss} > 0$.

1.3.5.2 Autarky Equilibrium

Here I briefly discuss autarky equilibrium under rational expectation. Generally, an autarky equilibrium steady state is an equilibrium where money has no value, $\phi_t = \phi_{t+1} = \phi^{ss} = 0$, money demand and supply are all zero, $a = \tilde{a} = 0$ and trade would not take place. In this model, in addition to money, the number of miners is also zero, $m = 0$. The intuition is clear: no miners would choose to mine when cryptocurrency is worth nothing, resulting in no agent wanting to hold cryptocurrency and no trade happening. In short, no cryptocurrency exists in this economy. This implies that the value of the very first coin of cryptocurrency must be traded at more than zero, otherwise, cryptocurrency will not exist.

1.3.5.3 Monetary Equilibrium

The money market equilibrium (and so equilibrium price ϕ_t) depends on agents' *ex-ante* expectation of tomorrow's price, and agents will based on the information available at that time to choose to hold money in the centralized market.

Proposition 1 (*Steady-state Monetary Equilibrium) Under perfect foresight (rational expectation) assumption, the existence of a monetary equilibrium requires agents to be sufficiently patient that* $r < \frac{\sigma\theta}{(1-\theta)}$.

This is consistent with the standard "folk theorem" in monetary theory. The intuition is that when r is very small, agents have ample patience; consequently, as long as the steady-state supply has not been reached, all agents would like to mine continuously if the occupation condition is satisfied. This will gradually lead to a monetary equilibrium steady state. Rational expectation says that tomorrow's price is the same as the expected price based on all available information at t, $\phi^e_{t+1} = \phi_{t+1}$, as shown in the (1.22), the ϕ^{ss} can be solved by the following,

$$\sigma\theta \frac{u'(\phi^{ss}) - c'(\phi^{ss})}{(1-\theta)u'(\phi^{ss}) + \theta c'(\phi^{ss})} = r \tag{1.27}$$

where $\phi^{ss} > 0$ and $r = \frac{1}{\beta} - 1$.

Specifically, when utility and cost functions are assumed, the unique monetary equilibrium steady state can be solved by the following. Assume $c'(\cdot) = 1$, (1.22) becomes,

$$\sigma\theta\frac{u'(q^{ss})-1}{(1-\theta)u'(q^{ss})+\theta}=r \tag{1.28}$$

In the steady state, holding a real balance is costly $\frac{\phi_t}{\phi_{t+1}}=1>\beta$. Agents will bring only enough assets that they expect to spend on q^* unit of goods in the CM. The maximization problem requires $u'(q^*)=c'(q^*)$, and the concave assumption gives, $u'(\cdot)>0$.
So it requires,

$$u'(q^{ss})=\frac{\sigma\theta+\sigma r}{\sigma\theta+\sigma r-r}>0 \tag{1.29}$$

Therefore, it requires $\frac{\alpha\sigma}{1-\sigma}>r$ to have a positive solution of q^{ss}, i.e., the existence of a monetary equilibrium requires agents to be sufficiently patient $\frac{\alpha\sigma}{1-\sigma}>r$. For example, assuming $c(q)=q$, and $c'(q^*)=1$, it is straightforward that when $\frac{\alpha\sigma}{1-\sigma}>r$, $\frac{\sigma\theta+\sigma r}{\sigma\theta+\sigma r-r}=u'(q^{ss})>u'(q^*)=1$, thus, the level of trade and output in a steady state are less than that of social optimal, $q^{ss}<q^*$.

1.3.6 General Equilibrium Dynamics

Now, let us look at the transitional dynamic equilibria. Given $\tilde{a}_0$ and ϕ_1^e, the sequences $\{\phi_t,\ \phi_{t+1}^e,\ q_t,\ p_t,\ a_t,\ a_{t+1},\ \tilde{a}_t,\ \tilde{a}_{t+1},\ m_t\}$ are the equilibria solutions to the system of equations (1.13) or (1.15)(1.18)(1.22) and the market clearing condition $a_t=\tilde{a}_t$. Notice the number of variables are more than the number of equations. Thus, although closed form solutions might not exist in general, non-zero equilibrium solutions do exist under some restrictions, and I show the equilibrium path by simulation.

The equilibrium path is time consistent, so without loss of generality, I characterize all mone-

tary dynamic equilibria starting with the lowest initial condition that cryptocurrency supply is zero, $\tilde{a}_0 = 0$. At any time t, $\tilde{a}_t$ on the equilibrium path is the same as starting from $\tilde{a}_0 = 0$ on the path reaching to $\tilde{a}_t$. When the initial cryptocurrency supply $\tilde{a}_0 = 0$, demand $a_0 = 0$, and therefore cryptocurrency worth nothing $\phi_0 = 0$. As a result, miners m, and goods q in the steady states are also zeros. This is the so-called non-Monetary stationary equilibrium. When new cryptocurrency is expected to be issued at a positive value $\phi^e_{t+1} > 0$, miners will choose to mine on the condition that the value of the mining occupation is greater than or equal to producing goods ($\Delta(\tilde{a}_t) \leq 0$). Hence, the result of the equilibrium values of the cryptocurrency is a nonempty, left-closed interval.

Let me derive the process of solving for the monetary equilibrium in general equilibrium. The money supply is exogenous, at each time period, the new cryptocurrency, $\tilde{a}_{t+1} - \tilde{a}_t$, is created according to the transition function (1.16) and the number of miners m_t is determined by the mining technology (1.18), which depends on how much is left to mine ($\bar{A} - \tilde{a}_t$). Therefore, the matching function $\alpha(1 - m_t)$ on that account is also determined exogenously. On the demand side, agents have perfect foresight ϕ^e_{t+1} and choose to bring the optimal a_{t+1} units of money to the next day. In equilibrium, market clearing $\tilde{a}_{t+1} = a_{t+1}$, thus, the equation (1.21) changes to below, which is not a function of a_{t+1}, but a function of $\tilde{a}_{t+1}$.

$$\phi_t = \beta\phi^e_{t+1}\left\{1 + \alpha(1-m_{t+1})\sigma\theta\frac{u'\big(q_{t+1}(\tilde{a}_{t+1},\phi^e_{t+1})\big) - c'\big(q_{t+1}(\tilde{a}_{t+1},\phi^e_{t+1})\big)}{(1-\theta)u'\big(q_{t+1}(\tilde{a}_{t+1},\phi^e_{t+1})\big) + \theta c'\big(q_{t+1}(\tilde{a}_{t+1},\phi^e_{t+1})\big)}\right\} \quad (1.30)$$

One thing to note is the causality intuition in the general equilibrium. On the demand side, agents take the price as given, using the F.O.C to determine the demand for liquidity a_{t+1}, and the causality is that knowing the price determines the demand. However, on the supply side, at any given time the money supply is exogenous, and the equilibrium prices are the results, which are determined endogenously based on the money supply. The causality

is that the quantity of the money supply determines the equilibrium price. Therefore, in general equilibrium, the solutions of the money supply $\tilde{a}_{t+1}$, demand a_{t+1}, and prices ϕ_t are determined simultaneously at any time. As mentioned it is possible to numerically solve for the system of equations and the solution depends on the initial values.

There are three cases to analyze the equilibrium solutions.

1. Money supply is abundant and it can satisfy the optimal solution q^* for all time t.

2. Money supply is scarce, and agents bring whatever available to the next period, the equilibrium solution is that $\tilde{a}_{t+1} = p_{t+1} \leq p*_{t+1}$ and $q_{t+1} \leq q^*_{t+1}$.

3. Money supply can be scarce in the beginning then it can become abundant or vice versa. The state of scarcity or abundance of the money supply relative to money demand can change along the equilibrium path, because ϕ_{t+1} and a_{t+1} together determine the bargaining budget, and both are endogenous variables.

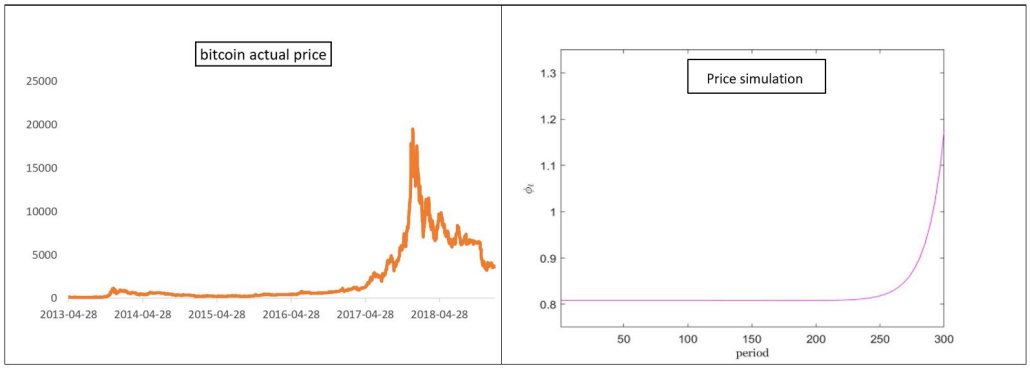

Figure 1.3: Simulation vs. Actual

Figure (1.3) shows the actual Bitcoin prices (2013-2019) vs. a simulation of the price equilibrium path. As shown in two figures, the prices movements are similar before the Bitcoin crash in January 2018. Intuitively, the value of money must appreciate over time to induce agents to mine because more money in circulation leads to mining speed decreases, therefore,

miners require higher value of the money to be compensated. Mining speed and scarcity of money left to mine is the main reasons that prices rise.

Perfect foresight, $\phi^e_{t+1} = \phi_{t+1}$, assumes that agents have full knowledge of the equilibrium distribution of all economic variables and unlimited computational power, know other agents' preference and beliefs, and also assumes market clearing conditions. Although rational expectation can bring desirable results, it seems unrealistic. In addition, once the agents' foresight changes, the equilibrium path can be altered and the steady states can be broken down at any time due to self-fulfilling beliefs, therefore, the monetary steady state is tenuous and not always "stable". I follow the definition of local stability for rational expectation of Van Zandt and Lettau (2003). They applied the usual definition of stability, however, its interpretation is no longer "robustness to small perturbations" but "indeterminacy", because the concept of "robustness to small perturbations" is inconsistent with rational expectations. Their definition of local stability is that for each neighborhood of the steady state, there is an open set of equilibria, for which the equilibrium path does not leave this neighborhood and the equilibrium path converges to the steady state ϕ^{ss}.

Empirically, the boom-and-bust features of cryptocurrency's price can be reviewed as triggered by optimistic or pessimistic self-fulfilling beliefs. A shift in expectation can lead agents to change trade contracts and consumption, then the realized price will reinforce future expectations. During this process, extreme price volatility can arise. This phenomenon can not be explained in the canonical rational expectation version of the model. In the following sections, I discuss replacing the rational expectation assumption with a learning mechanism expectation which will add more benefit generating price volatility and better explain the data.

1.4 Adaptive Learning

The rest of the paper models adaptive learning expectations by assuming forward-looking agents who act like econometricians and form beliefs to forecast prices. Agents use the "adaptive learning forecast rule" by which, agents extrapolate historical data, forecast prices and adjust forecast prices when new data becomes available. As Evans and Honkapohja (2001) explained, this belief structure has self-referential properties and can generate extremely volatile prices. The logic is that the forecast of tomorrow's price affects the current market price, and once the new current price is realized and observed, agents update their beliefs and the parameters in the forecast model; this in return will affect the next round of the current price. Therefore, in this environment, greater volatility can be generated as a response to economic change due to the self-referential property.

1.4.1 Learning rule

First, I begin to assume agents have a basic Perceived Law of Motion (PLM). The following equation illustrates how PLM works,

$$\hat{b}_t = \hat{b}_{t-1} + g_{t-1}(\phi_{t-1} - \hat{b}_{t-1}) \tag{1.31}$$

where $\hat{b}_t = \phi_t^e$ and g is the weight put on the forecast error $\phi_{t-1} - \hat{b}_{t-1}$.

In the literature, there are two ways to model the weight or learning gain g, either constant $g_t = g$ or decreasing $g_t = 1/t$. The intuition of the decreasing learning gain is that agents mainly focus on the most recent economics structure. The key difference between the two ways is that for the constant-learning-gain algorithm in stochastic models, it is possible to have endogenous fluctuations, as the economy occasionally escapes from the basin of at-

traction of one steady state to the basin of attraction of another steady state (Evans and Honkapohja (2001)). For simplicity, I also assume at time t $\phi^e_{t+1} = \phi^e_t$, which interpreted as tomorrow's expected price is the same as today's expected price. As explained in the Economic Environment section, agents only update their forecasts ϕ^e_{t+1} once during one period of time (including two sub-stages DM and CM), $\phi^e_{t+1} = \phi^e_t$ is the simplest way to forecast future $t+1$ at the beginning of period t, and ϕ^e_{t+1} will be updated at the beginning of the next day, period $t+1$, but when tomorrow arrives, the notation will be automatically changed to ϕ^e_t.

Using (1.22), PLM becomes the actual law of motion (ALM),

$$\phi_t = \beta\hat{b}_t\left\{1 + \ \alpha(1-m_{t+1})\sigma\theta\frac{u'(\hat{b}_t) - c'(\hat{b}_t)}{(1-\theta)u'(\hat{b}_t) + \theta c'(\hat{b}_t)}\right\} \equiv F(\hat{b}) \tag{1.32}$$

1.4.2 E-Stability

Following Evans and Honkapohja (2001), the condition of stability of the REE under adaptive learning requires that the parameter slowly adjusts from mapping of the PLM to ALM.

Under Learning and the assumption of forecast (1.31), when the algorithm has sufficiently small constant gain $g_t = g$ or decreasing gain, there exits a continuum of equilibria b converging to ϕ^{ss}, and ϕ^{ss} is locally stable, if and only if $|1+g[F'(b)-1]| < 1$, i.e iff $F'(b) \in (-\frac{2}{g}+1, 1)$. The derivative of $F(b)$ at the steady state is,

$$\begin{aligned} F'(b) =&\beta\Big\{1 + \sigma\theta\Big[\frac{u'(q^{ss}) - c'(q^{ss})}{(1-\theta)u'(q^{ss}) + \theta c'(q^{ss})}\phi^{ss} \\ &\frac{[u''(q^{ss}) - c''(q^{ss})][(1-\theta)u'(q^{ss}) + \theta c'(q^{ss})] - [u'(q^{ss}) - c'(q^{ss})][(1-\theta)u'(q^{ss}) + \theta c'(q^{ss})]}{[(1-\theta)u''(q^{ss}) + \theta c''(q^{ss})]^2}\Big]\Big\} \end{aligned} \tag{1.33}$$

Using (1.28) and the derivative becomes,

$$F'(b) = \beta\Big\{1 + \frac{1}{\beta} - 1 + \sigma\theta \frac{u''(q^{ss})}{[(1-\theta)u''(q^{ss}) + \theta c''(q^{ss})]^2}\Big\} \tag{1.34}$$

Due to the concavity assumption, $u''(q^{ss}) < 0$, $F'(b)$ could be less than 1, with some assumptions such as linearity of cost function. (The detailed steps are given in Appendix.)

Proposition 2 (*Steady-state monetary equilibria*) Under the adaptive learning rule (1.31), there exists at least two steady-state equilibria, an autarky steady state where $\phi^{ss} = 0$ and a monetary steady state with $\phi^{ss} > 0$, when learning gain is sufficiently small or decreasing, b asymptotically converges to ϕ^{ss}, $b \to \phi^{ss}$. The monetary steady-state monetary equilibrium is locally stable if and only if $|F'(\phi^{ss})| < 1$.

Corollary 1: There exists a sufficient constant gain, such that, $F'(b) < 1$ and $g < \frac{2}{1-F'(b)}$, monetary steady state $\phi^{ss} = b$ is locally stable.

Following Evans and Honkapohja (2001), under perfect foresight, as long as $-1 < F'(\phi^{ss}) < 1$, the monetary steady state equilibrium is always locally stable. Under adaptive learning, that the monetary steady-state monetary equilibrium is locally stable requires $|1 + g[F'(b) - 1]| < 1$, which can be interpreted as $F'(b) < 1$ and $g < \frac{2}{1-F'(b)}$. When g is very small, the equilibrium outcome is not affected but the stability can be altered. When $F'(b) < -1$, g can reach very close to 1, so the monetary steady state equilibrium will not be stable.

I demonstrate through numerical simulation examples of complex dynamics that arise from the learning gain parameter [12]. Figure (1.4)) shows a simulation example in which the mon-

[12]More simulation examples can be found in Section 1.4.3

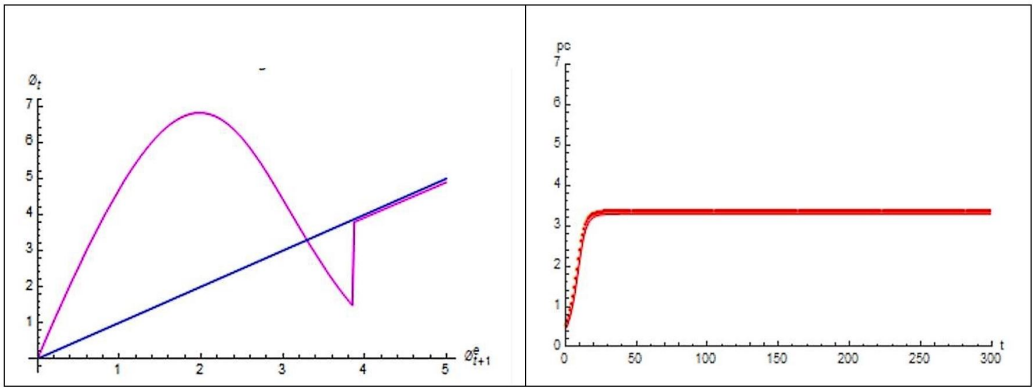

Figure 1.4: $g = 0.05$, (Left) Price diagram, (Right) Price simulation

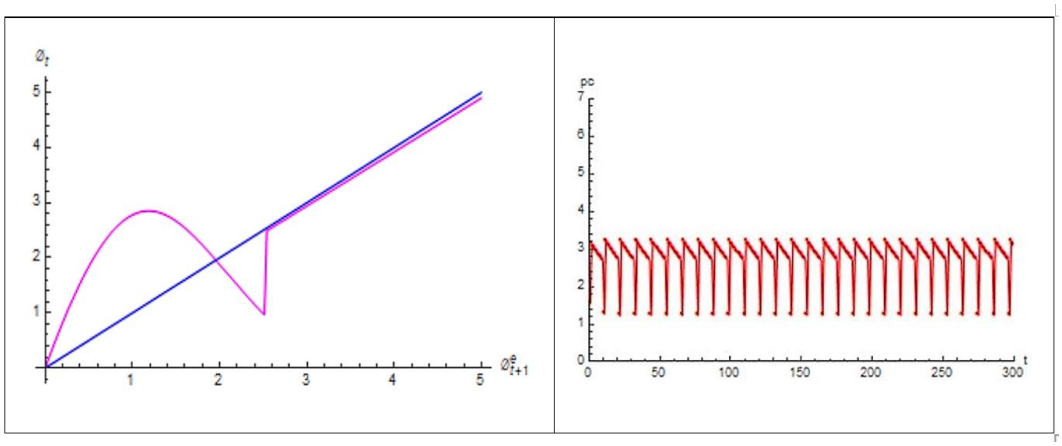

Figure 1.5: $g = 0.914$ (Left) Price diagram, (Right) Price simulation

etary steady state is learnable and locally stable with $g = 0.05$. When the learning gain parameter is large, chaotic cycles or bifurcation can be generated. This indeed appears to be the case shown in Figure (1.5) where g is set to 0.914. Prices move between a high and a low price level and it seems the oscillations permanently persist. Intuitively, learning captures the expectations feedback, as explained in Hommes (2013), where there are two different sets of feedback, and the realized price depends positively or negatively on the price forecast. In the case of positive (negative) feedback, an increase of forecast price causes the realized market price to go slightly up (down). As shown in Figure (1.5), it seems that the positive feedback and negative feedback alternatively dominates, therefore prices do not converge to

rational expectation equilibrium, but persistently oscillate.

1.4.3 Numerical Examples of the Economic Environment

Based on the adaptive learning theoretical analysis, I now seek to use examples to show the parameterization effects on the equilibrium paths, steady states and their stabilities. I will briefly examine different market structures, such as variations of bargain power, interest rates and discount rates, which are captured in the shape of $F(\cdot)$.

Bargaining power is defined as the ability to obtain the most favorable price possible under conditions prevailing in a market. Bargaining power variations could be one of the reasons for extreme price volatility. Assume a buyer's bargain power is θ, which implies that a miner's bargain power is also θ, and his trading partner, a producer, has $(1-\theta)$ bargain power. In Kalai bargaining, bargain power is the proportional share of which the agents split and obtain from the total social surplus. Therefore, θ is the share of surplus that buyers obtain, while $(1-\theta)$ is the share sellers obtain. Fig.(1.6) shows numerical examples to illustrate how the bargain power affects the price equilibrium path in this learning framework. Even if the initial prices are the same, after some periods of learning, the equilibrium paths lead to different steady states. The underlying intuition is due to feedback effect. The equilibrium price of the cryptocurrency is analogous to a miner's wage. With a higher bargain power against their trading partners, miners extract a higher portion of the social surplus, resulting in higher values from mining and holding money. Due to the feedback effect, the higher value of money attracts agents who want to engage in mining; however, by the law of motion of money supply, money increase is at a decreasing rate and this in turn urges miners to demand a higher price; therefore, money converges to a positive steady state value

eventually. As shown in the simulation, with the bargain power $\theta = 0.9$ in the left panel, the price converges to a positive value, while with $\theta = 0.4$ in the right panel, it seems that the price decreases and then shifts to a different regime, which eventually converges to a small but positive number. It makes sense empirically that the market power is not constant across a long time, therefore, the learning model can shed new light on the high volatility of cryptocurrency.

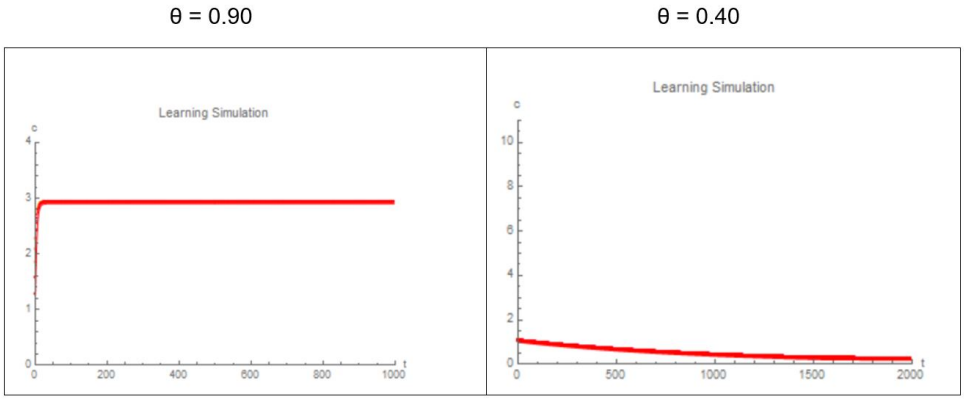

Figure 1.6: Price simulation with different bargain powers

The impact of the discount factor on the equilibrium price path is another example I examine. Figure (1.7) shows that even if the cryptocurrency starts at the same price, with different discount rates, the two equilibrium paths and steady state prices can be different. These price paths are actually numerical examples of Proposition 2. On the left side of the panel, agents live in an environment that has a higher discount rate $\beta = 0.98$, as demonstrated in the graph, price eventually converges to a positive steady state equilibrium; while with a very low discount rate of $\beta = 0.1$ shown on the right side of the panel, price converges very quickly to zero. The intuition is consistent with the "folk theorem" mentioned previously in rational expectation. When β is large, agents exhibit ample patience; consequently, under some constraint, this will gradually lead to a monetary equilibrium steady state. When β is very small, agents do not value too much of the future's consumption, holding money for the

distant future is actually not worth it and therefore money will eventually become worthless.

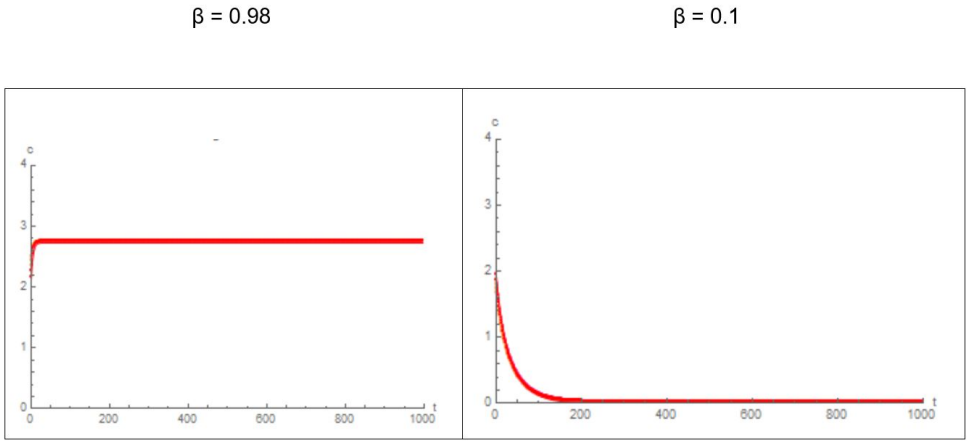

Figure 1.7: Price simulation with different discount rate

1.5 Conclusion

This paper relaxes the fundamental perfect foresight assumption (rational expectation), replaces it with a bounded rational in the Lagos and Wright (2005) and Choi and Rocheteau (2021) framework, and studies the following question: "What causes cryptocurrency's extreme price volatility?" Inspired by Evans and Honkapohja (2001), all agents use the adaptive learning rule to form their price expectations in this monetary search model, engage mining cryptocurrency to trade or produce goods to trade.

The primary contribution of this paper is that I use a constant-learning-gain to demonstrate how the learning gain affects monetary equilibria, their dynamics and their stabilities. The main results are that with a relative high learning gain in the adaptive learning algorithm, a period of doubling bifurcation can occur, which can lead to chaos or explosive paths. These endogenous dynamic results shed some light on the intensity of cryptocurrency's price

volatility. In addition, when buyers have higher bargain power, the price of cryptocurrency converges to a positive value. Ceteris paribus, however, when producers have higher bargain power, the price converges to zero equilibrium. The feedback effect, which plays a significant role in cryptocurrency's price volatility, provides the intuition behind this model.

Chapter 2

Cross-Sector Comovements in the COVID-19 Stock Market

Abstract

U.S. equity returns comoved remarkably during the COVID-19 pandemic. This study constructs a dynamic factor model to illuminate the sources and implications of these comovements. Estimation of the model using a Markov Chain Monte Carlo method reveals that the comovements had a weak daily oscillation pattern. Within that pattern, monetary policy significantly impacted the equity returns of several key sectors. In addition, cross-sector equity returns were shaped by news of monetary policies, fiscal stimulus, and unemployment. News about conventional and unconventional monetary policy shocked each sector in opposite directions. Interest-rate policy surprises had a stronger positive impact on equity returns than other unconventional monetary policy shocks. News about fiscal stimulus had the most substantial impact and triggered all sectors to rebound from the bear market at the end of March 2020. Applying Natural Language Processing sentiment analysis, this study also sheds light on the positive correlation between comovements and news sentiment.

Keywords: Comovements, Monetary Policy, Dynamic Factor Model, Markov Chain Monte Carlo, Bayesian Inference, Text Mining

2.1 Introduction

The turbulence in the U.S. stock market during the COVID-19 pandemic has sparked renewed interest in the long-time study of financial market comovements. Two different views on comovements of excess returns have been proposed in the literature: the traditional view attributes comovements to the expected fundamental values while an alternative view is sentiment- or friction-based. During the COVID-19 pandemic, the traditional view is inadequate to explain the comovement phenomena in the U.S. stock market. This empirical study constructs a Dynamic Factor Model (DFM) and decomposes the stock excess returns into fundamental and non-fundamental components. The model reveals that the non-fundamental components mainly drive the stock comovements during the pandemic.

Correlations in cross-sector returns are expected because macroeconomic conditions affected all sectors' expected earnings. What is puzzling is that despite the pandemic's disparate impacts on each sector, stocks from all sectors remained to comove excessively. For example, the left panel of Figure (2.1) shows that durable consumer goods production declined by 51% from February 2020 to April 2020[1], while the electric and gas output only decreased by 1.3%. The top right panel of Figure (2.1) shows that the hospitality industry's unemployment rates jumped from 5.7% in February 2020 to 39.3% in April 2020 due to the government's restric-

[1]Unemployment and GDP data are retrieved from `http://fred.stlouisfed.org`. Daily excess return data are retrieved from the Fama-French database library `http://mba.tuck.dartmouth.edu/pages/faculty/ken.french/data_library.html`

tions, while the finance industry only suffered an increase from 1.6% to 5.4%. Conversely, cross-sectors of the stock market moved closely together, especially during the beginning of the pandemic. (See the cross-sector excess returns in the bottom panel of Figure (2.1).) Additionally, at the end of March 2020, when the economy was still in recession, all sectors in the stock market comoved and rebounded together.

This study aims to explain the puzzle by measuring the latent non-fundamental forces that drove the comovements of stock returns. In this paper the non-fundamental force is market sentiment or latent sentiment, which propels the economy into periodic booms and busts.

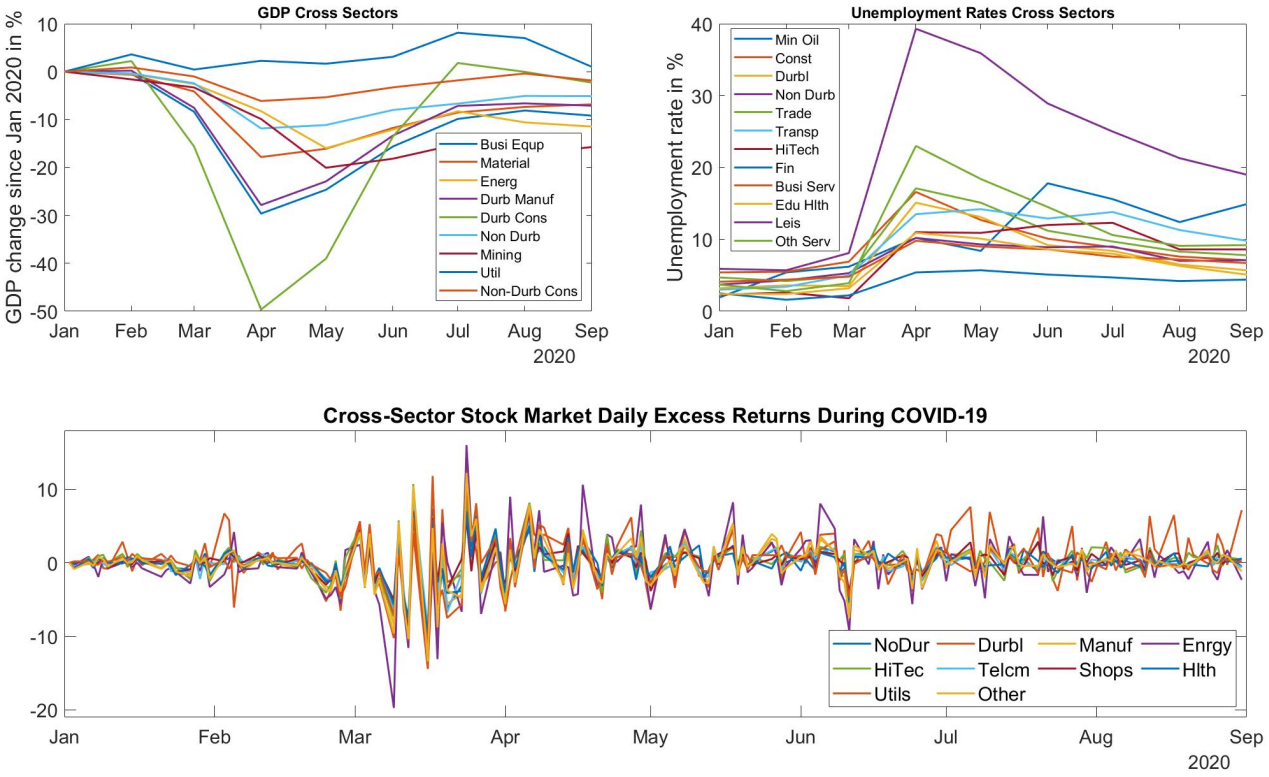

Figure 2.1: Cross-sector monthly unemployment, GDP, and daily stock indices from January 1, 2020 to August 31, 2020.

The main results of this study is that it reveals the size and patterns of the latent sentiment.

By controlling the known fundamental factors in a dynamic factor model, the unknown latent factor can be identified and measured. Using Bayesian Markov chain Monte Carlo (MCMC) approach, the study finds that, between January 1, 2020, and August 31, 2020, the latent sentiment has a weak daily oscillation pattern with an autoregressive coefficient of -0.09 in an AR(1) process. This result helps explain the stock market's extreme comovements, as well as the high volatility during the pandemic, especially in the beginning.

In addition, the study identifies and measures the impact of monetary policy and various news shocks on stock returns by controlling fundamentals and the latent factor variable. In particular, the model contains 43 fundamental variables (including macroeconomics variables, financial market variables, COVID-19 related variables), four dummy variables for shocks (conventional and unconventional monetary announcements, fiscal stimulus news, and unemployment news shocks), and one latent variable. The identifying assumption is that conditioning on the above controls, the impact of monetary policy and news shocks can be isolated and measured.

The results indicate that when the Fed cut its benchmark interest rates by 100 basis points, stock prices in all sectors rose immediately. The more prominent jumps were observed in the utilities and non-durable goods sectors, which are 11.35% and 7.33%, respectively. For any given sector, the conventional and unconventional monetary policy news shocked the sector in opposite directions. Of the positive monetary news shocks, the strongest shocks were from the interest rate policy surprises, while unconventional monetary policy news had a more sluggish impact on stock returns. Conversely, fiscal stimulus news had the most substantial positive impact and triggered all sectors to rebound from the bear market at the end of March 2020.

Furthermore, this study finds evidence of the positive linkage between the latent factor and the sentiment of the Fed's communication or media news, respectively. Wall Street Journal headlines are used as a proxy of the market sentiment. This study finds a positive correlation, 0.31, at the 95% statistically significant level by exploiting the Natural Language Processing (NLP) approach — Valence Aware Dictionary for Sentiment Reasoning (VADER) algorithm. Finally, this paper explores the associations between community mobility and stock returns and finds that different mobility data categories (e.g., visiting parks or staying in residential houses) have opposite associations with stock returns.

To the best of my knowledge, this paper is the first to examine comovements combined with monetary policy effects and policy news shocks during the COVID-19 pandemic. The existing finance literature suggest that the increased comovements are due to increased shared sentiment more than increased shared economic fundamentals. For example, Shiller (1989), using a simple present value model, shows that the comovements in stock prices cannot be accounted for by those in dividends. This argument provides an alternative view to the Efficient Markets Hypothesis (EMH) (see Fama (1970)). Pindyck and Rotemberg (1993), Vijh (1994), and Barberis et al. (2005), among others, examine the excess comovements between industry indices in the US and find significant excess comovements.

From a methodological viewpoint, this study is closely related to the DFM estimation literature. The method was initially developed by Geweke (1977) as an extension of the time series model for analyzing cross-sectional data. The influential work by Sargent and Sims (1977) develop the dynamic index models and provide evidence that one "index" can explain a large fraction of the variance in macroeconomic variables. Stock and Watson (1989) and Sargent (1989) using maximum likelihood and the Kalman filter estimate the DFM. Stock and Watson (2002) develop a static Principal Component Analysis (PCA) estimation. The

factor is essentially a weighted average with the eigenvectors of the sample variance matrix as the weights. There a few advantages of the PCA method, for example, it can deal with high dimensional data. In addition, the results of principal components are consistent and robust (see Bai and Perron (2003), Bai and Ng (2006)). Although its advantages, the PCA method remains limited. First, the principal components are computed ex-ante, treated as given in the estimation, therefore not suit for dynamics. Second, PCA method is not suitable for models have covariables. Chib and Greenberg (1996) and Chib et al. (2006) introduce blocking in the Markov Chain Monte Carlo (MCMC) method, which combines the efficient state space and the consistent nonparametric estimates approach. This blocking method allows MCMC to reduce correlations between draws efficiently by separating certain sets of parameters. Chan and Jeliazkov (2009) further improve the efficiency of the collapsed MCMC sampling by implementing a new blocking technique for the state space models. This study follows the collapsed MCMC method in Chan and Jeliazkov (2009) to investigate the puzzling comovements in the equity returns during the pandemic.

This study contributes to the emerging literature that investigates the impact of the COVID-19 pandemic on the economy. For example, Gormsen and Koijen (2020) develop a model of crisis that shows dividend futures can be a valuable tool for studying the evolving growth expectations in response to the coronavirus outbreak and subsequent policy responses. Cox et al. (2020) develop a dynamic asset pricing model to investigate the causality of stock market fluctuations. Different from those studies, this study adds to this growing body of literature related to the study of monetary and fiscal policy effects by providing evidence of the policy impact on the equity returns during the COVID-19 recession. In particular, this empirical study highlights monetary policy effects and the impact of conventional, unconventional monetary and fiscal policy shocks. Therefore, it is also related to the following research. Jinjarak et al. (2020) study both fiscal and monetary policies in the Euro-zone. Levin and Sinha (2020) assess the effectiveness of monetary forward guidance. Benmelech

and Tzur-Ilan (2020) and Bianchi et al. (2020) study both fiscal and monetary policies during the COVID-19 pandemic.

The remainder of the paper proceeds as follows. In Section 2, the Dynamic Factor Model is set up. Section 3, the model is derived, and the estimation steps are described. Section 4 describes the data sets, including financial market data, macroeconomics data, COVID 19 related information, policy announcements, and restrictions related data. Section 5 presents the estimation results, and policy implications. The linkage between the latent factor and news sentiment is also studied. The final section concludes.

2.2 Model

To illuminate the sources of the comovements and their implications, I construct a dynamic factor model (DFM). Let $y_{i,t}$ be the dependent variable, stock market excess returns or risk premia at the end of time t for sector i, where $i \in [1, 2, ..., n]$. Let $t = 1...T$ and $y_t = [y_{1,t}, y_{2,t}, ..., y_{n,t}]'$. Let X_t represent the independent variables, which include w_{t-1}, y_{t-1}, z_{t-1} and d_t[2]. Let w_{t-1} be the COVID-19 public health variables and community movement/mobility variables. Let z_{t-1} be the observed macro variables for all sectors lagged in time, which includes monthly GDP by sector, monthly unemployment rates by sector, M1 money stock, monthly Consumer Price Index, monthly Consumer Sentiment Index, and the daily Effective Federal Funds rate. Let d_t be a vector that includes four dummy variables representing conventional and unconventional monetary announcement shocks, fiscal stimulus news shocks, and unemployment news shocks. Let f_t be the unobservable comovement, which affects the dynamics of the excess returns of the stock market.

[2]Notation convention - we assume the values at the end of $t-1$ is equal to the values at the beginning of t and d_t is the contemporaneous shock during the day t.

The DF model takes the State Space representation as below,

Observation equation:

$$y_t = X_t\beta + Af_t + _t, \quad _t \sim N(0, \Omega) \tag{2.1}$$

State equation:

$$f_t = \gamma f_{t-1} + \mu_t, \qquad \mu_t \sim N(0, \sigma^2) \tag{2.2}$$

where $X_t = \begin{bmatrix} (1, w'_{t-1}, y'_{t-1}, z'_{t-1}, d'_t) & & \\ & (1, w'_{t-1}, y'_{t-1}, z'_{t-1}, d'_t) & \\ & \ddots & \\ & & (1, w'_{t-1}, y'_{t-1}, z'_{t-1}, d'_t) \end{bmatrix}$,

β is a vector containing the corresponding parameters ordered equation by equation, $\beta = vec\,([c : \lambda^w : \lambda^y : \lambda^z : \lambda^d]')$, $vec(\cdot)$ is a vectorization operator, which stacks the columns of a matrix one underneath the other into a vector. Let c be the intercept $n \times 1$ vector and λ^w, λ^z, λ^y, and λ^d be the regression coefficients in the observation equation. The factor loading A is a $n \times 1$ vector. γ is the autoregressive correlation of the state equation. Let $_t$ and μ_t denote the idiosyncratic errors that are in the zero-mean Gaussian distribution $N(0, \Omega)$ and $N(0, \sigma^2)$. Assume σ^2 is a scalar and Ω is a $n \times n$ diagonal covariance matrix with $(\omega_{11}, ..., \omega_{nn})$ on the diagonal and zeros on the off diagonal, which implies there is no concurrent correlation between $_{i,t}$ and $_{j,t}$ for all $i \neq j$[3].

[3]The concurrent correlation effects from cross sectors are absorbed by $y_{-i,t}$

Now stack equation (2.1) over time t, for $t = 1...T$, and we have,

$$y = \ X\beta + Af +, \ \ \sim N(\mathbf{0}, \ I_T \otimes \Omega) \tag{2.3}$$

where, $A = I_T \otimes A$, and

$$y = \begin{bmatrix} y_1 \\ \vdots \\ y_T \end{bmatrix}, \quad X = \begin{bmatrix} X_1 \\ \vdots \\ X_T, \end{bmatrix}, \quad f = \begin{bmatrix} f_1 \\ \vdots \\ f_T, \end{bmatrix}, \quad = \begin{bmatrix} _1 \\ \vdots \\ _T \end{bmatrix}$$

2.3 Estimation

In a DFM, both parameters and latent factors are regarded as random variables whose posteriors need to be sampled from. This study follows Chan and Jeliazkov (2009) as they improve the efficiency of the Markov Chain Monte Carlo (MCMC) sampling by implementing the integrated likelihood sampling. Instead of using the Kalman filter, they propose a new blocking technique by exploiting collapsed MCMC, sampling the loading parameter marginally over the factor vector f, and then drawing the factor f from its full-conditional distribution.

As the most challenging part in this estimation consists of sampling A and f from the posterior distribution, it is worthwhile to provide details of the derivation for factor f's conditional distribution before outlining the whole sampling procedure. First, the likelihood function $\pi(y|f, \beta, A, \Omega, \gamma, \sigma^2)$ is shown, followed by the conditional density $\pi(f|\gamma, \sigma^2)$. By Bayes' theorem, the posterior probability density $\pi(f|\ y, \beta, A, \Omega, \gamma, \sigma^2)$ can be immediately derived (See Koop (2003)). For compact writing, let θ represents $\{\beta, A, \Omega, \gamma, \sigma^2\}$ including all model parameters. Also, the covariant matrix X is regard as given, in this paper I drop

X from the conditioning set $\pi(f|y, X, \theta)$ to simplify the notation. By Bayes' theorem,

$$\pi(f|\ y, \theta) = \frac{\pi(y|\theta, f)\pi(f|\theta)}{\pi(y|\theta)} \tag{2.4}$$

the posterior probability density $\pi(f|\ y, \theta) \propto \pi(y|\theta, f)\pi(f|\theta)$.

As in (2.3) is Gaussian distribution, the conditional likelihood function is straightforward and also a Gaussian distribution,

$$\pi(y|\theta, f) \sim N\ (X\beta + Af,\ I_T \otimes \Omega) \tag{2.5}$$

Now, to explain the conditional density $f|\gamma, \sigma^2$, first rewrite equation (2.2),

$$f_t - \gamma f_{t-1} = \mu_t, \qquad \mu_t \sim N(0, \sigma^2) \tag{2.6}$$

Subsequently, stack equation (2.6) over time $t = \{1, 2, 3, ..., T\}$, and rewrite as following,

$$Hf = u \tag{2.7}$$

where

$$H = \begin{bmatrix} 1 & & & \\ -\gamma & 1 & & \\ & \ddots & & \\ & & -\gamma & 1 \end{bmatrix}, \quad f = \begin{bmatrix} f_1 \\ \vdots \\ f_T, \end{bmatrix}, \quad S = \begin{bmatrix} \frac{\sigma^2}{1-\gamma^2} & & & \\ & \sigma^2 & & \\ & & \ddots & \\ & & & \sigma^2 \end{bmatrix}$$

,

and,

$$u = \begin{bmatrix} \mu_1 \\ \vdots \\ \mu_T \end{bmatrix} \sim N(0, S), \tag{2.8}$$

The first top-left element in the covariance matrix S is the variance of the initial f_1, which is assumed distribute at the steady state of a first order autoregressive AR(1) process. Please refer to Chib and Greenberg (1994) for more details. The distribution is as below,

$$f_1 \sim N(0, \frac{\sigma^2}{1-\gamma^2}) \tag{2.9}$$

Following Fahrmeir and Kaufmann (1991), the conditional density of f can be derived as,

$$f|\gamma, \sigma^2 \ \sim N\Big(0, (\sigma^{-2}K)^{-1}\Big) \tag{2.10}$$

where the precision $\sigma^{-2}K = H'S^{-1}H$, and K $= \begin{bmatrix} 1 & -\gamma & & \\ -\gamma & 1+\gamma^2 & -\gamma & \\ & \ddots & \ddots & \ddots \\ & -\gamma & 1+\gamma^2 & -\gamma \\ & & -\gamma & 1 \end{bmatrix}$.

Now to express the conditional posterior, combine both (2.5) and (2.10),

$$[f|y, \theta] \sim N(\hat{f}, P^{-1})] \tag{2.11}$$

where the mean and precision are given as below,

$$P = \sigma^{-2}K + A'(I_T \otimes \Omega^{-1})A \tag{2.12}$$

$$\hat{f} = P^{-1}[A'(I_T \otimes \Omega^{-1})(y - X\beta)] \tag{2.13}$$

Following Chan and Jeliazkov (2009), this study employs their estimation method Metropolis– Hastings-within-Gibbs. The steps are as follows,

Step 1: Draw β from the conditional posterior marginalized out of f for the observation equation.

It is helpful to rewrite the model. Assume $\psi = Af+$; subsequently, the equation (2.3) becomes to the following,

$$y = X\beta + \psi, \quad \psi \sim N(0, \Sigma) \tag{2.14}$$

where Σ is a $nT \times nT$ covariance matrix, $\Sigma = [(I_T \otimes \Omega) + (I_T \otimes A)\sigma^2 K^{-1}(I_T \otimes A)']$ obtained from equations (2.3) and (2.10).

After a few steps of derivation (Please see Appendix B.7 for more details), the conditional posterior distribution of β is obtained:

$$[\beta|\ y, A, \Sigma, \gamma, \sigma^2] \sim N(\beta, B) \tag{2.15}$$

where the mean β and variance B are given by,

$$B = \left(B_0^{-1} + \sum_{t=1}^{T} X_t' \Omega^{-1} X_t - \tilde{X}_t' P^{-1} \tilde{X}_t \right)^{-1} \tag{2.16}$$

$$\beta = B \left(B_0^{-1} \beta_0 + \sum_{t=1}^{T} X_t' \Omega^{-1} y_t - \tilde{X}_t' P^{-1} \tilde{y} \right)^{-1} \tag{2.17}$$

where the compact notations $P = [\sigma^{-2} K + I_T (A' \Omega^{-1} A)]$, $\tilde{X}_t = A' \Omega^{-1} X_t$ and $\tilde{y}_t = A' \Omega^{-1} y_t$.

Step 2: Draw from the joint conditional posterior of A and f for the observation equation.

To generate draws of A and f from the joint distribution $[A, f | y, \beta, \Omega, \gamma, \sigma^2]$, two substeps are required.

Step 2.1 $[a |\ y, \beta, \Omega, \gamma, \sigma^2]$, sample a first independent of f

Step 2.2 $[f |\ y, \beta, A, \Omega, \gamma, \sigma^2]$, sample f and depends on a

This study follows Chan and Jeliazkov (2009) to generate the posterior density of A marginalized over f. By Bayes' Theorem,

$$\pi(A |\ y, \beta, \gamma, \Omega, \sigma^2) = \frac{\pi(A |\ y, f, \beta, \gamma, \Omega, \sigma^2) \pi(f |\ y, \beta, \gamma, \Omega, \sigma^2)}{\pi(f |\ y, A, \beta, \gamma, \Omega, \sigma^2)} \tag{2.18}$$

As both loading A and factor f are unknown, there are potential sign and scale identification issues for them. However, this can be solved by restricting the first element in the loading vector to 1, that is, $A = \{1, a'\}$. More details can be found in the study of Chan and Jeliazkov (2009). As the first element in the loading vector A is fixed as 1, replacing A with a, the posterior density of a, given $(y, \beta, \gamma, \Omega, \sigma^2)$ and marginalized over f, is as follows:

$$\pi(a|\ y, \beta, \gamma, \Omega, \sigma^2) = \frac{\pi(a|\ y, f, \beta, \gamma, \Omega, \sigma^2)\pi(f|\ y, \beta, \gamma, \Omega, \sigma^2)}{\pi(f|\ y, a, \beta, \gamma, \Omega, \sigma^2)} \tag{2.19}$$

$$\propto \frac{\pi(a|\ y, f, \beta, \gamma, \Omega, \sigma^2)}{\pi(f|\ y, a, \beta, \gamma, \Omega, \sigma^2)} \tag{2.20}$$

Notice that the loading parameter a is not involved in the term $\pi(f|\ y, \beta, \gamma, \Omega, \sigma^2)$ on the numerator, which therefore can be relegated to a constant, and can be scaled proportionately on both the denominator and numerator in calculating the acceptance ratio and eventually canceled out.

According to (2.20), the next step is to derive the numerator $\pi(a|\ y, f, \beta, \gamma, \Omega, \sigma^2)$. Please see more details in Appendix B.2. This section also skips explaining of denominator $\pi(f|y,$ $a, \beta, \gamma, \Omega, \sigma^2)$ as it has been derived in the equations (2.11), (2.12) and (2.13).

By Metropolis-Hastings (M-H) algorithm, a proposal density is tailored closely mimicking the posterior density. In practice, it is extremely important for the candidate generating density to have fatter tails than those of the target posterior. Let a^* be the draw from the tailored proposal, a student t distribution, of which, the mean $\hat{a}$ and negative inverse of Hessian, $\hat{A}$, are obtained by Maximum Likelihood Estimation. Let *df* be the degree of freedom, in general, df is chosen as a small number to ensure the fat details. The jumping distribution $q(a^*|a)$ represents the distribution for the current state a to jump to the next

state a^*. Rewrite the tailored proposal density as follows for notation convenience.

$$q(a^*|a) = q(a^*|\hat{a}, \hat{A}, df), \qquad q(a|a^*) = q(a|\hat{a^*}, \hat{A}^*, df) \tag{2.21}$$

Thus, the rate $\alpha(a, a^*)$ of accepting the next proposed draw a^* is,

$$\alpha(a, a^*) = min \left\{ 1, \frac{\pi(a^*|\ y, \beta, \gamma, \Omega, \sigma^2) q(a\ |\hat{a^*}, \hat{A}^*, df)}{\pi(a|\ y, \beta, \gamma, \Omega, \sigma^2) q(a^*|\hat{a}, \hat{A}, df)} \right\} \tag{2.22}$$

Please see more details in Appendix B.3.

The next step is step 2.2, which generates draws of f from $[f|\ y, a, \beta, \gamma, \Omega, \sigma^2)] \sim N(\hat{f}, P^{-1})$. This study follows Chan and Jeliazkov (2009) and implement an efficient way to compute the latent factors by employing forward and back substitution techniques. Usually, the variance matrix P^{-1} is obtained by inverting the precision matrix P from (2.12). However, this study uses Cholesky decomposition to avoid the daunting task of inverting a matrix and only invert the Cholesky factor. Let C be the Cholesky factor, such that $C'C = P$. Multiplying $C'C$ on both sides, equation (2.13) becomes,

$$C'C\hat{f} = A'(I_T \otimes \Omega^{-1})(y - X\beta) \tag{2.23}$$

Apply the forward substitution to solve $C\hat{f}$, and use the back substitution technique with the assumption $C'm = \zeta$ and $\zeta \sim N\ (0, 1)$ to solve $\hat{f}$. Draw ζ, and solve m backward, which is $m = C^{-1}\zeta$. This implies m is distributed in $N\ (0, P^{-1})$, where it has the idea variance. The subsequent step is to add the mean $\hat{f}$ from (2.12) to the result of m. Now, a draw of $[f|y, a, \beta, \gamma, \Omega, \sigma^2] \sim N\ (\hat{f}, P^{-1})$ is achieved.

Step 3: Draw from the conditional posterior of Ω for the observation equation.

Assuming Ω is a diagonal covariance matrix with $(\omega_{11}, ..., \omega_{nn})$ on the diagonal, and the conjugate inverse Gamma prior of the form, $\omega_{ii} \sim IG(d_0, D_0)$, the study generates draws of each variance ω_{ii} equation-by-equation, from the conditional posterior distribution, where $ii = \{11, ..., nn\}$. The conditional posterior distribution $[\Omega|y, \beta, A, f, \gamma, \sigma^2]$ is given by,

$$\omega_{ii} \sim IG(d, D) \tag{2.24}$$

$$d = \frac{d_0 + T}{2} \tag{2.25}$$

$$D = \frac{D_0 + e_i' e_i}{2} \tag{2.26}$$

where d_0 and D_0 are the inverse Gamma prior parameters, and e_i is the residue vector with T length from the ith observation equation.

Step 4: Draw from the conditional posterior of γ for the state equation.

To generate sample γ from the conditional posterior $[\gamma|y, f, \beta, A, \Omega, \sigma^2]$, the study adapts the usual time series Bayesian updating rules in Chib and Greenberg (1994) and Chib and Jeliazkov (2001). Draws of γ from its distribution until the factor is found in the stationary region; it is then subject to the usual M-H acceptance criterion. Specifically, let $F^* = [f_1, f_2, ..., f_{T-1}]$ and $F^{**} = [f_2, f_3, ..., f_T]$, and initial (γ_0, Γ_0). Draw a candidate γ^* according

to the distribution below,

$$\begin{aligned} \gamma^* &\sim N(\hat{\gamma}, \Gamma) && (2.27) \\ \hat{\gamma} &= \Gamma(\Gamma_0^{-1}\gamma_0 + F^{*\prime}F^{**}\sigma^{-2})^{-1} && (2.28) \\ \Gamma &= (\Gamma_0^{-1} + F'^{*}F^{*}\sigma^{-2})^{-1} && (2.29) \end{aligned}$$

Accept the proposed value γ^* with the M-H probability of move given by the ratio $\alpha(\gamma, \gamma^*)$, i.e.

$$\alpha(\gamma, \gamma^*) = min \left\{ 1, \frac{f_N(f_1|(0, \frac{\sigma^2}{1-\gamma^{*2}}))}{f_N(f_1|(0, \frac{\sigma^2}{1-\gamma^2}))} \right\} \quad (2.30)$$

Step 5: Draw from the conditional posterior of σ^2 for the state equation.

The way to generate draws of σ^2 from $[\sigma^2|\ y, \beta, A, f, \Omega, \gamma]$ is similar to step 3. From equations (2.7) and (2.8), the conditional distribution of σ^2 is given by an inverse Gamma distribution:

$$\begin{aligned} \sigma^2 &\sim IG(g, G) && (2.31) \\ g &= \frac{g_0 + T}{2} && (2.32) \\ G &= \frac{G_0 + u'u}{2} && (2.33) \end{aligned}$$

where the conjugate prior of $\sigma^2 \sim IG(g_0, G_0)$, $u = Hf = f_s - f_p$, $f_s = [f_1(1-\gamma)^{1/2}, f_2, ..., f_T]'$ and $f_p = [0, \gamma f_1, ..., \gamma f_{T-1}]'$.

MCMC Sampling Algorithm Summary

Step 1. Draw β from $[\beta|\ y, A, \Omega, \gamma, \sigma^2] \sim N(\beta, B)$.

Step 2. Draw A and f from the joint posterior distribution $[A, f|y, \beta, \Omega, \gamma, \sigma^2]$ through the following two sub-steps.

Step 2.1 Implement MH sampling, draw a from $[a|\ y, \beta, \Omega, \gamma, \sigma^2]$ independently of f.

Step 2.2 Sample f from $[f|\ y, \beta, A, \Omega, \gamma, \sigma^2] \sim N(\hat{f}, P^{-1})$.

Step 3. Draw Ω from the conditional posterior distribution $[\Omega|\ y, \beta, A, f, \gamma, \sigma^2] \sim IG(d, D)$.

Step 4. Implement MH sampling, and draw γ from the conditional posterior distribution: $[\gamma|\ y, \beta, A, f, \Omega, \sigma^2]$.

Step 5. Draw σ^2 from the conditional posterior distribution $[\sigma^2|\ y, \beta, A, f, \gamma, \Omega] \sim IG(g, G)$.

2.4 Data

There are 48 variables (including a latent variable) in the model, which are grouped into four categories. They are as follows: financial market data by sector with daily frequency; macroeconomics variables — comprising both daily and monthly frequency data; COVID-19 related data, including daily public health information and daily community mobility data; and dummy variables representing the announcements or news shocks.

First, the financial market dataset includes daily excess returns by sector and daily trading volume data, in total 11 variables. Daily excess returns are calculated by deducting the daily risk-free rates from the daily stock returns in sectors[4]. Based on the Standard Indus-

[4]Daily return data are retrieved from the Fama-French database library `http://mba.tuck.dartmouth.edu/pages/faculty/ken.french/data_library.html`

trial Classification (SIC) codes[5], each stock in NYSE, AMEX, and NASDAQ is assigned to one of the ten sectors: consumer non-durables; consumer durables; manufacturing; energy; high-tech; telephone and television transmission; wholesale and retail; healthcare; utilities; and other[6]. This study uses the daily NASDAQ market trading volume[7] as one proxy to capture the financial market sentiment (see Baker and Wurgler (2007)). The daily trading volume reveals the underlying different opinions on the stock market between buyers and sellers. However, having the trading volume variable as the only proxy to represent market sentiment still cannot capture the majority share of variations in stock prices. The next section explains that it is still necessary to include the latent factor as it is an essential driver for the stock market returns.

The second category is macroeconomic data, which includes 25 variables comprising daily Effective Federal Funds Rate (EFFR), monthly Gross Domestic Product (GDP) by sector, monthly unemployment rates by sector, monthly Consumer Price Index (CPI), monthly Consumer Sentiment Index, and monthly M1 money stock. All of these series are retrieved from the Federal Reserve Economic Data library (FRED)[8]. These series of data encompass daily or monthly frequency. The time-series literature comprises a few ways to handle this issue. Econometricians usually either aggregate the higher frequency data to a lower frequency or interpolate the lower frequency data to the higher frequency. However, these methods may result in the loss of helpful information while smoothing. Therefore, the estimated results can be biased. The study uses the original data only by keeping the monthly variables constant during the month, with the justification that monthly variables can be observed and updated once each month. However, it can cause a larger variance of the parameters on the

[5]SIC refers to `https://www.osha.gov/data/sic-manual`

[6]Other sector includes mines, construction, build management, transportation, hotels, entertainment, and finance.

[7]The daily trade volume in NASDAQ is obtained from http://www.nasdaqtrader.com/

[8]`https://fred.stlouisfed.org/`

monthly regressors than the daily regressors[9].

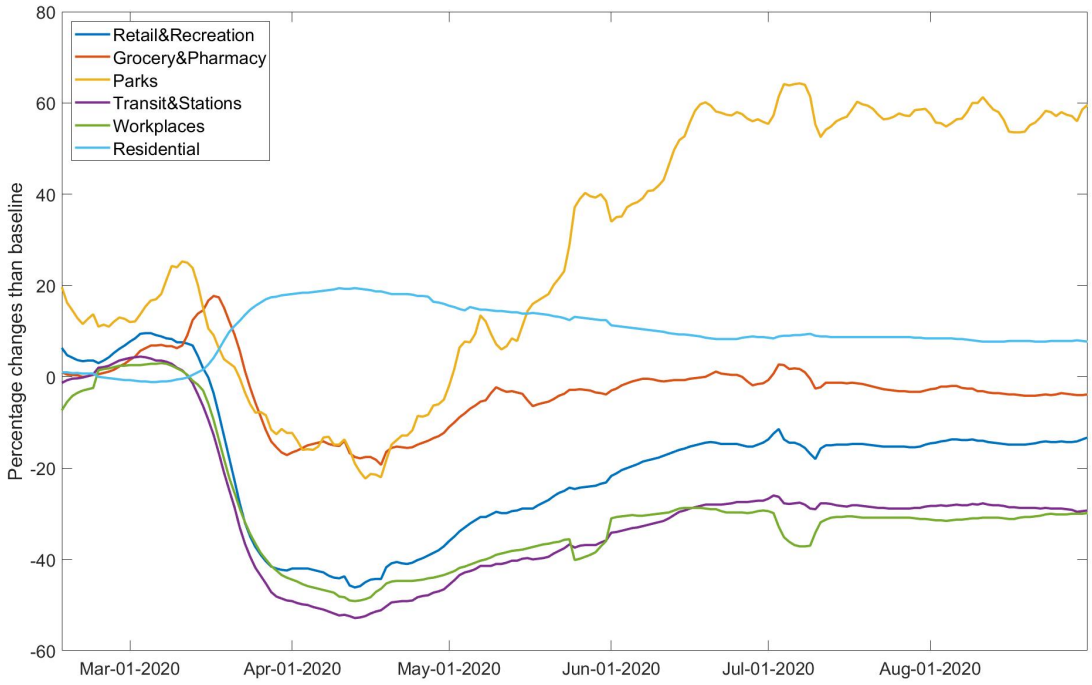

Figure 2.2: Google community mobility changes to baseline in 2020.
Data source: `https://www.google.com/covid19/mobility/`

The third category dataset is COVID-19 related information, including community mobility set and public health set, a total of seven variables. The subset of the community mobility dataset for the U.S. is obtained from Google's COVID-19 Global Community mobility data center[10]. The mobility level of the community is measured by the number of visits and time spent in a particular category of location. The six categories of the locations people visit are retail and recreation, grocery and pharmacy, residential areas, transit, parks, and workplaces, as shown in Figure (2.2). The mobility dataset starts from January 3, 2020, before COVID-19 was widespread worldwide. The initial five weeks (from January 3 to February 6, 2020) are issued as the baseline period[11]. The baseline values in each category are the

[9]This paper simulates 10,000 iterations with 3,000 burn-in to improve accuracy of the results
[10]`https://www.google.com/covid19/mobility/`. In their document, it also includes the data limitation.
[11]As one of the data limitations mentioned in the document of the data set, the chosen based line may

median value of the five-week baseline period, which has seven different values representing each day of a week. Google measures the mobility level in the degree of change by comparing it to the baseline values on the same day of a week. For example, Tuesday's visit to the grocery and pharmacy will only be compared to the baseline value of Tuesday visits to the grocery and pharmacy. Further, as the financial market data are only for weekdays except for holidays, the study uses the corresponding five weekdays for the mobility level and ignores the weekend data.

The COVID-19 public health status — the daily death rate variable — is collected from Our World In Data[12], which combines information from multiple sources such as the World Health Organization (WHO), Johns Hopkins University, and the European Center for Disease Prevention and Control. The study uses the daily new deaths attributed to COVID-19 smoothed per million people series in the data set. The first three deaths attributed to COVID-19 in the U.S. reported as of March 2, 2020, stand at a rounding rate of 0.001 per million[13].

This study creates four dummy variables to identify and assess the impact of shocks from monetary policy announcements, fiscal policy announcements, and government restrictions for different sectors. They represent the shocks of conventional monetary policy announcement, unconventional monetary policy announcement, fiscal news, and Unemployment rates news. The Conventional monetary policy includes lowering the target range for the federal funds rate and increasing the Federal Reserve's holdings of Treasury securities and agency Mortgage-Backed Securities (MBS). As the lower bound of the target range is near zero, the

not be the perfectly normal baseline days, because a short period of the year cannot represent normal for all regions in the U.S.

[12] `https://ourworldindata.org/coronavirus`

[13] `https://www.nytimes.com/2020/04/22/us/coronavirus-first-united-states-death.html`, this new information may shift the timeline of the virus's spread through the U.S. a few weeks earlier than previously believed on February 26, 2020.

Federal Reserve has created several trillion dollars of loan facilities to support the economy, and this is the unconventional monetary policy. See more details in Appendix B.1.

Finally, all data are transformed into stationary series. See Appendix B.5 for more details of the data and the process of transformation.

2.5 Estimation Results

2.5.1 Latent Factor and Loading Parameters

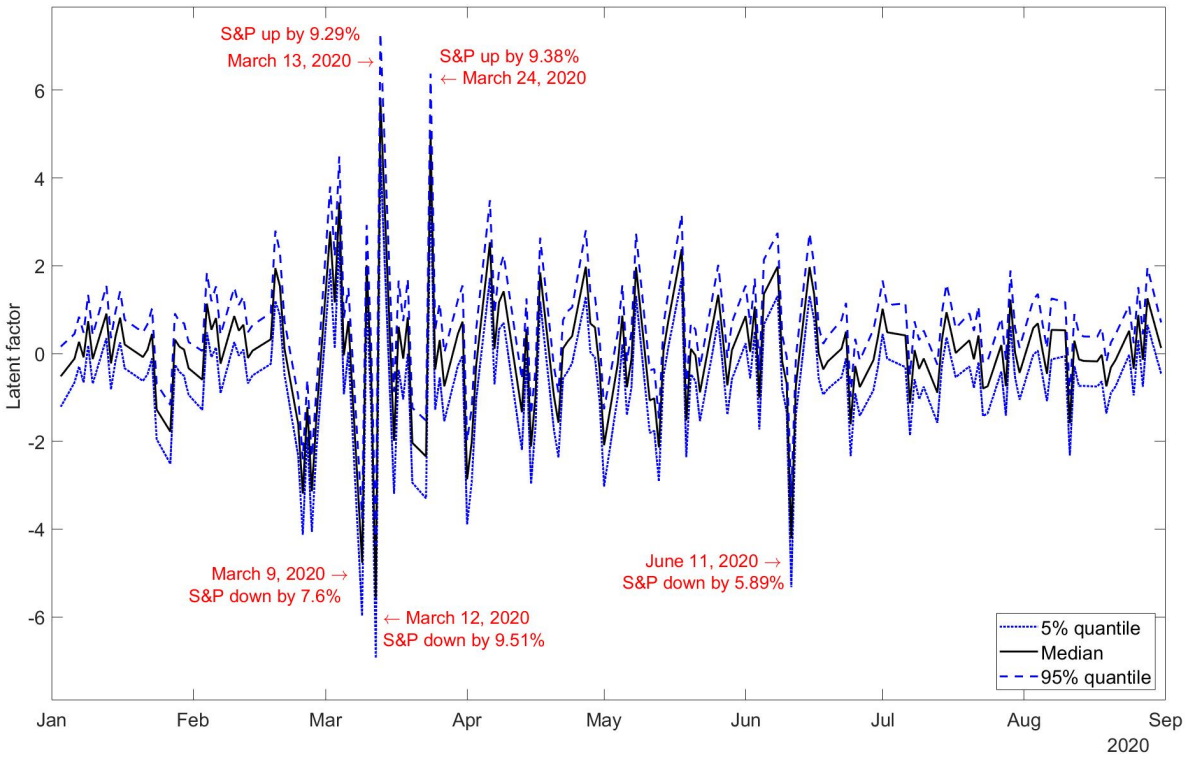

Figure 2.3: Latent factor estimation at 5%, 50% and 95% quantiles from January 2020 to August 2020.

The results of the estimated posterior distribution of the latent factor are presented in Figure

(2.3). The black line in the middle indicates the median value of the posterior distribution along with 5% and 95% quantile bands; the narrowness of the band suggests that the factor is estimated rather precisely. Figure (2.3) shows that there are three dives on March 9, March 12, and June 11, 2020, decreasing by 712%, 940% and 513% from the previous days, respectively. These estimation results are consistent with the fact that the Dow Jones Index dropped by -7.79%, -9.99%, and -12.93% on those three days. These three events also coincide with world events and monetary policy news. On March 11, 2020, the WHO upgraded the status of the coronavirus outbreak from an epidemic to a pandemic, and two days later, on March 13, 2020, the president of the U.S. declared a national emergency. The results of the latent factor, market sentiment, in those hectic events reflect the impact of these shocks on investors. Unprecedentedly, the stock crash in March only caused a short-lived bear market, and in April, the stock market rebounded into a bull market, indicating the extremely restless pattern of the latent sentiment. On June 11, 2020, one day after the Fed announced that interest rates would remain near zero to 2022, signaling a long road to recovery, the U.S. stock market suffered its worst one-day sell-off since March. This phenomenon can be explained by the possibility that forward guidance is also a negative signal to the market in addition to the growing fears of a second wave of COVID-19 cases. Not coincidentally, following each dive, the market shows a significant jump. The latent factor reflects this high volatility behavior with two considerable spikes shown in Figure (2.3). These spikes are on March 14 and March 24, 2020, with the values increasing by 204% and 312%, respectively.

On March 3 and March 15, 2020, FOMC announced lowering the benchmark rates by a half and one percentage points, respectively, and ended at zero. The estimated results of the latent sentiment on those announcement days suggest a decrease by 59% and 134%, respectively,[14] from their previous trading days. The decreasing comovements suggest that

[14]This number is calculated by comparing the factors between March 16, 2020, and March 13, 2020, due to weekend announcement.

collectively with other sources of shocks, the conventional monetary policy (lowering the target rate to zero and increasing holding Treasury securities and agency MBS) is not sufficiently powerful to overcome the underlying restless latent sentiment to support the stock market. Note: These declining comovements do not represent negative effects of the monetary policy. These estimated results are the isolated comovements after controlling all macroeconomics effects, including effects of various policies and news shocks. Effects of monetary policy are explained in Section (2.5.2), and news impact is in Section (2.5.3).

2.5.1.1 Persistence Properties of the Dynamic Latent Sentiment

To measure the evolution of the latent factors, this study collects the autoregressive coefficients (2.2) at each step of the estimation procedure to obtain their distribution. The latent factors have a negative and small autocorrelation, -0.0868; the 45% and 55% quantiles of this distribution are -0.0936 and -0.0764, respectively. See Figure (2.4). These results can help explain the volatility of the latent sentiment and weak mean reverse pattern. For example, during the nine trading days (between March 9 and March 19, 2020), the market did not simply tumble linearly, however, on four of the nine days, the market rose by nearly 5% after the previous day crash. The estimated median of the variance of the dynamic latent factor is 2.201 (see Figure (2.5)).

2.5.1.2 Loading Parameters

The loading parameter for each sector can be understood as a multiplier effect on the market comovements. Figure (2.6) displays the estimated distributions for the loading parameters. The first sector — non-durable goods — is assumed as the benchmark. The highest medium values of the loading parameters are 1.91, the energy sector; 1.67, the durable sector; and

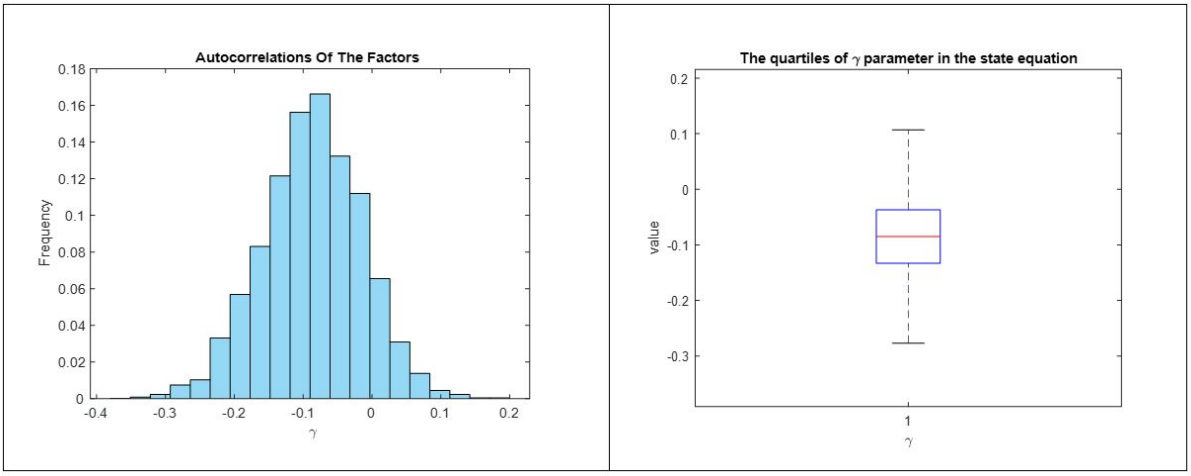

Figure 2.4: Persistence properties of the dynamic factors.

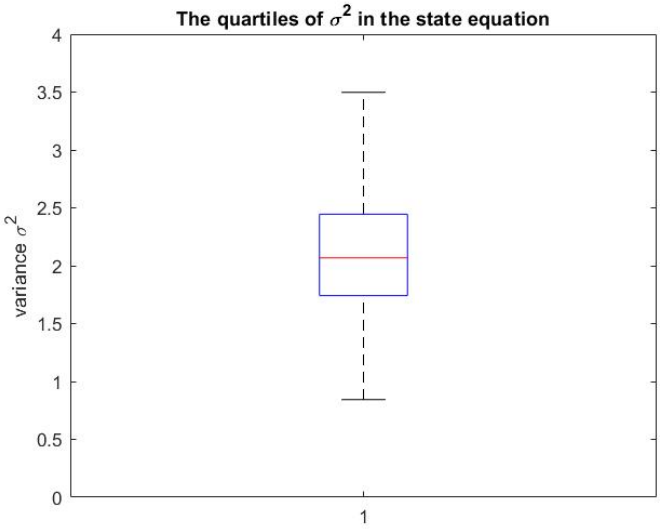

Figure 2.5: Boxplot for variance of the dynamic latent factor

1.64, the other sector. As the comovements permeate the whole market across sectors, it is valuable to consider the whole picture of the equity market to determine how sectors evolve during the pandemic. Figure (2.7) gives a three-dimensional depiction of these comovements across sector and time; the "sector" axis in this graph arrays the different sectors in the order given in Figure (2.6). The vertical axis is the latent factor in each sector. The colors illuminate the comovements and volatility of the market.

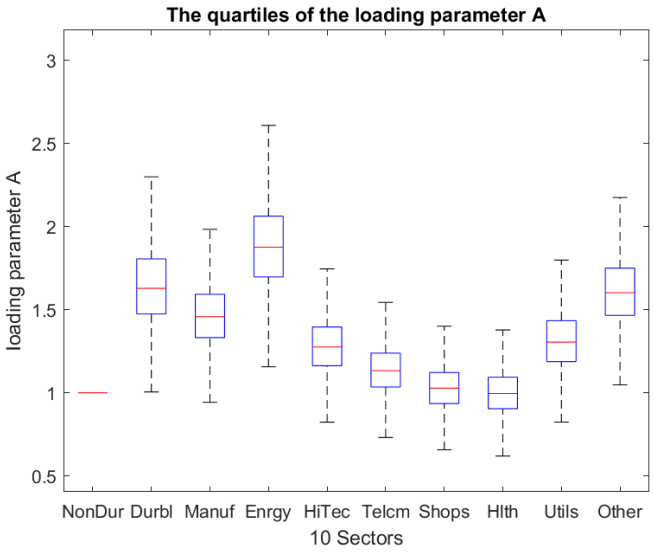

Figure 2.6: Estimated loading vector
Coefficients in the figure NoDur, 1; Durbl, 1.67; Manuf, 1.48; Enrgy, 1.91; HiTec, 1.30; Telcm, 1.15; Shops, 1.04; Hlth,1.01; Utils, 1.33; Other,1.64.

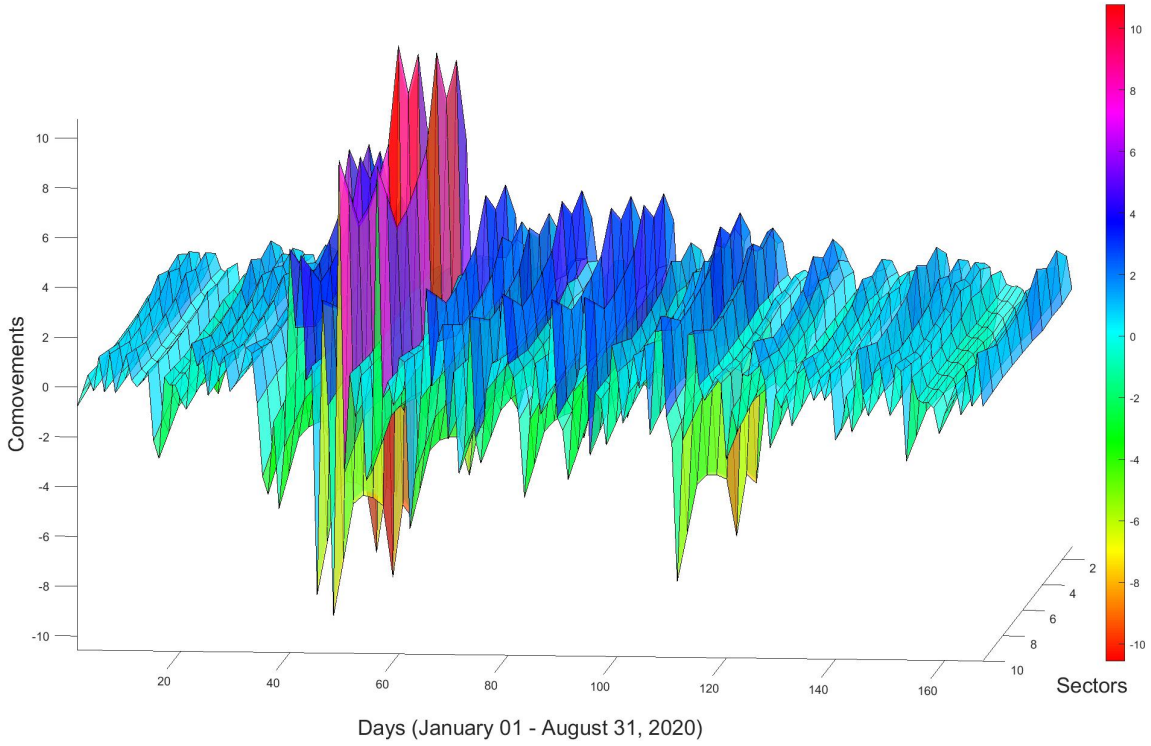

Figure 2.7: Comovements across sector and time. Sectors: 1-NoDur, 2-Durbl, 3-Manuf, 4-Enrgy, 5-HiTec, 6-Telcm, 7-Shops, 8-Hlth, 9-Utils, 10-Other

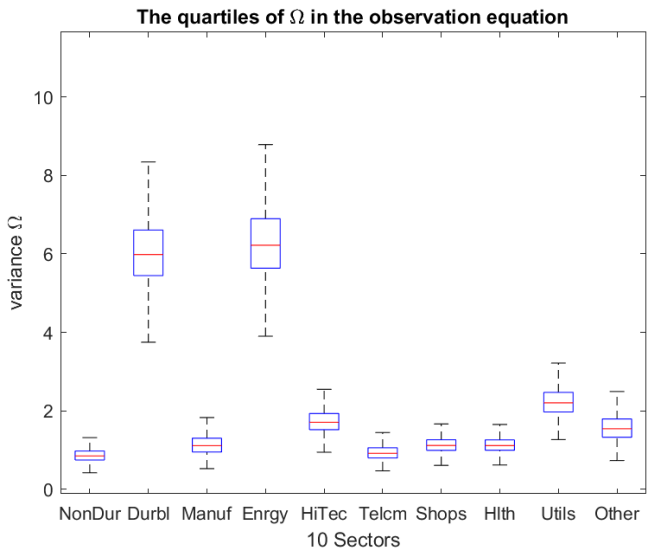

Figure 2.8: Boxplot for variance of the observation equation

Figure (2.8) displays the variances of the idiosyncratic risks in all ten sectors. After controlling the macroeconomic condition, monetary policy effects, news shocks, and their comovements, the remaining risks are relatively small with a medium variance less than 2 for most sectors, except for the high-risk energy and durable goods sectors.

2.5.2 Monetary Policy Interest Rates Effect

First, the study briefly analyzes the effects of the monetary policy interest rates on the stock returns during the sample data between January 1 and August 31, 2020. Subsequently, in the next section, this paper examines the policy news shocks on the stock returns as part of monetary policy impact analysis. The effects of the interest rates on stock returns are reported in Table (2.1), and the quantile boxplot is reported in Figure (2.9). It shows that utilities and non-durable consumer goods sectors are the most sensitive to interest rates. The results show that if the Fed Effective Funds Rate is decreased by one percentage point, specifically, the utilities and non-durable goods stock returns increase by 11.35% and 7.328%, respectively; the overall market of ten sectors was a 4.18% increase. These estimation re-

sults are in congruence with the empirical data — between March 16, 2020 and March 17, 2020, the stock market jumped up by 11.81% in utilities and 7.40% in non-durable goods, were very close to my estimations 11.35% and 7.328%, when the Fed announced reducing interest rates by one percentage point on the evening of March 15, 2020[15]. These two sectors are defensive sectors. Whether the economy and the stock market are good or bad, people still need the necessities, such as food, water, and electricity. However, durable goods stock prices are less responsive to lower interest rates. That households reduced durable goods expenditures during the COVID-19 recession due to uncertainty about future income, made the interest rate policy accommodation less responsive in the durable goods sector.

Table 2.1: Estimated Coefficients on the Effective Federal Funds Rate (EFFR)

	NoDur	**Durbl**	**Manuf**	**Enrgy**	**HiTec**	**Telcm**	**Shops**	**Hlth**	**Utils**	**Other**
EFFR	-7.328	-0.849	-4.522	-2.508	-2.990	-2.451	-3.250	-4.097	-11.35	-2.501

Note: The negative signs imply that the excess returns of stocks and EFFR move in opposite directions.

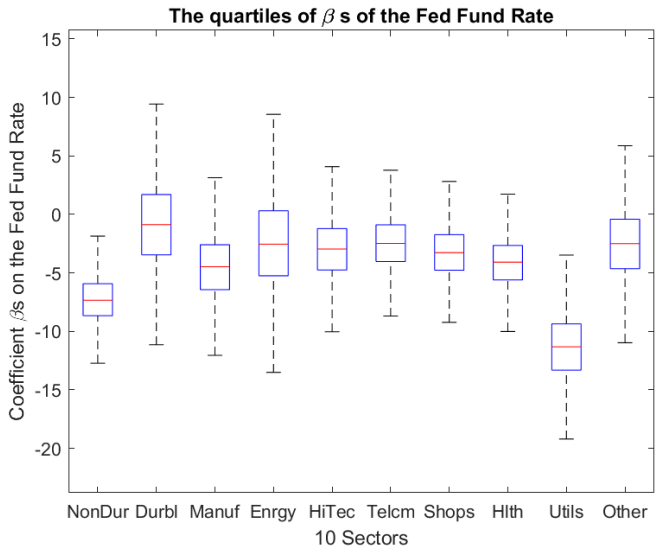

Figure 2.9: Boxplot for the estimated βs on the Fed Funds Rate variable

[15]Since March 15 is a Sunday, this paper counts the next trading day as the monetary policy day for prediction purpose.

2.5.3 Announcement Shocks

Since the first coronavirus death that shocked the U.S. media at the end of February in 2020, there was an enormous amount of news and information broadcasting every day. There was collective news including spikes of new deaths and cases, oil price tank, government's stay-at-home and closure of business orders, monetary policy announcement, fiscal stimulus, and unemployment rate announcements. When such news is released, it has a significant effect on economic activities and the financial market. To attempt to separate the impact of an amalgam of news, the constructed four dummy variables representing four types of shocks: conventional, unconventional monetary policy announcement, fiscal stimulus announcement, and unemployment rate announcement[16].

2.5.3.1 Monetary Policy Announcement Shocks

Distinguishing the impact of announcements between a conventional monetary policy and an unconventional monetary policy is one of the essential results of this study. A conventional monetary policy in the U.S. refers to the Federal Reserve altering the target interest rate and opening market operations, for instance, purchasing Treasury securities and agency MBS. Conversely, an unconventional monetary policy is a situation where the Federal Reserve pursues an alternative monetary policy, such as Large Scale Asset Purchase (LASP) or forward policy guidance, when facing the Zero Lower Bound (ZLB) constraint, to influence interest rates to reach its dual mandate of full employment and stable prices. At the beginning of COVID-19, the Fed announced the conventional monetary policy of lowering the benchmark interest rate to ZLB on March 3 and March 15, 2020, respectively. Immediately after reach-

[16]Dummy variables are either one or zero. One represents an announcement for that day. It is possible that news leaks before the official day of the announcement, and it is also possible there are multiple sources of shocks on that same day, but they capture the major shocks on the financial market of that day.

Table 2.2: The impact of News shocks

Estimated Coefficients of The four dummy variables										
Dummy Variable	**NoDur**	**Durbl**	**Manuf**	**Enrgy**	**HiTec**	**Telcm**	**Shops**	**Hlth**	**Utils**	**Other**
Conventional MP News	1.711	-1.544	1.300	1.095	-0.856	0.786	-0.598	-0.464	1.440	-0.461
Unconventional MP News	-0.006	0.783	-0.086	0.222	0.688	0.030	0.231	0.288	-0.371	0.447
Fiscal News	4.265	4.448	6.267	6.883	3.986	4.592	1.256	4.213	5.980	6.147
Unemployment News	0.475	-0.043	0.383	0.228	-0.666	0.157	-0.351	-0.127	0.010	0.189

ing the constrain, on March 17, 2020, the Federal Reserve Board announced establishment of a Commercial Paper Funding Facility (CPFF) to support the flow of credit to households and businesses. Subsequently, there were 15 announcements regarding unconventional monetary policies establishing nine new lending facilities from the middle of March to May 2020 (See the event details in Appendix B.1). These interventions can also be reviewed as signals that the Fed acknowledges the economy is suddenly heading toward the brink of recession and "they will do whatever they can" to help support the economy.

Table (2.2) reports the estimated impact of four different news, including conventional and unconventional monetary policy announcement, fiscal stimulus and unemployment news. Coefficients are in units of percentage. For instance, the top left number 1.711 implies that, on average, the conventional monetary policy announcement shock caused excess return on the non-durable goods sector by 1.711% at the end of that announcement day. One caveat is that it is "average" effects, because the FOMC cut half percent on March 3; on March 15, 2020, a full one percent is cut and reached ZLB. I also present the corresponding coefficients' distribution in Figure (2.10) and Figure (2.11) for the non-durable and utility sectors[17]. As shown in the quantile box plots, the coefficients' inter-quantile ranges are all centered and the variances are quite small, which imply the results are significant.

[17]Graphs for other sectors are also available upon request. Notched boxplot version is also available implying results significance.

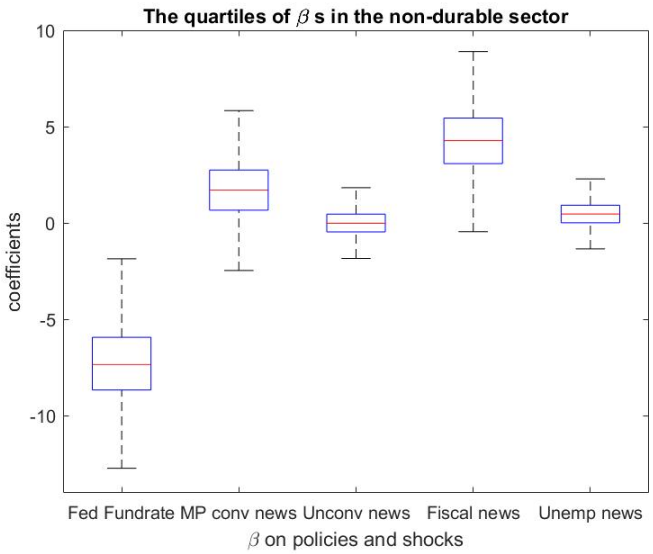

Figure 2.10: Boxplot for the impact of news shocks in non-durable sector

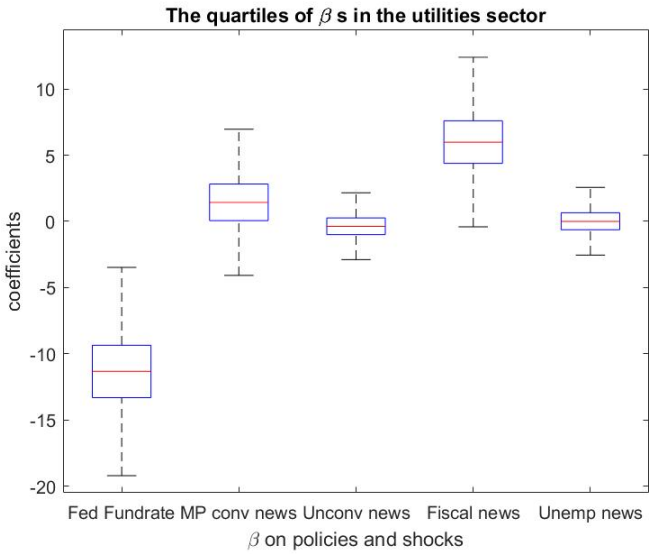

Figure 2.11: Boxplot for the impact of news shocks in utilities sector

In addition to Table (2.2), Figure (2.12) helps us visually explain the differences between the two types of monetary policy announcement impact. The bars labeled blue in Figure (2.12) indicate the impact of the announcements regarding conventional monetary policy shocks, while the bars labeled in red are the impact of the unconventional monetary policy shocks.

The positive impact of the announcements of conventional monetary policy is 1.711% in non-durable consumer goods, 1.440% in utilities, 1.300% in manufacturing, 1.095% in energy and 0.786% in communication sectors. These results are expected and similar to the interest rate effects because defensive sectors in the stock market are sensitive to the interest rate. Further, another reason that could contribute to the announcement impact is the striking phenomenon of consumers' panic-buying to stock-up essentials during the beginning of the COVID-19 pandemic. For example, when the WHO advised that the best defense against Coronavirus was hand soap, sanitizer, and wearing masks, many consumers immediately began to purchase large quantities of these items. This led to a surge in demand, prompting producers to increase their production. Therefore, with the announced cutting interest rate, the non-durable goods sector responded to it positively. However, durable goods and high-tech sectors responded to the announcement shock negatively on a relatively larger scale. The GDP for durable consumer goods decreased by more than 26% between March and April 2020. As mentioned in Section 2.5.2, the second conventional monetary policy of cutting interest rates announced on Sunday morning (March 15, 2020) could be a negative signal that the Fed Reserve acknowledges that a recession is coming in the near future. Therefore, it is reasonable to believe that lowering the interest rates did not positively impact durable goods and other sectors.

The red bars shown in Figure (2.12) present the impact of the unconventional monetary policy shocks on the stock market. There were overall 16 FOMC announcements, which have created nine new lending facilities from the middle of March till that of May 2020. For the same sector, the estimated effects for the unconventional monetary policy shocks have opposite directions to the impact of the conventional monetary policy shocks[18]. As indicated in Table (2.2), the magnitude of the impact is smaller for both positive or negative. For energy, shops, health, and other sectors, there is essentially no impact. Durable goods and high-tech

[18]Except for the health sector, both are negative. However, unconventional policy shock is close to zero.

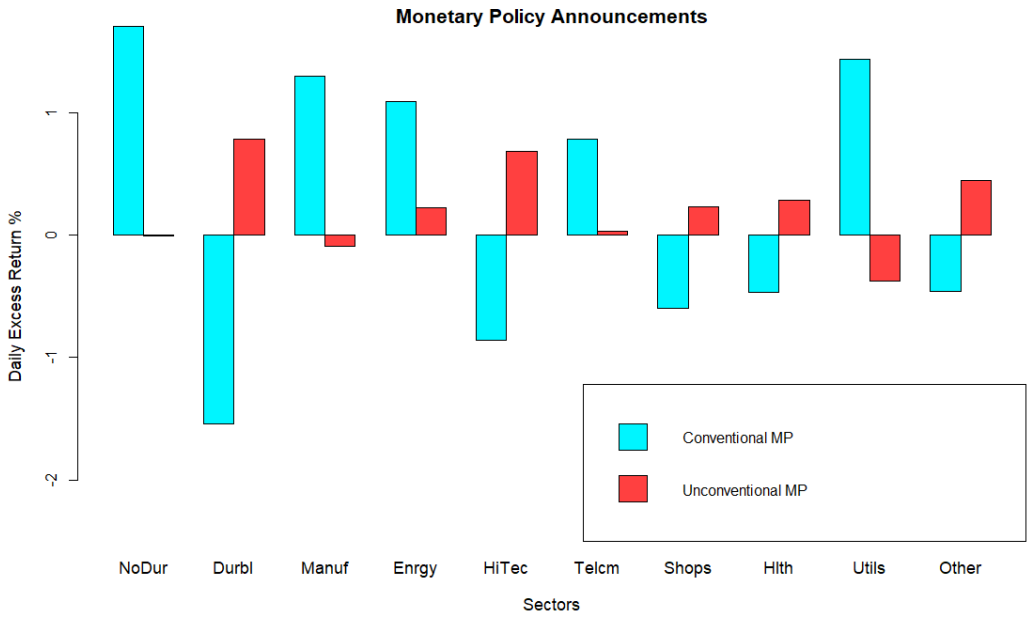

Figure 2.12: The impact of conventional and unconventional monetary policy shocks on stock market cross ten sectors.

sectors display 0.783% and 0.688% sluggish increases on risk premia from unconventional monetary policy shocks, while those announced shocks negatively impact the rest sectors. It seems reasonable to interpret the mixed signs of the coefficients demonstrating enormous uncertainties and volatility on the stock market cross sectors during the first two months of the COVID-19 crisis.

Table 2.3: Estimated coefficients of three dummy variables

Dummy Variable	**NoDur**	**Durbl**	**Manuf**	**Enrgy**	**HiTec**	**Telcm**	**Shops**	**Hlth**	**Utils**	**Other**
Monetary Policy News	0.262	0.402	0.119	0.334	0.453	0.140	0.123	0.152	-0.125	0.294
Fiscal News	4.481	4.254	6.387	7.074	3.751	4.714	1.200	4.133	6.242	6.003
Unemployment News	0.413	-0.003	0.320	0.180	-0.619	0.124	-0.325	-0.104	-0.074	0.224

Few announcements that are difficult to classify as conventional or unconventional only. For example, on March 23, 2020, the Federal Reserve issued the FOMC statement that announced to continue purchasing Treasury securities and agency MBS can be regarded as an open market operation or a forward guidance policy. In addition, on that same day, the Fed

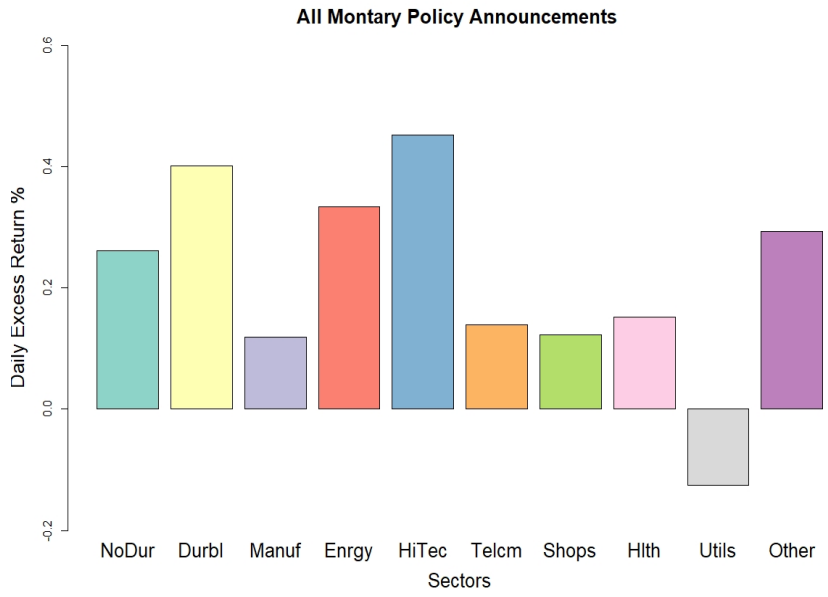

Figure 2.13: The impact of both conventional and unconventional monetary policy announcements cross sector (with a total of three dummy variables).

also created three new facilities-the Primary Market Corporate Credit Facility (PMCCF), the Secondary Market Corporate Credit Facility (SMCCF), and the Term Asset-Backed Securities Loan Facility (TALF). Overall, as the main "surprise" is establishing new facilities, this study classifies it as an unconventional monetary policy shock focused. Owing to these reasons, the study attempts to investigate the overall effects of the shocks of the monetary policy regardless of whether they are conventional and unconventional by re-estimating the model (2.1) with three dummy variables in total: monetary policy, fiscal stimulus, and unemployment shocks. See the results[19] in Table (2.3) and Figure (2.13). As Figure (2.13) shows, the overall monetary policy announcement shocks on stocks are positive (except the utilities sector) during the sample period.

[19]As the number of total independent variables reduced by one, all coefficients estimation results changed, but the changes for non-dummy variable coefficients are trivial. Therefore, I only report the coefficients for the three dummy variables.

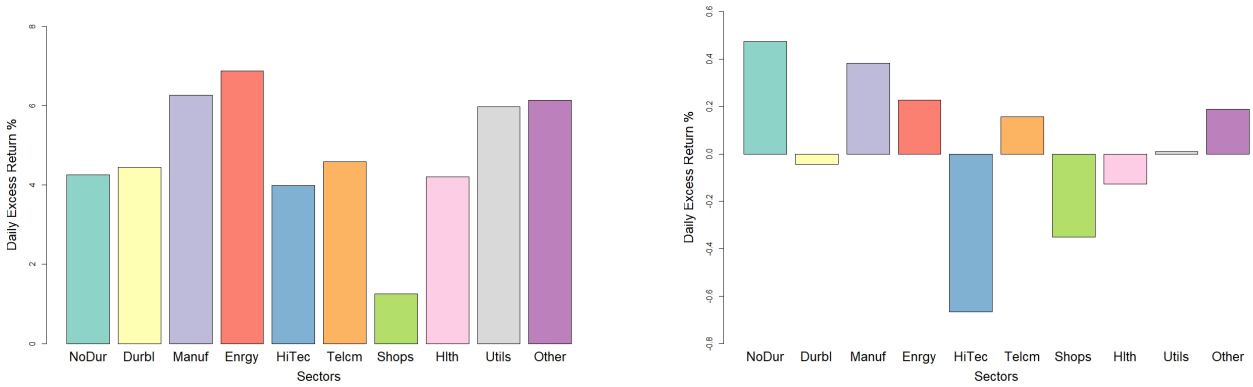

(a) Fiscal Policy Announcements

(b) Unemployment Announcements

Figure 2.14: Fiscal policy and unemployment news announcements impact
Left panel: The impact of the $2.2 trillion fiscal stimulus announcement. Right panel: The impact of unemployment rate news from the Department of Labor.

2.5.3.2 Fiscal Stimulus Announcement Shocks

Conversely, the announcement of fiscal stimulus has a strong positive impact on all ten stock market sectors. See the third row in Table (2.2) and left panel in Figure (2.14). There is distinct focus between fiscal policy and monetary policy. Fiscal stimulus is regarded as spending power that can directly help a business that suffers from the COVID-19 pandemic or people who need financial support. Monetary policy, however, has lending powers that can make secured loans to institutions, companies, or individuals to help the economy. Another reason that can also explain the significant positive effect of the fiscal stimulus package is timing. Before the fiscal stimulus package, the market of March 23 was at the lowest point, where the S&P 500 has dropped by 31.32 % since the beginning of 2020. Concerning the $2.2 trillion fiscal stimulus package passed by the Senate on the night of March 25, 2020 [20], the stock market responded to the news immediately and pivoted to a new direction with a remarkable rebound from the bottom and manifested a strong positive impact on all ten sectors.

[20]Even the final stimulus package was officially signed off on the late night of March 25, 2020, some newspapers had leaking the news and announced "The Senate appeared close to reaching a deal on a massive stimulus bill" since March 24, 2020. For example, `https://www.cbsnews.com/news/senate-coronavirus-economic-stimulus-package-bill-2020-03-24/`

2.5.3.3 Unemployment Rate News Shocks

The Bureau of Labor Statistics (BLS) releases the employment situation summary on the first Friday of every month[21]. Historically, if this release comes in significantly different from consensus estimates, it can lead to fluctuations in the stock market to fluctuate. The impact of the unemployment rate news is reported in the last row in Table (2.2) and right panel of Figure (2.14), where there are mixed positive and negative results across sectors. There are five sectors, (e.g., durable goods and manufacturing) that have positive impacts after the unemployment rates are announced. The remaining sectors (e.g., high-tech and shops) have negative impacts due to the release. The nature of the shocks could explain these findings. When presented with surprising news, optimist and pessimist investors have different expectations and may have different market behaviors. In February 2020, the U.S. unemployment rate of 3.5% was at the lowest in 50 years. When the coronavirus started to spread quickly in the U.S., the unemployment rate in April 2020 surged from 10.3% to 14.7%, the largest over-the-month increase for all data available in history. The leisure and hospitality industries' unemployment rates were the worst and reached 39.3% in April 2020. When these rates of unemployment were issued, the stock market tumbled immediately. The durable goods and energy sector slumped by 6.36% and 6.33%, respectively, on that Friday. However, as the stock market constantly involves investors' different attitudes, a shock to the opposite directions can also happen. For example, on June 5, 2020, although the unemployment rates of the leisure and hospitality industry in May were still 35.9%, it was much better than the market's expectation. The Dow Jones jumped up by 6.8%, and S&P 500 rose by 4.9% immediately. This hectic financial behavior during the COVID-19 pandemic also substantiates that the latent factor is a vital variable in the model and play a crucial role in

[21]Job report is released at 8:30 a.m. EST on the first Friday of every month `https://www.bls.gov/schedule/news_release/empsit.htm`

explaining the hectic movements of the stock prices during the COVID-19 stock market.

2.5.4 Latent Factor and Sentiment Indicators

We do not know what the latent factor exactly includes, by definition, but we can explore it by associating it with something we can measure. This section aims to use the sentiment analysis technique to explore the linkage between the latent factor and the market sentiment, which is extracted from the multi-dimensional aspects of information released. This paper examines Federal Open Market Committee (FOMC) communications and Wall Street Journal daily news. Notably, the study does not claim any causality due to data limitation but focuses on the correlations between the estimated latent factor and market sentiment.

2.5.4.1 Text Mining Techniques

There is an emerging interest in text mining or Natural Language Processing (NLP) in big data, and many soft computing methods and techniques have been developed. Although text mining is widely applied in computer science, it is still relatively new in economics and finance. This section applies two different techniques, sentiment lexicon and rule-based model (in addition to sentiment lexicon). They both show that the latent factor and the sentiment of the communications or news headlines are positively correlated.

The first technique is a sentiment lexicon term-frequency tool that identifies the sentiment polarity of words and texts. Although many algorithms are built to construct a sentiment lexicon with sentiment-aware word embedding, most of them focus on product reviews, movie reviews, and emotional states. Loughran and McDonald (2011) have shown that dictionaries

developed in other fields can be possibly ineffective for economics and finance texts and may result in misclassification errors. Given the formal characteristics of the Fed's communication, this study chooses to use Loughran and McDonald Sentiment Word Lists[22] and build the Dictionary Sentiment Score (DSS). This method is a common way of measuring market sentiment in the finance literature, where word lists are chosen to reflect the positive and negative tone and applied to text. See the literature Tetlock (2007), Tetlock et al. (2008), Loughran and McDonald (2011), and Loughran and McDonald (2014).

The dictionary sentiment score is defined as,

$$DSS = \frac{(N_{pos,t} - N_{neg,t})}{N_{tot,t}} 100\% \tag{2.34}$$

where $N_{pos,t}$ is the number of positive tone words in the context released at time t, $N_{neg,t}$ is the number of negative tone words released at time t, and $N_{tot,t}$ is the total number of words of the context released at time t. The formula gives a percentage measure, which can be greater than zero, classified as a positive sentiment, less than zero, classified as a negative sentiment, or equal to (round to) zero, classified as a neutral tone.

The second technique used in this study is called Valence Aware Dictionary for Sentiment Reasoning (VADER), which combines both lexicon sentiment analysis and embodies grammatical and syntactical conventions that express and emphasize sentiment intensity. VADER is an NLP algorithm created in 2014 and is a fully open source under the MIT License[23]. This algorithm is sensitive to both polarity (positive/negative) and the intensity of emotions. It is attuned to several domain contexts, such as NY Times editorials, movie reviews, product

[22] `https://sraf.nd.edu/textual-analysis/resources/`

[23] Hutto, C.J. Gilbert, E.E. (2014). VADER: A Parsimonious Rule-based Model for Sentiment Analysis of Social Media Text. Eighth International Conference on Weblogs and Social Media (ICWSM-14). Ann Arbor, MI, June 2014.

reviews, and performs exceptionally well in social media texts.

2.5.4.2 Event Study of FOMC Communication and Latent Factor

The Federal Open Market Committee (FOMC) holds eight regularly scheduled meetings during one calendar year. During the sample period between January 2020 and August 2020, the FOMC holds seven meetings and six press conferences, including two unscheduled meetings and one canceled scheduled meeting. FOMC meetings' statements and the press conference's scripts that are always released on the same day as the events happen, therefore can be used for sentiment analysis. The FOMC meetings' minutes are not included because minutes usually are released three weeks later after the date of the policy decision.

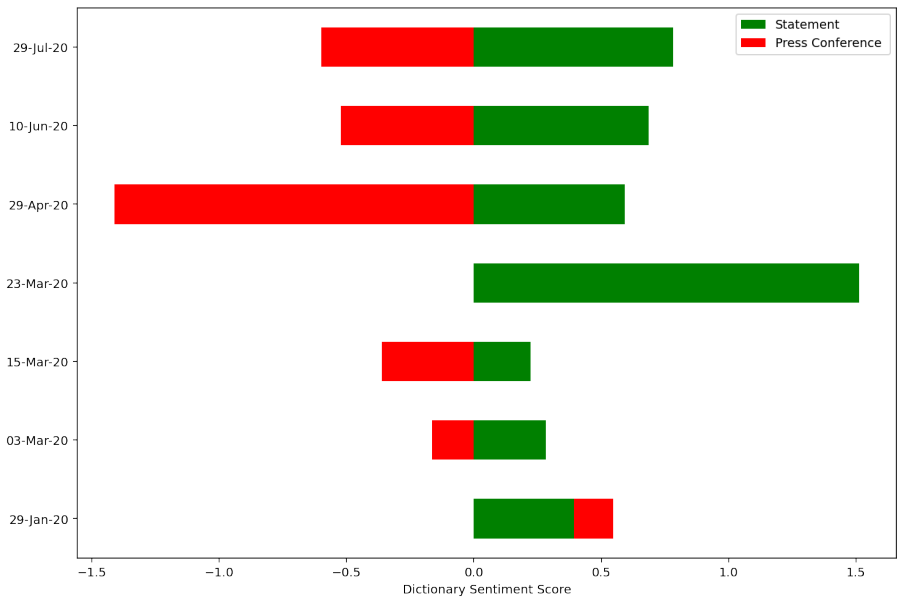

Figure 2.15: DSS Analysis of the Fed Communications

First, the study applies the DSS method to the text of FOMC statements and the press conference transcripts downloaded from the Fed Reserve's website[24]. This method demon-

[24] www.federalreserve.gov

strates success in extracting sentiment from the text, and the results are presented in Figure (2.15). Overall, FOMC statements are concise communications (total of 760 words on average from the sample), which have high quality in the sense that Committees use words precisely, and the formats of the statements are also very consistent; all DSS appear positive. The FOMC press conference gives a market update and answers reporters' questions after a Fed's monetary policy meeting. The transcripts have a longer length (a total of 8190 words on average), and all the DSS appear as negative tones since the COVID-19 breakout. For example, consider the following scripts excerpt from the March 15, 2020 conference:

"Against this favorable backdrop, the virus presents significant economic challenges. Like others, we expect that the illness and the measures now being put in place to stem its spread will have a significant effect on economic activity in the near term. Those in the travel, tourism, and hospitality industries are already seeing a sharp drop in business. In addition, the effects of the outbreak are restraining economic activity in many foreign economies, which is causing difficulties for U.S. industries that rely on global supply chains. The weakness abroad will also weigh on our exports for a time. Moreover, the energy sector has recently come under stress because of the large drop in global oil prices. Inflation, which has continued to run below our symmetric 2 percent objective, will likely be held down this year by the effects of the outbreak."

This excerpt has a total of 139 words including one positive tone word, ['favorable'], and 10 negative tone words, ['against', 'challenges', 'drop', 'difficulties', 'weakness', 'under', 'stress', 'drop', 'below', 'down']. The entire press conference scripts on March 15, 2020, has a -0.36% DSS ratio, which has a total word count of 7471 with 140 positive tone words, and 167 negative tone words. See Figure (2.15).

Next, the study combines the contents from both statements and press conferences' scripts

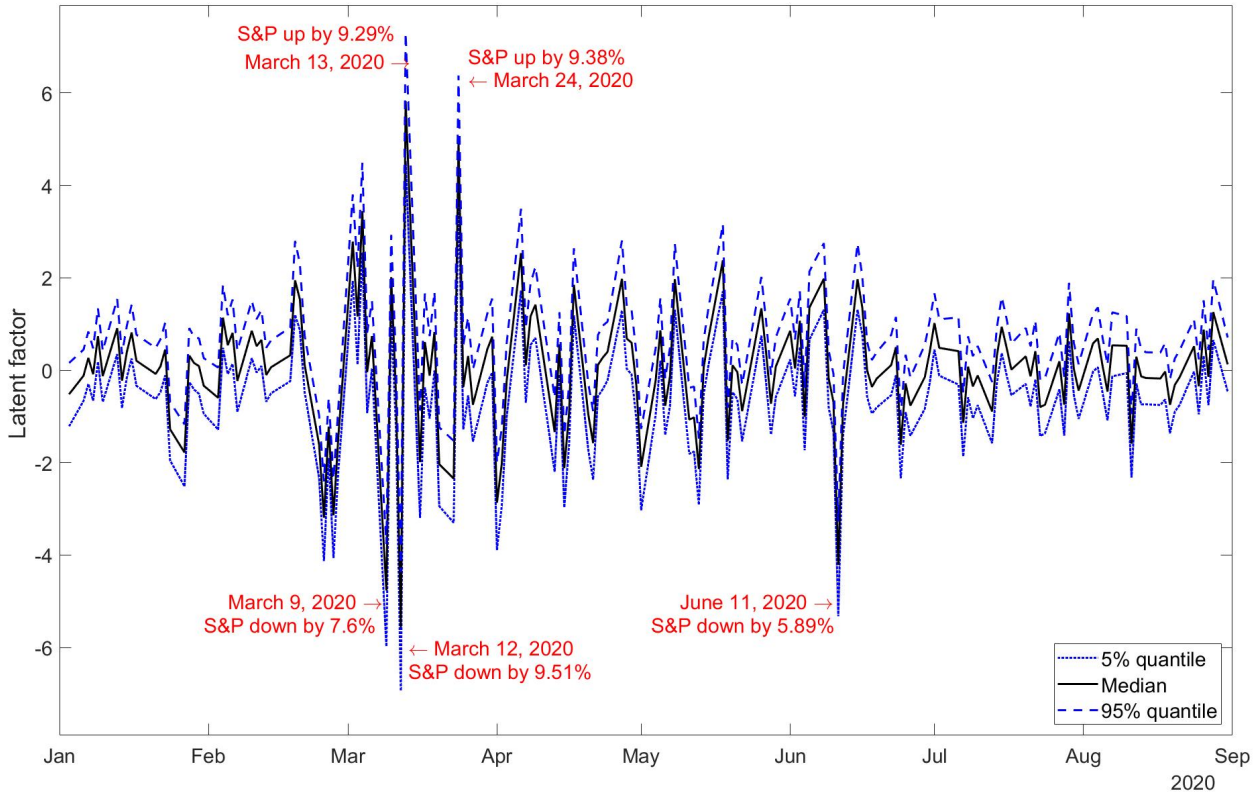

Figure 2.16: Latent factor value and change in DSS of the Fed Communications

and study the links between FOMC communications and the latent factor. Figure (2.16) visually shows the change in sentiment scores during the seven FOMC meetings. The most significant positive change of the sentiment was on March 23, 2020, and only an FOMC statement was released. The DSS is six times the last communication from FOMC, and the stock market pivoted to a new direction on March 23, 2020, and ended the bear market. This event is shown as a significant spike in Figure (2.16), where the study plots both changes in DSS and the values of the latent factor together. The most significant negative change in the DSS ratio was on March 15, 2020, when the FOMC announced reducing interest rates by one percentage point. In the previous section, Figure (2.3) shows the latent movement in the stock market plunged by 134% on the following trading day. Overall, it is evident that the latent movement and the changes in the sentiment of the Fed communications are

positively associated.[25]

2.5.4.3 Wall Street Journal Headlines And Latent Factor

FOMC communication textual data is scarce during the sample period. However, there are incredibly abundant information and news from the internet and social media. The shortfall of this type of data is that they are noisy[26], and some might not be trustworthy. The study scrapes the daily headline news from Wall Street Journal (WSJ) as a proxy of diversified aspects of market news[27]. For example, here are some examples of WSJ headlines on March 15, 2020, and a full-day sample is presented in Appendix (B.8).

"U.S.
Top Health Official Urges Americans to Stay Home Amid Coronavirus
U.S. Economy
Fed Slashes Rates to Fight Coronavirus Slowdown Coronavirus Social-Distancing Forces Painful Choices on Small Businesses
Schools
New York City Schools to Close Over Coronavirus
Economy
Fed Takes Emergency Actions as Virus Pushes Economy Toward Recession
Election 2020
Democratic Debate Between Sanders and Biden: The Moments That Mattered"

The bubble chart Figure (2.17) and (2.18) visually show sentiment scores using DSS or

[25]Due to the limitation of data, I do not draw any statistical inference.
[26]In the sample period, in addition to the COVID-19 pandemic, we also have news about the 2020 U.S. presidential election, which can also impact the stock market.
[27]WSJ archive website: `https://www.wsj.com/news/archive/years`

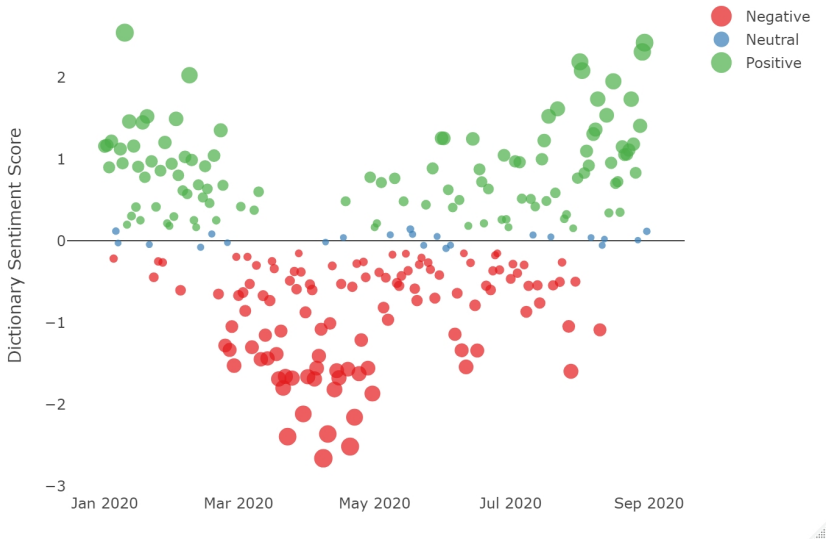

Figure 2.17: DSS for the WSJ headlines

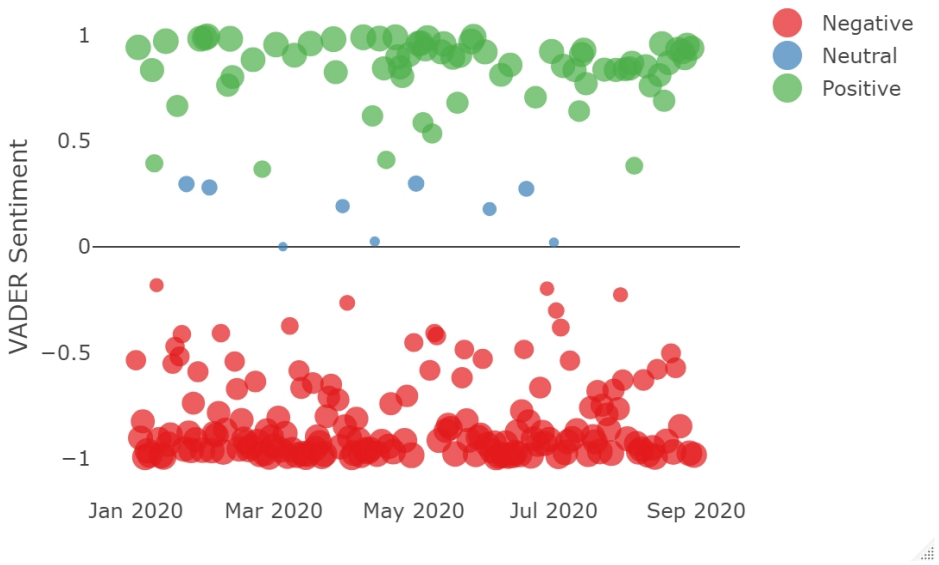

Figure 2.18: VADER for the WSJ headlines

VADER algorithm. The bubbles' diameters and the shade of the colors reflect the changes in sentiment intensity of the WSJ headlines from January 1, 2020, to August 31, 2020. Figure (2.17) is the result from the DSS method showing a vague V-shaped trajectory. The sentiment scores from the VADER algorithm are plotted in Figure (2.18), where negative sentiments dominate throughout the sample period because this method estimates both

sentiment valence (intensity) and sentiment polarity. Two regressions, regressing the daily changes in the latent factor on the changes of the DSS ratios and the changes of VADER scores, are constructed separately. The first regression obtains a positive coefficient of 0.184, the second also obtains a positive coefficient, 0.315, and both are at the 95% statistic significant level. From both NLP techniques, results show that the positive correlations between the latent comovement of the stock market and sentiment extracted from the WSJ headlines. The results validate the contribution of having the latent factor in the model; without latent factors, shown in Section 2.3, it becomes an omitted variable problem. As initially mentioned, this does not mean that the WSJ headlines trigger the stock market's movements, nor does the market causes some of the headlines reported. Owing to both the stock market and the WSJ headlines data in low daily frequency, high-frequency data are required to research their causality and bring more insights.

2.5.5 Government Restrictions

The COVID-19 impacts the economy through both direct and indirect channels. The direct channel is that it impacted laborers' health and their ability to work, especially during the first half year of 2020. There are also various indirect channels, one of which is through the government's restrictions, such as stay-home orders or the closure of non-essential business. Community mobility data can capture this kind of information. People's voluntary activities, such as grocery shopping or visiting a park, reflect their psychological state during the pandemic. Therefore, it is reasonable to assume that financial market returns are associated with mobility levels because they are associated with economic activities and people's psychological states.

Table (2.4) reports the estimated coefficients on the six categories of mobility level for each

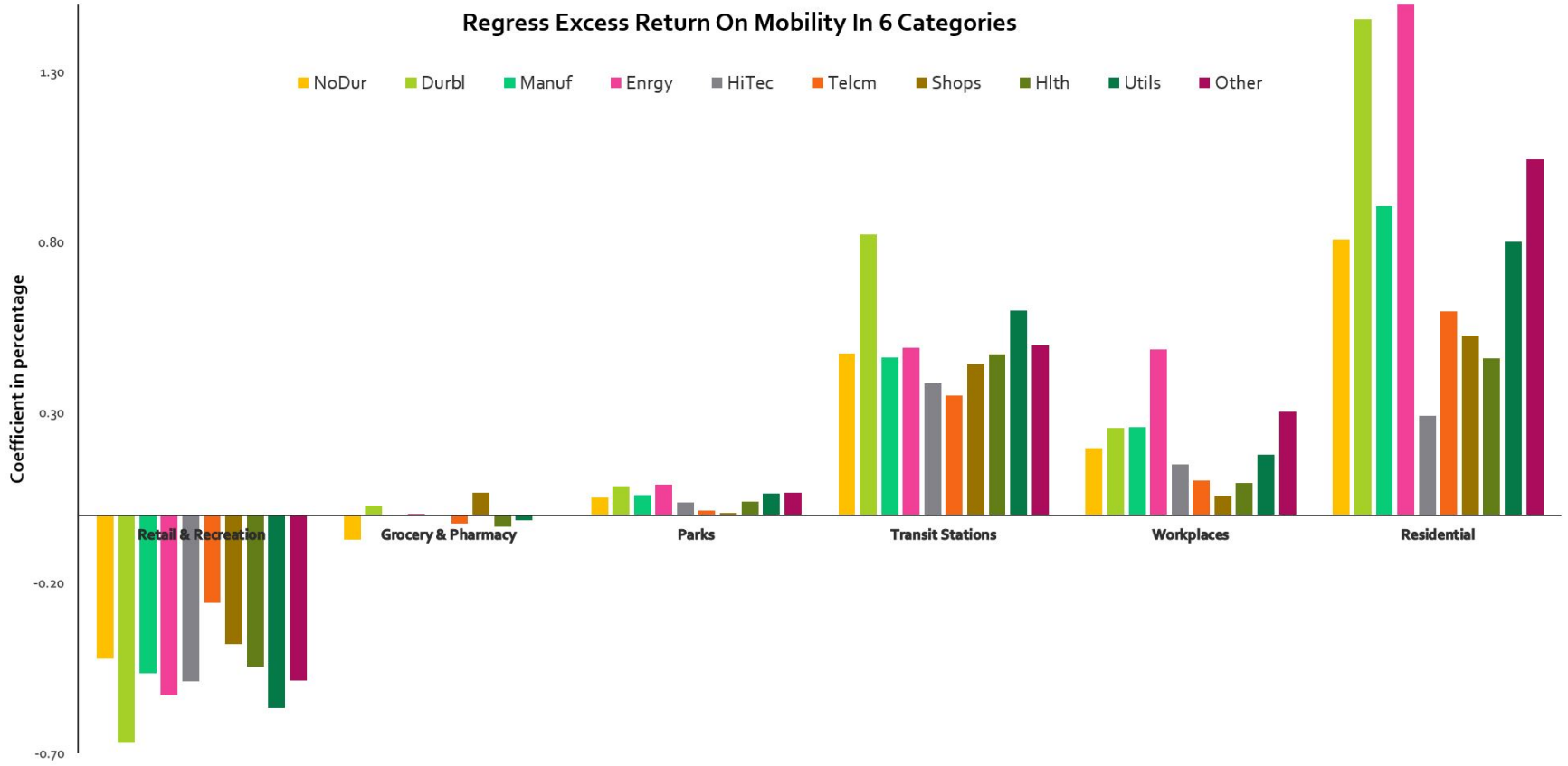

Figure 2.19: Regression coefficients of the six Mobility variables

Table 2.4: Estimated Coefficients On Mobility In Six Categories

	Retail Rec	Grocery	Parks	Transit	Workplaces	Residential
NonDur	-0.42%	-0.07%	0.05%	0.47%	0.20%	0.81%
Durbl	-0.67%	0.03%	0.08%	0.82%	0.26%	1.46%
Manuf	-0.47%	0.00%	0.06%	0.46%	0.26%	0.91%
Enrgy	-0.53%	0.01%	0.09%	0.49%	0.49%	1.63%
HiTec	-0.49%	0.00%	0.04%	0.39%	0.15%	0.29%
Telcm	-0.26%	-0.02%	0.01%	0.35%	0.10%	0.60%
Shops	-0.38%	0.07%	0.01%	0.44%	0.06%	0.53%
Hlth	-0.45%	-0.03%	0.04%	0.47%	0.10%	0.46%
Utils	-0.57%	-0.02%	0.06%	0.60%	0.18%	0.80%
Other	-0.49%	0.00%	0.07%	0.50%	0.30%	1.04%

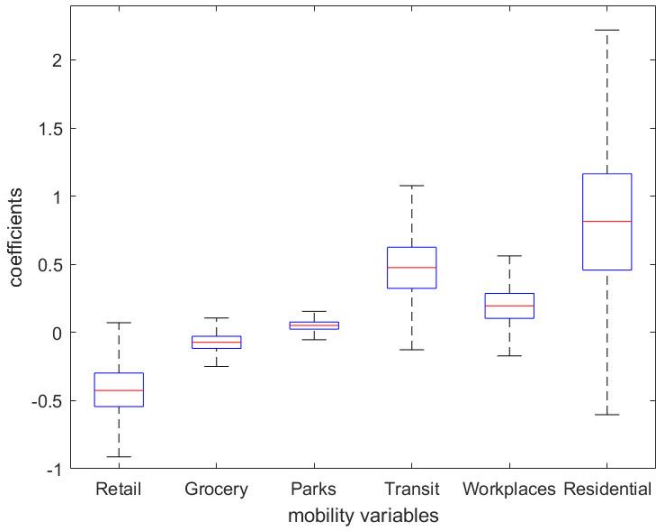

Figure 2.20: Boxplot for mobility coefficients in non-durable sector

sector. All numbers are in percentage point shown in Table (2.4) and Figure (2.19). The retail and recreation category coefficients are all negative, the grocery and pharmacy coefficients are close to zero, and the rest are all positive. I also include non-durable and utility sectors' boxplots, see Figure (2.20) and Figure (2.21). Graphs for other sectors are also available upon request.

The community mobility level in the residential category has been increasing since March 2020 due to the stay-at-home order, and the average level for all states in the U.S. has reached 20% more time relative to the baseline. Since May 2020, some states have eased up

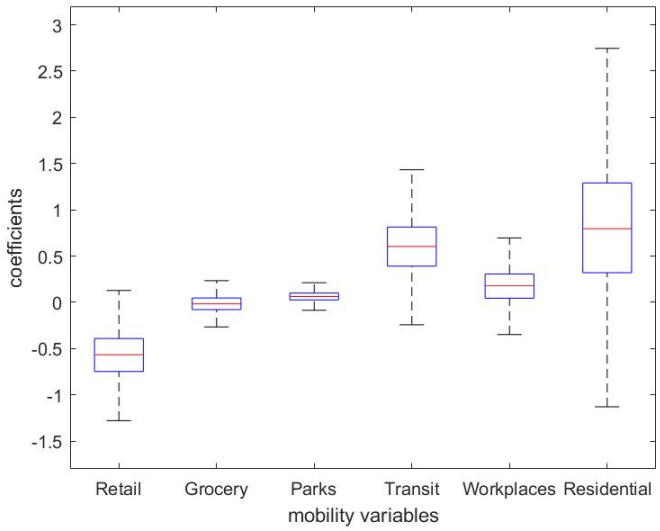

Figure 2.21: Boxplot for mobility coefficients in utility sector

and released lockdown orders. As of August 31, 2020, the level of staying-at-home is still 10% more than the baseline. The correlations between stay-home levels and stock returns are positive for all sectors, with the highest correlations, 0.0163, in the energy sector, and 0.0146 in the durable goods sector. These results imply, respectively, that a one percent increase in the stay-home level is correlated with a 1.63% and 1.46% rise in the energy and durable goods sector.

Visits to workplaces and transit are remarkably similar because the local government highly regulates them both. In the middle of March 2020, the government ordered the closure of non-essential businesses to help prevent the spread of COVID-19. Both visits have declined by 50% compared to the baseline at the end of March 2020 and the beginning of April 2020. Since May 2020, some state governments have slowly relaxed COVID-19 restrictions on businesses to help the economy recover. Positive associations are shown in Table (2.4) and Figure (2.19) between visits to work or transit and returns on the stock market. The positive association mirrors the correlation between public health status and the public economy. The coefficients of the visit to the workplace are much smaller than those of visits to

transit. One possible reason is that many jobs and economic activities can be conducted at home. Therefore, the association between visiting the workplace and the economy is smaller.

Visits to parks have been dropped by 20% and picked up since the beginning of May. Moreover, in August, it has reached 60% more than the baseline before COVID times. The coefficients on park visits are also positive in a smaller magnitude in all sectors. Positive associations are due to visits that are voluntary activities; the more visits, the less people are worried, and the more optimism there is about economic recovery. Therefore, more visits to parks are correlated with increases in the stock market returns.

In the middle of March 2020, visits to the retail and recreation stores immediately declined when the closures of non-essential businesses and social distancing protocols went into effect. In the middle of April 2020, visits to retail shops decreased by 50% from the baseline level, while the stock market rebounded. At the end of August 2020, visits to retail stores and recreation are only at 87% of the baseline, while the stock market recovered and was in a rally. Hence, the correlation between visits in the retail and recreation stores and stock market returns are all negative across sectors.

Visits to grocery and pharmacy stores are considered essential trips. Since June 2020, the visits are back to the baseline level. Without the coronavirus pandemic, the number of visits should not be associated with asset returns. As shown in Table (2.4), manufacturing, high-tech, and other sectors have zero coefficients. However, at the beginning of COVID-19, grocery and drug store visits dramatically increased due to consumers' panic-buying behavior. Stock prices plummeted simultaneously, causing the non-durable goods sector stock to show a negative association, -0.07%, while revenue grew in the shops sector, showing a positive association, +0.07%, between stock returns in the shops sector and visits to grocery

and pharmacy stores.

2.6 Conclusions

This study examines the cross-sector comovements that occurred in the U.S. stock market during the COVID-19 pandemic. The findings confirm that the latent sentiment is the driving force behind financial market behaviors. In addition, the latent sentiment had a weak daily oscillation pattern with a -0.09 autoregressive coefficient in an AR(1) process. This pattern explains the stock market's extreme comovements and high volatility.

Moreover, this study estimates the impact of the monetary policy interest rate on each stock market sector. The results indicate that when the Fed Effective Funds Rate was reduced by one percentage point, utilities and non-durable goods stock returns substantially jumped by 11.35% and 7.328%, respectively. In addition, this study explores the impact of news shocks, including monetary policy news, fiscal stimulus news, and unemployment news, on cross-sector equity returns. For any given sector, the conventional and unconventional monetary policy news shocked the sector in opposite directions. Of the positive monetary news shocks, the strongest shocks were from the interest rate policy surprises, while unconventional monetary policy news had a more sluggish impact on stock returns. Conversely, fiscal stimulus news had the most substantial positive impact and triggered all sectors to rebound from the bear market at the end of March 2020.

Furthermore, by applying Natural Language Processing (NLP) sentiment analysis, this study sheds light on the positive correlation between comovements and news sentiment. Using the

Wall Street Journal headlines as proxies of the market sentiment, the study finds a positive correlation, 0.31, at the 95% statistically significant level, between the comovements and market news sentiment.

Finally, in estimating the associations between the cross-sector asset returns and the government's social distancing policy, this study finds that the stay-at-home orders and restrictions on transit have positive associations with asset returns. Conversely, increases in retail and recreation activities have negative associations with asset returns in general. Owing to the government's policies and restrictions enacted to protect public health by slowing the spread of COVID-19, some economic activities have been curtailed in the short term. However, in the long term, these government restrictions help the public's welfare and the economy. Future studies to explore the different impacts between government restrictions and voluntary social distancing could provide fruitful results.

Bibliography

B. Aruoba, G. Rocheteau, and C. Waller. Bargaining and the value of money. *Journal of Monetary Economics*, 54(8):2636–2655, 2007. ISSN 0304-3932. doi: https://doi.org/10.1016/j.jmoneco.2007.07.003. URL https://www.sciencedirect.com/science/article/pii/S0304393207000876.

J. Bai and S. Ng. Confidence intervals for diffusion index forecasts and inference for factor-augmented regressions. *Econometrica*, 74(4):1133–1150, 2006. URL https://EconPapers.repec.org/RePEc:ecm:emetrp:v:74:y:2006:i:4:p:1133-1150.

J. Bai and P. Perron. Computation and analysis of multiple structural change models. *Journal of Applied Econometrics*, 18(1):1–22, 2003. URL https://EconPapers.repec.org/RePEc:jae:japmet:v:18:y:2003:i:1:p:1-22.

M. Baker and J. Wurgler. Investor sentiment in the stock market. *Journal of Economic Perspectives*, 21(2):129–152, June 2007. doi: 10.1257/jep.21.2.129. URL https://www.aeaweb.org/articles?id=10.1257/jep.21.2.129.

N. Barberis, A. Shleifer, and J. Wurgler. Comovement. *Journal of Financial Economics*, 75(2):283–317, 2005. ISSN 0304-405X. doi: https://doi.org/10.1016/j.jfineco.2004.04.003. URL https://www.sciencedirect.com/science/article/pii/S0304405X04001308.

E. Benmelech and N. Tzur-Ilan. The determinants of fiscal and monetary policies during the covid-19 crisis. NBER Working Papers 27461, National Bureau of Economic Research, Inc, July 2020. URL https://ideas.repec.org/p/nbr/nberwo/27461.html.

B. Biais, C. Bisière, M. Bouvard, and C. Casamatta. The Blockchain Folk Theorem. *The Review of Financial Studies*, 32(5):1662–1715, 04 2019. ISSN 0893-9454. doi: 10.1093/rfs/hhy095. URL https://doi.org/10.1093/rfs/hhy095.

F. Bianchi, S. C. Ludvigson, and S. Ma. Belief Distortions and Macroeconomic Fluctuations. NBER Working Papers 27406, National Bureau of Economic Research, Inc, June 2020. URL https://ideas.repec.org/p/nbr/nberwo/27406.html.

W. Branch and B. McGough. Heterogeneous beliefs and trading inefficiencies. *Journal of Economic Theory*, 163(C):786–818, 2016. doi: 10.1016/j.jet.2016.02.003. URL https://ideas.repec.org/a/eee/jetheo/v163y2016icp786-818.html.

M. M. Bray and N. E. Savin. Rational expectations equilibria, learning, and model specification. *Econometrica*, 54(5):1129–60, 1986. URL https://EconPapers.repec.org/RePEc:ecm:emetrp:v:54:y:1986:i:5:p:1129-60.

J. Chan and I. Jeliazkov. Efficient simulation and integrated likelihood estimation in state space models. *International Journal of Mathematical Modelling and Numerical Optimisation*, 1:101–120, 2009.

S. Chib and E. Greenberg. Bayes inference in regression models with arma (p, q) errors. *Journal of Econometrics*, 64:183–206, 1994.

S. Chib and E. Greenberg. Markov chain monte carlo simulation methods in econometrics. *Econometric Theory*, 12(3):409–431, 1996. URL https://EconPapers.repec.org/RePEc:cup:etheor:v:12:y:1996:i:03:p:409-431_00.

S. Chib and I. Jeliazkov. Marginal likelihood from the metropolis-hastings output. *Journal of the American Statistical Association*, 96:270–281, 2001. URL https://EconPapers.repec.org/RePEc:bes:jnlasa:v:96:y:2001:m:march:p:270-281.

S. Chib, F. Nardari, and N. Shephard. Analysis of high dimensional multivariate stochastic volatility models. *Journal of Econometrics*, 134(2):341–371, 2006. URL https://EconPapers.repec.org/RePEc:eee:econom:v:134:y:2006:i:2:p:341-371.

J. Chiu and T. Koeppl. Blockchain-based settlement for asset trading. *Review of Financial Studies*, 32(5):1716–1753, 2019. URL https://EconPapers.repec.org/RePEc:oup:rfinst:v:32:y:2019:i:5:p:1716-1753.

M. Choi and G. Rocheteau. Money mining and price dynamics. *American Economic Journal: Macroeconomics*, 13(4):246–94, October 2021. doi: 10.1257/mac.20200034. URL https://www.aeaweb.org/articles?id=10.1257/mac.20200034.

J. Cox, D. L. Greenwald, and S. C. Ludvigson. What explains the covid-19 stock market? Working Paper 27784, National Bureau of Economic Research, September 2020. URL http://www.nber.org/papers/w27784.

G. Evans and S. Honkapohja. Learning dynamics. In J. B. Taylor and M. Woodford, editors, *Handbook of Macroeconomics*, volume 1, Part A, chapter 07, pages 449–542. Elsevier, 1 edition, 1999. URL https://EconPapers.repec.org/RePEc:eee:macchp:1-07.

G. W. Evans and S. Honkapohja. *Learning and Expectations in Macroeconomics*. 2001.

L. Fahrmeir and H. Kaufmann. On kalman filtering, posterior mode estimation and fisher scoring in dynamic exponential family regression. *Metrika: International Journal for Theoretical and Applied Statistics*, 38(1):37–60, 1991. URL https://EconPapers.repec.org/RePEc:spr:metrik:v:38:y:1991:i:1:p:37-60.

E. Fama. Efficient capital markets: A review of theory and empirical work. *Journal of Finance*, 25:383–417, 1970.

R. Garratt and N. Wallace. Bitcoin 1, bitcoin 2,....: An experiment in privately issued outside monies. *Economic Inquiry*, 56(3):1887–1897, 2018. URL https://EconPapers.repec.org/RePEc:bla:ecinqu:v:56:y:2018:i:3:p:1887-1897.

J. Geweke. The dynamic factor analysis of economic time series. *Latent Variables in Socio-Economic Models*, 1977. URL https://ci.nii.ac.jp/naid/10026983658/en/.

F. Glaser, K. Zimmermann, M. Haferkorn, and M. C. Weber. Bitcoin - asset or currency? revealing users' hidden intentions. *PSN: Exchange Rates & Currency (International) (Topic)*, 2014.

N. J. Gormsen and R. S. J. Koijen. Coronavirus: Impact on stock prices and growth expectations. Working Paper 27387, National Bureau of Economic Research, June 2020. URL http://www.nber.org/papers/w27387.

C. Gu, F. Mattesini, C. Monnet, and R. Wright. Endogenous credit cycles. *Journal of Political Economy*, 121(5):940 – 965, 2013. URL https://EconPapers.repec.org/RePEc:ucp:jpolec:doi:10.1086/673472.

L. P. Hansen and T. J. Sargent. Recursive linear models of dynamic economies. Working Paper 3479, National Bureau of Economic Research, October 1990. URL http://www.nber.org/papers/w3479.

C. Hommes. Reflexivity, expectations feedback and almost self-fulfilling equilibria: Economic theory, empirical evidence and laboratory experiments. Tinbergen Institute Discussion Papers 13-206/II, Tinbergen Institute, 2013. URL https://EconPapers.repec.org/RePEc:tin:wpaper:20130206.

Y. Jinjarak, R. Ahmed, S. Nair-Desai, W. Xin, and J. Aizenman. Accounting for global covid-19 diffusion patterns, january-april 2020. Working Paper 27185, National Bureau of Economic Research, May 2020. URL http://www.nber.org/papers/w27185.

E. Kalai. Proportional solutions to bargaining situations: Interpersonal utility comparisons. *Econometrica*, 45(7):1623–30, 1977. URL https://EconPapers.repec.org/RePEc:ecm:emetrp:v:45:y:1977:i:7:p:1623-30.

G. Koop. *Bayesian econometrics*. John Wiley and Sons Inc., 2003. ISBN 978-0-470-84567-7.

R. Lagos and R. Wright. A unified framework for monetary theory and policy analysis. *Journal of Political Economy*, 113(3):463–484, 2005. ISSN 00223808, 1537534X. URL http://www.jstor.org/stable/10.1086/429804.

A. T. Levin and A. Sinha. Limitations on the Effectiveness of Monetary Policy Forward Guidance in the Context of the COVID-19 Pandemic. NBER Working Papers 27748, National Bureau of Economic Research, Inc, Aug. 2020. URL https://ideas.repec.org/p/nbr/nberwo/27748.html.

T. Loughran and B. McDonald. When is a liability not a liability? textual analysis, dictionaries, and 10-ks. *Journal of Finance*, 66(1):35–65, 2011. URL https://EconPapers.repec.org/RePEc:bla:jfinan:v:66:y:2011:i:1:p:35-65.

R. Lucas. Adaptive behavior and economic theory. *The Journal of Business*, 59(4):S401–26, 1986. URL https://EconPapers.repec.org/RePEc:ucp:jnlbus:v:59:y:1986:i:4:p:s401-26.

A. Marcet and T. Sargent. Convergence of least-squares learning in environments with hidden state variables and private information. *Journal of Political Economy*, 97(6):1306–22, 1989. URL https://EconPapers.repec.org/RePEc:ucp:jpolec:v:97:y:1989:i:6:p:1306-22.

E. Nosal and G. Rocheteau. *Money, Payments, and Liquidity*, volume 1. The MIT Press, 1 edition, 2011. URL https://EconPapers.repec.org/RePEc:mtp:titles:0262016281.

E. Pagnotta and A. Buraschi. An equilibrium valuation of bitcoin and decentralized network assets. 2018. URL https://ssrn.com/abstract=3142022.

R. Pindyck and J. Rotemberg. The comovement of stock prices. *The Quarterly Journal of Economics*, 108(4):1073–1104, 1993. URL https://EconPapers.repec.org/RePEc:oup:qjecon:v:108:y:1993:i:4:p:1073-1104.

G. Rocheteau and R. Wright. Money in search equilibrium, in competitive equilibrium, and in competitive search equilibrium. *Econometrica*, 73(1):175–202, 2005. URL https://EconPapers.repec.org/RePEc:ecm:emetrp:v:73:y:2005:i:1:p:175-202.

G. Rocheteau and R. Wright. Liquidity and asset-market dynamics. *Journal of Monetary Economics*, 60(2):275–294, 2013. URL https://EconPapers.repec.org/RePEc:eee:moneco:v:60:y:2013:i:2:p:275-294.

T. Sargent. Two models of measurements and the investment accelerator. *Journal of Political Economy*, 97(2):251–87, 1989. URL https://EconPapers.repec.org/RePEc:ucp:jpolec:v:97:y:1989:i:2:p:251-87.

T. Sargent. A primer on monetary and fiscal policy. *Journal of Banking Finance*, 23 (10):1463–1482, 1999. URL https://EconPapers.repec.org/RePEc:eee:jbfina:v:23:y:1999:i:10:p:1463-1482.

T. Sargent and C. Sims. Business cycle modeling without pretending to have too much a priori economic theory. Working Papers 55, Federal Reserve Bank of Minneapolis, 1977. URL https://EconPapers.repec.org/RePEc:fip:fedmwp:55.

L. Schilling and H. Uhlig. Some simple bitcoin economics. *Journal of Monetary Economics*, 106(C):16–26, 2019. URL https://EconPapers.repec.org/RePEc:eee:moneco:v:106:y:2019:i:c:p:16-26.

R. J. Shiller. Comovements in stock prices and comovements in dividends. *The Journal of Finance*, 44(3):719–729, 1989. ISSN 00221082, 15406261. URL http://www.jstor.org/stable/2328779.

J. H. Stock and M. W. Watson. New indexes of coincident and leading economic indicators. In *NBER Macroeconomics Annual 1989, Volume 4*, pages 351–409. National Bureau of Economic Research, Inc, 1989. URL https://EconPapers.repec.org/RePEc:nbr:nberch:10968.

J. H. Stock and M. W. Watson. Forecasting using principal components from a large number of predictors. *Journal of the American Statistical Association*, 97(460):1167–1179, 2002. ISSN 01621459. URL http://www.jstor.org/stable/3085839.

T. Van Zandt and M. Lettau. Robustness of adaptive expectations as an equilibrium selection device. *Macroeconomic Dynamics*, 7(1):89–118, 2003. URL https://EconPapers.repec.org/RePEc:cup:macdyn:v:7:y:2003:i:01:p:89-118_01.

A. M. Vijh. The spinoff and merger ex-date effects. *Journal of Finance*, 49(2):581–609, 1994. URL https://EconPapers.repec.org/RePEc:bla:jfinan:v:49:y:1994:i:2:p:581-609.

W. H. Wallace. Depository institutions deregulation and monetary control act of 1980. *Proceedings*, pages 200–201, 1980. URL https://EconPapers.repec.org/RePEc:fip:fedgpr:y:1980:p:200-201.

M. Woodford. Learning to believe in sunspots. *Econometrica*, 58(2):277–307, 1990. URL https://EconPapers.repec.org/RePEc:ecm:emetrp:v:58:y:1990:i:2:p:277-307.

Appendix A

1

A.1 Appendix : Proof of a_{t+1}

This section proves that, regardless, if agents are producers or miners, they choose to hold the same a_{t+1} for tomorrow.

At the beginning of the CM, the agent's problem,

$$W_t(a_t, \phi_t) = \max_{X_t, h_t, a_{t+1}} \{U(X_t) - h_t + \beta V^e_{t+1}(a_{t+1}, \phi_{t+1})\} \tag{A.1}$$

$$\text{s.t.} \quad a_t\phi_t + h_t = \ a_{t+1}\phi_t + X_t \tag{A.2}$$

$$V^e_{t+1}(a_{t+1}, \phi_{t+1}) = \ p^m_{t+1} V^m_{t+1}(a_{t+1}, \phi^e_{t+1}) + (1 - p^m_{t+1}) V^p_{t+1}(a_{t+1}, \phi^e_{t+1}) \tag{A.3}$$

where p^m_{t+1} is the probability of an agent to become a miner at time $t+1$. Note that since the total population is a unit, m_t is exogenous and agents have the information of the m_t path, $p^m_{t+1} = m_{t+1}$. I emphasize that even if the probabilities are unknown, a_{t+1} does not depend on the probabilities.

Let me first focus on the $V^e_{t+1}(a_{t+1}, \phi_{t+1})$ term,

$$V^e_{t+1}(a_{t+1}, \phi_{t+1}) = \ p^m_{t+1} V^m_{t+1}(a_{t+1}, \phi^e_{t+1}) + (1 - p^m_{t+1}) V^p_{t+1}(a_{t+1}, \phi^e_{t+1}) \tag{A.4}$$

Using the value functions (1.6) (1.7) indexed by $t+1$, the expected value function (A.4) becomes,

$$\begin{aligned} V^e_{t+1}(a_{t+1}, \phi_{t+1}) = (1 - p^m_{t+1}) \Bigg\{ & \alpha(\tau)\sigma \Big\{ u[q(a_{t+1}, \phi^e_{t+1})] - p(a_{t+1}, \phi^e_{t+1})\phi^e_{t+1} \Big\} \\ & + a_{t+1}\phi^e_{t+1} + \sigma \frac{\alpha(\tau)}{\tau} \Big\{ - c[q(\tilde{a}_{t+1}, \phi^e_{t+1})] + p(\tilde{a}_{t+1}, \phi^e_{t+1})\phi^e_{t+1} \Big\} \Bigg\} + \\ & p^m_{t+1} \Bigg\{ \alpha(\tau)\sigma \Big\{ u[q(a_{t+1}, \phi^e_{t+1})] - p(a_{t+1}, \phi^e_{t+1})\phi^e_{t+1} \Big\} + a_{t+1}\phi^e_{t+1} + \phi^e_{t+1}\Lambda \Bigg\} \end{aligned} \tag{A.5}$$

As mentioned in the DM section, $\tilde{a}_{t+1}$ appears in the producer's third term, which represents the number of tokens held by other agents, who are buyers. The reason that it is $\tilde{a}_{t+1}$, and not a_{t+1}, is that there is no credit in this economy; therefore, the trade payment is essentially limited by the buyer's assets, not the seller's. Recall the Kalai proportional bargaining (1.12), $(1-\theta)\Big[u(q) - p\phi^e_t\Big] = \theta\Big[- c(q) + p\phi^e_t\Big]$, the payment is subject to the combination of utility function, cost function and the buyer's budget, reference to (1.14) $p = \min\Big\{ \frac{(1-\theta)u(q^*)+\theta c(q^*)}{\phi^e_t}, a^{buyer} \Big\}$. With the linearity assumption of the cost function, the trade term (q, p) is determined by the shape of $u(\cdot)$ and a^{buyer}. Therefore I distinguish $\tilde{a}_{t+1}$ and a_t. The importance of this is that later I will be able to drop this term to make the equation expression easier for the maximum problem.

Continue simplifying,

$$V^e_{t+1}(a_{t+1},\phi_{t+1}) = \alpha(\tau)\sigma\Big\{u[q(a_{t+1},\phi^e_{t+1})] - p(a_{t+1},\phi^e_{t+1})\phi^e_{t+1}\Big\} + a_{t+1}\phi^e_{t+1}$$
$$+ (1-p^m_{t+1})\sigma\frac{\alpha(\tau)}{\tau}\Big\{ - c[q(\tilde{a}_{t+1},\phi^e_{t+1})] + p(\tilde{a}_{t+1},\phi^e_{t+1})\phi^e_{t+1}\Big\} + p^m_{t+1}\phi^e_{t+1}\Lambda \quad \text{(A.6)}$$

Then substitute (A.6) into (A.1), the agent's maximum problem becomes,

$$\max_{a_{t+1}}\Bigg\{ - a_{t+1}\phi_t \;+\; \beta\Big\{ a_{t+1}\phi^e_{t+1} + \;\alpha(\tau)\sigma\;\{u[q(a_{t+1},\phi^e_{t+1})] - p(a_{t+1},\phi^e_{t+1})\phi^e_{t+1}\}$$
$$+ (1-p^m_{t+1})\Big\{\sigma\frac{\alpha(\tau)}{\tau}\Big\{ - c[q(\tilde{a}_{t+1},\phi^e_{t+1})] + p(\tilde{a}_{t+1},\phi^e_{t+1})\phi^e_{t+1}\Big\}\Big\} + p^m_{t+1}\phi^e_{t+1}\Lambda\Big\}\Big\} \quad \text{(A.7)}$$

Divided by β and dropping the last two terms without a_{t+1}, the buyer's problem reduces to,

$$\max_{a_{t+1}}\Bigg\{ - (\frac{\phi_t}{\beta\phi^e_{t+1}} - 1)\; a_{t+1}\phi^e_{t+1} \;+\; \alpha(\tau)\sigma\Big\{u[q(a_{t+1},\phi^e_{t+1})] - p(a_{t+1},\phi^e_{t+1})\phi^e_{t+1}\Big\}\Big\} \quad \text{(A.8)}$$

Therefore, when forward looking agents make decisions of a_{t+1} for tomorrow, regardless of the probability of becoming of miners or producers, they eventually face the same maximum problem, which is, they will always choose to hold the same assets a_{t+1} at the end of the CM.

A.2 Appendix: Proof of Proposition 1

Proof of Proposition 1.

In steady state, $\phi_t = \phi^e_{t+1}$ and $m = 0$, therefore, (1.22) gives,

$$1 = \beta\Big\{1 + \sigma\theta\frac{u'(\phi^{ss}) - c'(\phi^{ss})}{(1-\theta)u'(\phi^{ss}) + \theta c'(\phi^{ss})}\Big\} \tag{A.9}$$

Simplify,

$$\sigma\theta\frac{u'(\phi^{ss}) - c'(\phi^{ss})}{(1-\theta)u'(\phi^{ss}) + \theta c'(\phi^{ss})} = \frac{1}{\beta} - 1 \tag{A.10}$$

where $r = \frac{1}{\beta} - 1$, therefore,

$$\sigma\theta\frac{u'(\phi^{ss}) - c'(\phi^{ss})}{(1-\theta)u'(\phi^{ss}) + \theta c'(\phi^{ss})} = r \tag{A.11}$$

$$\left|\sigma\theta\frac{u'(\phi^{ss}) - c'(\phi^{ss})}{(1-\theta)u'(\phi^{ss}) + \theta c'(\phi^{ss})}\right| = r \tag{A.12}$$

where $\phi^{ss} > 0$.

Specifically, when utility and cost functions are assumed, the unique monetary equilibrium steady state can be solved by the following. Assume $c'(\cdot) = 1$, (1.22) becomes,

$$1 + \ \sigma\theta\frac{u'(q^{ss}) - 1}{(1-\theta)u'(q^{ss}) + \theta} = \frac{1}{\beta} \tag{A.13}$$

solving $u'(q^{ss})$ obtains,

$$u'(q^{ss}) = \frac{\sigma\theta + \sigma r}{\sigma\theta + \sigma r - r} > 0 \tag{A.14}$$

where $r = \frac{1}{\beta} - 1$.

In the steady state, holding a real balance is costly $\frac{\phi_t}{\phi_{t+1}} = 1 > \beta$. Agents will bring only enough assets that they expect to spend on q^* unit of goods in the CM. The maximization problem requires $u'(q^*) = c'(q^*)$, and the concave assumption gives, $u'(\cdot) > 0$.
So it requires,

$$u'(q^{ss}) = \frac{\sigma\theta + \sigma r}{\sigma\theta + \sigma r - r} > 0 \tag{A.15}$$

It is obviously, the numerator $\sigma\theta + \sigma r > 0$. Therefore, it requires the denominator $\sigma\theta + \sigma r - r > 0$, i.e

$$(1 - \sigma)r < \sigma\theta \tag{A.16}$$

$$r < \frac{\alpha\sigma}{1 - \sigma} \tag{A.17}$$

Therefore, the existence of a monetary equilibrium requires agents to be sufficiently patient $\frac{\alpha\sigma}{1-\sigma} > r$. For example, assuming $c(q) = q$, and $c'(q^*) = 1$, it is straightforward that when $\frac{\alpha\sigma}{1-\sigma} > r$, $\frac{\sigma\theta+\sigma r}{\sigma\theta+\sigma r-r} = u'(q^{ss}) > u'(q^*) = 1$, thus, the level of trade and output in steady state are less than that of social optimal, $q^{ss} < q^*$.

A.3 Appendix: Proof of Proposition 2

Proof of Proposition 2.

From Appendix B and the derivative of (A.11) is,

$$F'(\phi^{ss}) = \beta + \beta\alpha\sigma\frac{u'(\phi^{ss}) - c'(\phi^{ss})}{(1-\theta)u'(\phi^{ss}) + \theta c'(\phi^{ss})} + \beta\alpha\sigma\phi^{ss}$$
$$\frac{(u''(\phi^{ss}) - c''(\phi^{ss}))((1-\theta)u'(\phi^{ss}) + \theta c'(\phi^{ss})) - (u'(\phi^{ss}) - c'(\phi^{ss}))((1-\theta)u''(\phi^{ss}) + \theta c''(\phi^{ss}))}{(1-\theta)u'(\phi^{ss}) + \theta c'(\phi^{ss})^2} \tag{A.18}$$

Using the linearity property assumption of the cost function $c'(\phi^{ss}) = 1, c''(\phi^{ss}) = 0$, simplify this equation and obtain,

$$F'(\phi^{ss}) = \beta\left\{1 + \sigma\theta\frac{u'(\phi^{ss}) - c'(\phi^{ss})}{(1-\theta)u'(\phi^{ss}) + \theta c'(\phi^{ss})} + \sigma\theta\frac{u''(\phi^{ss})}{((1-\theta)u'(\phi^{ss}) + \theta c'(\phi^{ss}))^2}\right\} \tag{A.19}$$

Using the fact (A.10)

$$\sigma\theta\frac{u'(\phi^{ss}) - c'(\phi^{ss})}{(1-\theta)u'(\phi^{ss}) + \theta c'(\phi^{ss})} = \frac{1}{\beta} - 1 \tag{A.20}$$

$$F'(\phi^{ss}) = \beta\left[1 + \frac{1}{\beta} - 1 + \sigma\theta\frac{u''(\phi^{ss})}{((1-\theta)u'(\phi^{ss}) + \theta c'(\phi^{ss}))^2}\right] \tag{A.21}$$

Continue simplifying above, (A.21) becomes,

$$F'(\phi^{ss}) = 1 + \beta\sigma\theta\frac{u''(\phi^{ss})}{((1-\theta)u'(\phi^{ss})} \tag{A.22}$$

Using the property of $u'(\phi^{ss}) > 0$ and $u''(\phi^{ss}) < 0$, it is clear that $F'(\phi^{ss}) < 1$.

Now, let us look at the condition for $F'(\phi^{ss}) > -1$, we require

$$\beta \frac{\sigma\theta u''(\phi^{ss})}{(1-\theta)u'(\phi^{ss})} > -2 \tag{A.23}$$

Simplify above, give a sufficient learning parameter small g, the steady-state monetary equilibrium is locally stable if and only if $|F'(\phi^{ss})| < 1$, i.e.,

$$\frac{u''(\phi^{ss})}{u'(\phi^{ss})} > -2\frac{(1-\theta)}{\sigma\theta\beta} \tag{A.24}$$

Now put everything together, according to Evans and Honkapohja (2001) under the learning and the assumption of forecast (1.31), when the algorithm has sufficiently small constant gain $g_t = g$ or decreasing gain, there exits a continuum of equilibria b converging to ϕ^{ss}. And ϕ^{ss} is locally stable, if and only if $|1 + g[F'(b) - 1]| < 1$, i.e iff $F'(b) \in (-\frac{2}{g} + 1, 1)$. Therefore, the IFF local stability condition for the steady-state monetary equilibrium is,

$$g\left[\beta \frac{\sigma\theta u''(\phi^{ss})}{(1-\theta)u'(\phi^{ss})}\right] < 2 \tag{A.25}$$

Appendix B

2

B.1 Appendix: The conditional posterior of β

This part is to explain the detail steps of how to obtain (2.16) and (2.17) in the estimation step 1. Starting from the equation (2.14) below,

$$y = X\beta + \psi, \qquad \psi \sim N(0, \Sigma)$$

where,

$$\Sigma = [(I_T \otimes \Omega) + (I_T \otimes A)\sigma^2 K^{-1}(I_T \otimes A)'] \tag{B.1}$$

As shown in Koop (2003), given Σ and assuming a natural conjugate prior $\pi(\beta) \sim N(\beta_0, B_0)$, the posterior distribution of β are given by the following expressions,

$$[\beta|\ y, A, \Sigma, \gamma, \sigma^2] \sim N(\beta, B) \tag{B.2}$$

where,

$$B = \Big(B_0^{-1} + X'\Sigma^{-1}X\Big)^{-1} \tag{B.3}$$

$$\beta = B\Big(B_0^{-1}\beta_0 + X'\Sigma^{-1}y\Big) \tag{B.4}$$

The existence of the inverse matrix Σ^{-1} is the most tricky step in solving the mean and variance in the posterior distribution. I follow the steps from Chan and Jeliazkov (2009) employing Woodbury Matrix Identity formula as shown below,

$$(E + FGH)^{-1} = E^{-1} - E^{-1}F(G^{-1} + HE^{-1}F)^{-1}HE^{-1} \tag{B.5}$$

It is straight forward to obtain,

$$\begin{aligned}
\Sigma^{-1} &= [(I_T \otimes \Omega) + (I_T \otimes A)\sigma^2 K^{-1}(I_T \otimes A)']^{-1} \\
&= (I_T \otimes \Omega^{-1}) - (I_T \otimes \Omega^{-1})(I_T \otimes A)\Big[\sigma^{-2}K + (I_T \otimes A)'(I_T \otimes \Omega^{-1}(I_T \otimes A)\Big]^{-1} \\
&\quad (I_T \otimes A)'(I_T \otimes \Omega^{-1}) \\
&= (I_T \otimes \Omega^{-1}) - (I_T \otimes \Omega^{-1}A)\Big[\sigma^{-2}K + I_T(A'\Omega^{-1}A)\Big]^{-1} \\
&\quad (I_T \otimes A'\Omega^{-1})
\end{aligned} \tag{B.6}$$

Using the compact notation $P = [\sigma^{-2}K + I_T(A'\Omega^{-1}A)]$ and combining (B.3), (B.4) and (B.6), the mean and variance for the posterior can be obtained as following,

$$B = \left(B_0^{-1} + X'\Big[(I_T \otimes \Omega^{-1}) - (I_T \otimes \Omega^{-1}A)P^{-1}(I_T \otimes A'\Omega^{-1})\Big]X\right)^{-1} \tag{B.7}$$

$$\beta = B\Big(B_0^{-1}\beta_0 + X'\Big[(I_T \otimes \Omega^{-1}) - (I_T \otimes \Omega^{-1}A)P^{-1}(I_T \otimes A'\Omega^{-1})\Big]y\Big) \tag{B.8}$$

Simplify above and obtain,

$$B = \left(B_0^{-1} + \sum_{t=1}^{T} X_t'\Omega^{-1}X_t - \tilde{X}_t'P^{-1}\tilde{X}_t\right)^{-1} \tag{2.16}$$

$$\beta = B\left(B_0^{-1}\beta_0 + \sum_{t=1}^{T} X_t'\Omega^{-1}y_t - \tilde{X}_t'P^{-1}\tilde{y}\right)^{-1} \tag{2.17}$$

where $\tilde{X}_t = A'\Omega^{-1}X_t$ and $\tilde{y}_t = A'\Omega^{-1}y_t$.

B.2 Appendix: Details of step 2.1 sample $[a|\ y, \beta, \Omega, \gamma, \sigma^2]$

This part is to explain the steps of how to obtain draw a from $[a|\ y, \beta, \Omega, \gamma, \sigma^2]$ in details.

I follow Chan and Jeliazkov (2009) to generate the posterior density of A marginalized over f. By Bayes' Theorem,

$$\pi(A|\ y, \beta, \gamma, \Omega, \sigma^2) = \frac{\pi(A|\ y, f, \beta, \gamma, \Omega, \sigma^2)\pi(f|\ y, \beta, \gamma, \Omega, \sigma^2)}{\pi(f|\ y, A, \beta, \gamma, \Omega, \sigma^2)} \tag{B.9}$$

Since both loading A and factor f are unknown, there is potential sign and scale identification issues for them, however, this can be solved by restricting the first element in the loading vector to 1, i.e. $A = \{1, a'\}$. More details can be found in Chan and Jeliazkov (2009). As the first element in the loading vector A is fixed as 1, replacing A with a, the posterior density of a, given $(y, \beta, \gamma, \Omega, \sigma^2)$ and marginalized over f, is as follows,

$$\pi(a|\ y, \beta, \gamma, \Omega, \sigma^2) = \frac{\pi(a|\ y, f, \beta, \gamma, \Omega, \sigma^2)\pi(f|\ y, \beta, \gamma, \Omega, \sigma^2)}{\pi(f|\ y, a, \beta, \gamma, \Omega, \sigma^2)} \tag{B.10}$$

$$\propto \frac{\pi(a|\ y, f, \beta, \gamma, \Omega, \sigma^2)}{\pi(f|\ y, a, \beta, \gamma, \Omega, \sigma^2)} \tag{B.11}$$

Notice the loading parameter a is not involved in the term $\pi(f|\ y, \beta, \gamma, \Omega, \sigma^2)$ on the numerator, which therefore can be relegated to a constant, and can be scaled proportionately on both denominator and numerator in calculating the acceptance ratio and eventually cancelled out.

According to (B.11), the next step is to derive the numerator $\pi(a|\ y, f, \beta, \gamma, \Omega, \sigma^2)$.

The equation (2.3) can be rewritten as,

$$y = X\beta + FA+, \quad \sim N(\mathbf{0},\ I_T \otimes \Omega) \tag{B.12}$$

where $F = diag(f_1, f_2, ..., f_T)$.

Assume a conjugate prior of $a \sim N(a_0, A_0)$, then the conditional posterior of a also follows Gaussian distribution,

$$\begin{aligned}
[a|\ y, f, \beta, \gamma, \Omega, \sigma^2] &\sim N(\bar{a}, V_a) && \text{(B.13)}\\
\bar{a} &= V_a[A_0^{-1}a_0 + F'(I_T \otimes \Omega)^{-1}(y - X\beta)] && \text{(B.14)}\\
V_a &= [A_0 + F'(I_T \otimes \Omega)^{-1}F]^{-1} && \text{(B.15)}
\end{aligned}$$

I skip explaining of denominator $\pi(f|\ y, a, \beta, \gamma, \Omega, \sigma^2)$ as it has been derived in the equations (2.11), (2.12) and (2.13).

By M-H sampling, a proposal density is tailored closely mimicking the posterior density. In practice, it is very important for the candidate generating density to have fatter tails than those of the target posterior. Let a^* be the draw from the tailored proposal, a student t distribution, of which, the mean $\hat{a}$ and negative inverse of Hessian, $\hat{A}$, are obtained by Maximum Likelihood Estimation. Let df be the degree of freedom, in general, df is chosen as a small number to ensure the fat details. The jumping distribution $q(a^*|a)$ represents the distribution for the current state a to jump to the next state a^*. Rewrite the tailored

proposal density as below for notation convenience.

$$q(a^*|a) = q(a^*|\hat{a}, \hat{A}, df), \qquad q(a|a^*) = q(a|\hat{a^*}, \hat{A^*}, df) \tag{B.16}$$

Thus, the rate $\alpha(a, a^*)$ of accepting the next proposed draw a^* is,

$$\alpha(a, a^*) = min \left\{ 1, \frac{\pi(a^*|\ y, \beta, \gamma, \Omega, \sigma^2) q(a\ |\hat{a^*}, \hat{A^*}, df)}{\pi(a|\ y, \beta, \gamma, \Omega, \sigma^2) q(a^*|\hat{a}, \hat{A}, df)} \right\} \tag{B.17}$$

B.3 Appendix: The acceptance ratio of α

Metropolis-Hastings algorithm can take many different forms. The algorithm in this paper is a special case, which is often referred to M-H within Gibbs. This appendix briefly explains the M-H sampler in the algorithm step 2(1) and how the acceptance rate (B.17) is derived.

Let a^* be the tailored proposed value, a draw from a student t distribution, of which the mean $\hat{a}$, and the variance as the negative inverse of the Hessian, $\hat{A}$ obtained by using maximum likelihood. The notation $q(a^*|a)$, is the proposed density, representing if the current state is a, then the proposed density $q(a^*|a)$ generates a^* in the next state. Thus, in the M-H algorithm the probability accepting the proposed draw a^* is,

$$\alpha(a, a^*) = min\left\{1, \frac{\pi(a^*|\ y, \beta, \gamma, \Omega, \sigma^2) q(a|\hat{a^*}, \hat{A}^*, df)}{\pi(a|\ y, \beta, \gamma, \Omega, \sigma^2) q(a^*|\hat{a}, \hat{A}, df)}\right\} \tag{B.18}$$

Recall the posterior density of a marginalized over f is $\pi(a|\ y, \beta, \gamma, \Omega, \sigma^2) \propto \frac{\pi(a|\ y, f, \beta, \gamma, \Omega, \sigma^2)}{\pi(f|\ y, a, \beta, \gamma, \Omega, \sigma^2)}$, hence, the probability of accepting the proposed draw a^* becomes,

$$\alpha(a, a^*) = min\left\{1, \frac{\frac{\pi(a^*|\ y, f, \beta, \gamma, \Omega, \sigma^2)}{\pi(f|\ y, a^*, \beta, \gamma, \Omega, \sigma^2)} q(a|a^*)}{\frac{\pi(a|\ y, f, \beta, \gamma, \Omega, \sigma^2)}{\pi(f|\ y, a, \beta, \gamma, \Omega, \sigma^2)} q(a^*|a)}\right\} \tag{B.19}$$

B.4 Appendix: MCMC Sampling Algorithm Detailed Summary

Step 1. Draw β from $[\beta|\ y, A, \Omega, \gamma, \sigma^2] \sim N(\beta, B)$, as specified by (2.15), (2.16) and (2.17).

Step 2. Draw A and f from the joint posterior distribution $[A, f|y, \beta, \Omega, \gamma, \sigma^2]$ by the following two sub-steps,

Step 2.1 Sample a first from $[a|\ y, \beta, \Omega, \gamma, \sigma^2]$ independently of f. Implement M-H sampling by drawing the proposed candidate a^* from the student $T(\hat{a}, \hat{A}, df)$ with an accepting rate at α from (B.17),

$$\alpha(a, a^*) = min\left\{1, \frac{\pi(a^*|\ y, \beta, \gamma, \Omega, \sigma^2)q(a|\hat{a^*}, \hat{A^*}, df)}{\pi(a|\ y, \beta, \gamma, \Omega, \sigma^2)q(a^*|\hat{a}, \hat{A}, df)}\right\}$$

Step 2.2 Sample f from $[f|\ y, \beta, A, \Omega, \gamma, \sigma^2] \sim N(\hat{f}, P^{-1})$ as specified by (2.12) and (2.13). I also make use to Cholesky decomposition and back substitution according to (2.23).

Step 3. Draw Ω from the conditional posterior distribution $[\Omega|\ y, \beta, A, f, \gamma, \sigma^2] \sim IG(d, D)$ as specified by (B.13), (2.25) and (2.26).

Step 4. Draw γ from the conditional posterior distribution $[\gamma|\ y, \beta, A, f, \Omega, \sigma^2]$ as specified by (2.27) (2.28) and (2.29), with an accepting rate at $\alpha(\gamma, \gamma^*)$ from (2.30),

$$\alpha(\gamma, \gamma^*) = min\left\{1, \frac{f_N(f_1|(0, \frac{\sigma^2}{1-\gamma^{*2}}))}{f_N(f_1|(0, \frac{\sigma^2}{1-\gamma^2}))}\right\}$$

Step 5. Draw σ^2 from the conditional posterior distribution $[\sigma^2|\ y, \beta, A, f, \gamma, \Omega] \sim IG(g, G)$ as specified by (2.31), (2.32) and (2.33).

B.5 Appendix: Monetary Policy Announcement Shocks

Type	Date	Time	Event	Main Information
Conventional	2020-03-03	10:00 AM	Lower benchmark rate	Lower the target range for the federal funds rate by 1/2 percentage point, to 1 to 1.25 percent.
Conventional	2020-03-15	5:00 PM	-Lower benchmark rate	Lower the target range for the federal funds rate by 1 percentage point, to 0 to 0.25 percent. reduced the interest rate on discount window loans by 1.5 percentage points, bringing it to 0.25 percent.
Unconventional	2020-03-17	10:45 AM	Establishment CPFF	The Federal Reserve Board announced today that it will establish a Commercial Paper Funding Facility (CPFF) to support the flow of credit to households and businesses.
Unconventional	2020-03-17	6:00 PM	Establishment PDCF	The Federal Reserve Board on Tuesday announced that it will establish a Primary Dealer Credit Facility (PDCF).
Unconventional	2020-03-18	11:30 PM	Establishment MMLF	The Federal Reserve Board establishes a Money Market Mutual Fund Liquidity Facility (MMLF) which will make loans available to eligible financial institutions secured by high-quality assets by the financial institution from money market mutual funds purchased.
Unconventional	2020-03-19	9:00 AM	U.S. Dollar liquidity arrangements with other Central Banks	The Federal Reserve announces the establishment of temporary U.S. dollar liquidity arrangements with other central banks. These new facilities will support the provision of U.S. dollar liquidity in amounts up to $60 billion each for the Reserve Bank of Australia, the Banco Central do Brasil, the Bank of Korea, the Banco de Mexico, the Monetary Authority of Singapore, and the Sveriges Riksbank and $30 billion each for the Danmarks National bank, the Norges Bank, and the Reserve Bank of New Zealand. These U.S. dollar liquidity arrangements will be in place for at least six months.
Unconventional	2020-03-20	10:00 AM	Extended U.S. Dollar liquidity arrangements with other Central Banks	The Bank of Canada, the Bank of England, the Bank of Japan, the European Central Bank, the Federal Reserve, and the Swiss National Bank are today announcing a coordinated action to further enhance the provision of liquidity via the standing U.S. dollar liquidity swap line arrangements. These central banks have agreed to increase the frequency of 7-day maturity operations from weekly to daily. These daily operations will commence on Monday, March 23, 2020, and will continue at least through the end of April. The central banks also will continue to hold weekly 84-day maturity operations.
Conventional	2020-03-23	8:00 AM	FOMC statement	The Federal Reserve will continue to purchase Treasury securities and agency MBS to support smooth market functioning and effective transmission of monetary policy to broader financial conditions.

Continued on next page

Figure B.1: Federal Reserve Announcements

Note: If policy announced after the trading hours, the dummy variable will reflect on the next trading day.

Type	Date	Time	Event	Main Information
Unconventional	2020-03-23	8:00 AM	Establishment of PMCCF, SMCCF, and TALF, expand MMLF, CPLF	-Supporting the flow of credit to employers, consumers, and businesses by establishing new programs that, taken together, will provide up to $300 billion in new financing. The Department of the Treasury, using the Exchange Stabilization Fund (ESF), will provide $30 billion in equity to these facilities. -Establishment of two facilities to support credit to large employers – the Primary Market Corporate Credit Facility (PMCCF) for new bond and loan issuance and the Secondary Market Corporate Credit Facility (SMCCF) to provide liquidity for outstanding corporate bonds. -Establishment of a third facility, the Term Asset-Backed Securities Loan Facility (TALF), to support the flow of credit to consumers and businesses. The TALF will enable the issuance of asset-backed securities (ABS) backed by student loans, auto loans, credit card loans, loans guaranteed by the Small Business Administration (SBA), and certain other assets. -Facilitating the flow of credit to municipalities by expanding the Money Market Mutual Fund Liquidity Facility (MMLF) to include a wider range of securities, including municipal variable rate demand notes (VRDNs) and bank certificates of deposit. -Facilitating the flow of credit to municipalities by expanding the Commercial Paper Funding Facility (CPFF) to include high-quality, tax-exempt commercial paper as eligible securities. In addition, the pricing of the facility has been reduced.
Unconventional	2020-03-31	8:30 AM	Establishment FIMA Repo Facility	Establishment of a temporary repurchase agreement facility for foreign and international monetary authorities (FIMA Repo Facility) to help support the smooth functioning of financial markets, including the U.S. Treasury market, and thus maintain the supply of credit to U.S. households and businesses.
Unconventional	2020-04-6	2:00 PM	Establish a facility to provide term financing backed by PPP loans	Federal Reserve will establish a facility to facilitate lending to small businesses via the Small Business Administration's Paycheck Protection Program (PPP) by providing term financing backed by PPP loans. Agencies announce changes to the community bank leverage ratio.
Unconventional	2020-04-9	8:30 AM	Provide up to $2.3T in loans. Bolster SBA's PPPLF. Establish MSLP. Expand the PMCCF, SMCCF, and TALF.	Took additional actions to provide up to $2.3 trillion in loans to support the economy. This funding will assist households and employers of all sizes and bolster the ability of state and local governments to deliver critical services during the coronavirus pandemic. Establishment of the MSLP. Expand the PMCCF, SMCCF, and TALF.
Unconventional	2020-04-23	5:45 PM	Expansion of the PPPLF	the Federal Reserve announces it is working to expand access to its Paycheck Protection Program Liquidity Facility (PPPLF) for additional SBA-qualified lenders as soon as possible.

Continued on next page

Figure B.2

Type	Date	Time	Event	Main Information
Unconventional	2020-04-27	4:30 PM	Expansion of the MLF	the Federal Reserve Board announces an expansion of the scope and duration of the Municipal Liquidity Facility. The facility, which was announced on April 9 as part of an initiative to provide up to $2.3 trillion in loans to support U.S. households, businesses, and communities, will offer up to $500 billion in lending to states and municipalities to help manage cash flow stresses caused by the coronavirus pandemic.
Unconventional	2020-04-29	2:00 PM	FOMC statement	The Fed decided to maintain the target range for the federal funds rate at 0 to 1/4 percent (Forward Guidance). Support the flow of credit to households and businesses, the Federal Reserve will continue to purchase Treasury securities and agency residential and commercial mortgage-backed securities in the amounts needed to support smooth market functioning, thereby fostering effective transmission of monetary policy to broader financial conditions. In addition, the Open Market Desk will continue to offer large-scale overnight and term repurchase agreement operations. The Committee will closely monitor market conditions and is prepared to adjust its plans as appropriate.
Unconventional	2020-04-30	10:00 AM	Expand the Main Street Lending Program	the Federal Reserve Board announces it is expanding the scope and eligibility for the Main Street Lending Program.
Unconventional	2020-04-30	5:15 PM	Expand PPPLF	the Federal Reserve expands access to its Paycheck Protection Program Liquidity Facility (PPPLF) to additional lenders, and expands the collateral that can be pledged.
Unconventional	2020-05-11	10:30 AM	Update MLF	The Municipal Liquidity Facility (MLF) , which was established under Section 13(3) of the Federal Reserve Act, with approval of the Treasury Secretary, will offer up to $500 billion in lending to states and municipalities to help manage cash flow stresses caused by the coronavirus pandemic.
Unconventional	2020-05-12	1:15 PM	Update TALF	Federal Reserve publishes updates to the term sheet for the Term Asset-Backed Securities Loan Facility (TALF) and announces information to be disclosed monthly for the TALF and the Paycheck Protection Program Liquidity Facility.

Figure B.3

B.6 Appendix: Data Transformation Summary

The column trans-code denotes the following data transformation for a series x: (1) No transformation; (2) Change: Δx_t; (3) Growth rate: $\Delta log(x_t)$; (4) Indexing: $\frac{x_t}{benchmark}$; (5) Normalizing: $\frac{x_t - min}{max - min}$.

ID	Trans-Code	Name/FRED	Description	Frequency
1	1	NoDur	Stock Returns by Secotor	Daily
2	1	Durbl	Stock Returns by Secotor	Daily
3	1	Manuf	Stock Returns by Secotor	Daily
4	1	Enrgy	Stock Returns by Secotor	Daily
5	1	HiTec	Stock Returns by Secotor	Daily
6	1	Telcm	Stock Returns by Secotor	Daily
7	1	Shops	Stock Returns by Secotor	Daily
8	1	Hlth	Stock Returns by Secotor	Daily
9	1	Utils	Stock Returns by Secotor	Daily
10	1	Other	Stock Returns by Secotor	Daily
11	3	IPBUSEQ	Industrial Production: Equipment: Business Equipment	Monthly
12	3	IPZ53010S	Industrial Production: Materials Excluding Energy Materials	Monthly
13	3	IPB53300S	Industrial Production: Energy Materials	Monthly
14	3	IPDMAN	Industrial Production: Durable Manufacturing (NAICS)	Monthly
15	3	IPDCONGD	Industrial Production: Durable Consumer Goods	Monthly
16	3	IPNMAN	Industrial Production: Non-Durable Manufacturing (NAICS)	Monthly
17	3	IPMINE	Industrial Production: Mining, Quarrying, and Oil and Gas Extraction: Mining (NAICS = 21)	Monthly
18	3	IPUTIL	Industrial Production: Utilities: Electric and Gas Utilities (NAICS = 2211,2)	Monthly
19	3	IPNCONGD	Industrial Production: Non-Durable Consumer Goods	Monthly
20	3	LNU04032230	Unemployment Rate - Mining, Quarrying, and Oil and Gas Extraction, Nonagricultural	Monthly
21	3	LNU04032231	Unemployment Rate - Construction Industry	Monthly
22	3	LNU04032233	Unemployment Rate - Durable Goods Industry	Monthly
23	3	LNU04032234	Unemployment Rate - Non Durable Goods Industry	Monthly
24	3	LNU04032235	Unemployment Rate - Wholesale and Retail Trade	Monthly
25	3	LNU04032236	Unemployment Rate - Transportation and Utilities Industry	Monthly
26	3	LNU04032237	Unemployment Rate - Information Industry	Monthly
27	3	LNU04032238	Unemployment Rate - Financial Activities Industry	Monthly
28	3	LNU04032239	Unemployment Rate - Professional and Business Services	Monthly
29	3	LNU04032240	Unemployment Rate - Education and Health Services	Monthly

Continued on next page

Figure B.4: Data Transformation

ID	Trans-Code	Name/FRED	Description	Frequency
30	3	LNU04032241	Unemployment Rate - Leisure and Hospitality	Monthly
31	3	LNU04032242	Unemployment Rate - Other Services Industry	Monthly
32	3	M1SL	M1 Money Stock	Monthly
33	3	CPIAUCSL	Consumer Price Index for All Urban Consumers	Monthly
34	4	UMCSENT	University of Michigan: Consumer Sentiment, Index 2020 : M1 = 1	Monthly
35	5	Death Rate	COVID-19 Death Rate Smoothed	Daily
36	3	Trade Volume	NASDAQ Stock Market Trade Volume	Daily
37	1*	Retail, Recreation	Google Community Mobility	Daily
38	1*	Grocery, Pharmacy	Google Community Mobility	Daily
39	1*	Parks	Google Community Mobility	Daily
40	1*	Transit Stations	Google Community Mobility	Daily
41	1*	Workplaces	Google Community Mobility	Daily
42	1*	Residential	Google Community Mobility	Daily
43	2	DFF	Effective Federal Funds Rate	Daily
44	1	MPC	MP Conventional Announcement Dummy Variable	Daily
45	1	MPUNC	MP Unconventional Announcement Dummy Variable	Daily
46	1	FISC	Fiscal announcement Dummy Variable	Daily
47	1	UNEMP	Unemployment Announcement Dummy Variable	Daily

Figure B.5: Data Transformation

Note: An asterisk is tagged these variables to indicate that they been adjusted from the source.

B.7 Appendix: Estimation of β

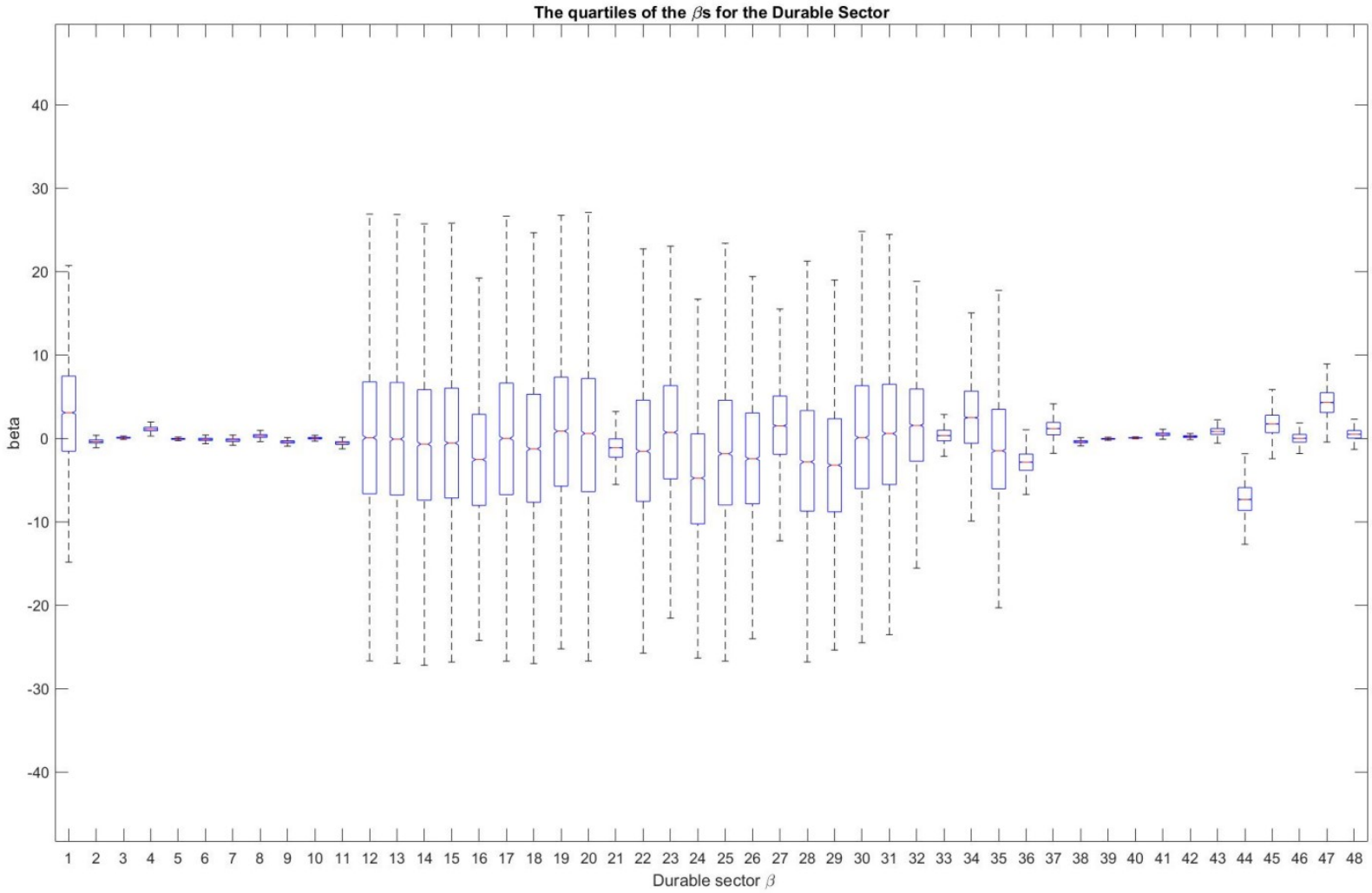

Figure B.6: 48 βs

Note: the order numbers of the coefficients are the same order numbers as in Appendix (B.6) but adding one, because the first coefficient is for the intercept. Graphs for other sectors are also available upon request.

B.8 Appendix: Sample of Wall Street Journal headlines on March 15, 2020

This is a one-day sample to show that the sentiment analysis captures collective news shocks during the sample period (January 1, 2020 - August 31, 2020). The news headlines include all aspects of the society, i.e., health, education, economy, business, election, world news shocks, etc.

Election 2020

Inside and Outside the Democratic Debate, a World Transformed

Election 2020

Biden, Sanders Split on Policy, Unite Against Trump

World

Coronavirus Measures Put New Limits on Daily Life

Business

United Starts Union Talks as Cuts Deepen

New York

De Blasio to Ban Dining at New York City Restaurants, Bars, Cafes

Election 2020

Democratic Debate Between Sanders and Biden: The Moments That Mattered

Business

Wynn, MGM to Temporarily Close Las Vegas Strip Casinos Over Coronavirus

Journal Reports: Wealth Management

Travel vs. Environmentalism? Millennials Try to Do Both

Europe

European Nations Impose Stricter Novel Coronavirus Measures

U.S.

Top Health Official Urges Americans to Stay Home Amid Coronavirus

U.S. Economy

Fed Slashes Rates to Fight Coronavirus Slowdown

Health Policy

Census Worker Tests Positive for Novel Coronavirus

Markets

Biggest U.S. Banks Halt Buybacks to Free Up Capital for Coronavirus

U.S.

Fliers Back From Abroad Face Long, Crowded Lines at Airports

U.S.

Trump Says He Is Considering Pardoning Michael Flynn

Review Outlook

Virus Relief but New Business Burdens

Review Outlook

The Federal Reserve Returns to 2008

Review Outlook

Mississippi's Biggest Loser

State Street

Coronavirus Roils New York Election Plans

Commentary Don't Credit the Minimum Wage for Growing Paychecks

Commentary

Let the Fed Administer an Antiviral Shot

Bookshelf

‘Experimentation Works’ and ‘The Power of Experiments’ Review: Test, Test and Test Again

Notable Quotable

Notable Quotable: ISIS on the Coronavirus

Inside View

Crisis Means a New Business Era

The Americas

Economic Flu Stalks Latin America

Economy

Economy Week Ahead: Focus on Fallout From the Coronavirus

Election 2020

Joe Biden Nods to Liberals With College Tuition, Bankruptcy Proposals

Schools

New York City Schools to Close Over Coronavirus

Economy

Fed Takes Emergency Actions as Virus Pushes Economy Toward Recession

U.S.

Despite Coronavirus, Some Religious Services Continue

Business

Coronavirus Prompts Abercrombie, Nike, Others to Close Shops

Middle East

Blue and White Leader Gantz to Get First Shot at Forming Israeli Government

Europe

Germany Accuses U.S. of Trying to Lure a Drug Maker Working on Coronavirus Vaccine

The A-Hed

Brine With a Dash of Beet Juice—A Pungent Cocktail for Icy Roads

New York

Gov. Cuomo Wants to Close New York City's Public-School System

Business

Grocers Fail to Keep Up With Demand as Pandemic Spreads

Business

For Airlines, a Week That Went From Bad to Worse

TikTok to Stop Using China-Based Moderators to Monitor Overseas Content

World

As Virus Spreads, Governments Rush to Secure Ventilators

New York

Homemade Hand Sanitizer Hits New York Store Shelves

Business

Sports, Retailers, Airlines, Autos: The Damage Across Business

Politics

Adam Schiff Says Former Aide Tests Positive for Virus

Media Marketing

Domestic Box Office Suffers Worst Weekend in Nearly 20 Years

Letters

On the Readmission of Criminal Immigrants

Letters

Schumer's Intimidating Supreme Court Rant

Letters

Fed Actions Should Truly Promote Liquidity

Letters

Graduate-School Regression Had Other Compensations

Letters

The Fed Liquidity Stimulus Must Be Enough to Succeed

Business

Coronavirus Social-Distancing Forces Painful Choices on Small Businesses